UNIVERSITÀ DEGLI STUDI DI UDINE

Dipartimento di Scienze Mediche e Biologiche

CORSO DI DOTTORATO DI RICERCA IN SCIENZE E TECNOLOGIE CLINICHE
XXV CICLO

TESI DI DOTTORATO DI RICERCA

MULTIMERIN2: an extracellular matrix protein regulating angiogenesis by VEGF-A/VEGFR2 pathway

DOTTORANDO
Dott.ssa Roberta Colladel

RELATORE
Prof. Alfonso Colombatti

CORRELATORE
Dott. Maurizio Mongiat

COORDINATORE
Prof. F.S. Ambesi Impiombato

Anno Accademico
2012/2013

TABLE OF CONTENTS

SUMMARY

Angiogenesis, the formation of new blood capillaries from pre-existing vessels, is a physiological process tightly regulated by a number of pro- and anti-angiogenic molecules and plays an important role in supporting tumor growth. In the latest years it has become clear that the different cellular and proteic components of the microenvironment are pivotal regulators of tumor development. In this contest many extracellular matrix (ECM) molecules have been recognized as prominent negative or positive modulators of tumor angiogenesis and tumor growth.

MULTIMERIN2 (MMRN2), also known as Endoglyx-1, is a ~160 kDa ECM glycoprotein belonging to the EMI-Domain ENdowed (EDEN) protein family. It is specifically deposited along the blood vessels in tight juxtaposition with endothelial cells (ECs) and is also present at the luminal side of the vessels, suggesting an important role in the regulation of EC function. MMRN2 displays a pan-endothelial expression pattern both in normal and tumoral vasculature. However, prior to the study presented in this thesis, the function of this molecule has remained concealed.

Given its strategic localization we hypothesized that MMRN2 could affect EC function and angiogenesis. By means of multiple assays, we show that MMRN2 significantly impairs EC migration and the formation of a functional vessel network. The interaction of ECs with MMRN2 causes an impaired activation of VEGFR2, the chief VEGF-A receptor involved in the regulation of angiogenesis. Furthermore these studies demonstrate that the interference of MMRN2 with the VEGF/VEGFR2 axis occurs via the sequestration of VEGF-A, likely preventing the interaction with its receptor.

Next the possibility that this effect could affect tumor growth was tested in vivo. The over-expression of MMRN2 by a sarcoma cell line dramatically reduced their tumorigenic potential. Accordingly, tumors from MMRN2 over-expressing cells were characterized by a significant decrease of the vascular density. Moreover, in agreement with the evidence of a direct binding between these two molecules, immunostainings performed on the tumor sections showed that VEGF-A co-localizes with MMRN2.

Newly generated results further strengthen our published data. First we have demonstrated that MMRN2 does not interact with other two members of the VEGF family regulating angiogenesis: VEGF-B and PlGF, suggesting that MMRN2 specifically impairs angiogenesis via VEGF-A/VEGFR2 pathway. Through the construction of a series of deletion mutants, we have started to dissect the

region involved in binding to VEGF-A and in the anti-angiogenic effects and pinpointed an N-terminal region included between Δ1 and Δ1-2 MMRN2 fragments.

Simultaneously we have also generated preliminary evidences indicating that MMRN2 may regulate VEGF-A signaling also by impairing the availability of VEGFR2 on the ECs' membrane, as assessed by immunofluorescence analysis.

The anti-angiogenic effects of MMRN2 were then corroborated and tested in a sophisticated experimental setting using spheroids embedded in a fibrin gel overlaid with fibroblasts. This 3D *in vitro* model will allow us to investigate the effects of MMRN2 in combination with different molecules to better understand its role in angiogenic process.

Taken together our results suggest that MMRN2, which is normally deposited along the blood vessels, may represent a homeostatic molecule. Indeed this hypothesis is supported by the finding that the tips of the newly form vessels departing from aortic rings embedded in type I collagen matrices are devoid of MMRN2. In accordance with these findings also the developing retinas from P3 pups display a weak MMRN2 deposition as opposed to retinas from adult mice. Based on these evidences, MMRN2 can be conceived as a stabilizer for the blood vessels. Once deposited it obstructs the formation of new vessels MMRN2, unless degraded.

In conclusion these findings indicate that MMRN2 plays a crucial role in the regulation of EC function, neoangiogenesis and tumor growth. We hypothesize that secreted and deposited MMRN2 may function as a homeostatic barrier halting the sprouting of novel vessels, suggesting that this ECM protein could represent a promising novel tool for the development of new antiangiogenic drugs for clinical practice.

ABBREVIATIONS

Ad MMRN2: Adenovirus MMRN2

BM: Basement Membrane

Coll I: type I collagen

DOX: Doxycycline

EC: Endothelial Cell

ECM: Extracellular Matrix

FBS: Fetal Bovine Serum

FGF: Fibroblast Growth Factor

HUVEC: Human Umbilical Vein Endothelial Cell

MMRN2: MULTIMERIN2

PBS: Phosphate Buffered Saline

siRNA: Small Interfering RNA

TUNEL: TdT-mediated dUTP Nick End Labeling

VEGF: Vascular Endothelial Growth Factor

VEGFR2: Vascular Endothelial Growth Factor Receptor 2

INTRODUCTION

1. ANGIOGENESIS

Blood vessels are a complex network of tubes that transport oxygenated blood and nutrients throughout the body.

The most essential component of blood vessels is the endothelial cell (EC). Every vessel, from the aorta down to the smallest capillaries, consists of a monolayerof EC, called the endothelium, arranged in a mosaic pattern around a central lumen through which blood can flow. Outside the endothelium there is an extracellular lining called the basement membrane (BM), separating the EC from the surrounding connective tissue. This is composed of protein fibres, mainly laminin and collagen, and may also contain peri-endothelial supporting cells. BM proteins possess multiple binding sites for cell adhesion molecules and many motifs serve as ligands for cell surface receptors. Binding of cell surface receptors to BM proteins initiates intracellular signaling pathways that influence cellular behavior. BM components guide cellular differentiation and inhibit or promote cell proliferation and migration (LeBleu V.L. *et al.*, 2007). Cell–cell contacts and cell–BM contacts, mediated respectively by cadherins and integrins, are extremely important and loss of either or both can lead to local destabilization of the endothelium and EC apoptosis (Lobov I.B. *et al.*, 2002). The peri-endothelial cells include pericytes in the microvasculature (capillaries) and smooth muscle cells in larger vessels. These cells play a particularly important role in maintaining blood vessels in the stable-state and are involved in the regulation of blood flow (HirschiK.K. *et al.*, 1996; Rucker H.K. *et al.*, 2000). Larger vessels have a thick wall of smooth muscle cells outside the BM, whereas capillaries consist only of the endothelium, BM and pericytes. A layer of connective tissue, known as the stroma, separates the vessel from the functional tissue of an organ, the parenchyma. The stroma is principally composed of fibroblasts, which secrete a matrix of extracellular protein fibres, such as collagen and fibronectin (Raza A. *et al*., 2010).

The formation of the blood vessels is one of the earliest and tightly regulated events in organogenesis and it occurs through two processes: vasculogenesis and angiogenesis. Vasculogenesis is the *de novo* formation of blood vessels from angioblasts. It occurs in the extra-embryonic and intra-embryonic tissues of the embryos. Vasculogenesis is a dynamic process that involves cell–cell and cell–ECM interactions directed spatially and temporally by growth factors and morphogens. This process includes the differentiation of mesodermal stem cells into

angioblasts which migrate under a growth factor stimulus to form blood islands and give rise to ECs (Ema M.*et al.*, 2003).

In contrast to vasculogenesis, angiogenesis is the formation of new capillaries from pre-existing vessels. This is a complex process that requires the interaction between different cell types, the ECM and several cytokines and growth factors. During angiogenesis, the capillary plexus is remodelled by sprouting, microvascular growth and finally by fusion into a mature and functional vascular bed. Angiogenesis also includes vessel penetration into avascular regions of the tissue and is crucially dependent on the correct interactions between ECs, pericytes, interacting externally with the endothelium, and stromal cells, such as fibroblasts, and their association with the ECM and the vascular BM (Yancopoulos G.D. *et al.*, 2000).

In the adult the angiogenetic process takes place only in particular occasions including wound healing, inflammation, endometrial re-growth during the menstrual cycle, and following tissue grafting or ischemia to allow the maintenance of physiological homeostasis and tissue integrity (Carmeliet P., 2003).

Multiple, sequential steps are required for effective angiogenesis **(Fig.1)**:

1) Expression of potent pro-angiogenic factors and mitogens for ECs, such as VEGF-A, that guides ECs into avascular areas (Ferrara N. *et al.,* 2003).

2) Activation of the membrane type 1 matrix metalloproteinase (MT1-MMP) that plays a major role in the ECM remodelling, directly by degrading several ECM components (collagens, fibronectin, laminin and proteoglycan) and indirectly by activating pro-MMP2 (Sato H. *et al.*, 1994). As a result, ECs lose their contact with BM laminin and are exposed to interstitial collagen. This change helps to trigger signaling cascades in the ECs that lead to cytoskeleton reorganization and sprouting morphogenesis (Rhodes M.J.C. *et al*., 2007). Subsequently, these cells become motile and align into chords.

3) Recruitment of pericytes and vascular smooth muscle cells to nascent vessels once EC proliferation is arrested; this provides stabilization, remodelling and maturation signals (Folkman J., 2006).

4) Expression of tissue inhibitor of metalloproteinases 2 (TIMP2) in ECs and TIMP3 in pericytes following the contact between ECs and pericytes which switches off the proteolytic phenotype in ECs (Saunders W.B. *et al*., 2006).

5) Tight sealing of the vessel lumen by adjacent ECs held together by tight junctions and adherens junctions (Bazzoni G. *et al*., 2004). A BM is then produced by ECs in cooperation with surrounding cells to provide structural support and maintain the EC quiescence (LeBleu V.L. *et al.*, 2007).

6) Pruning of excess or unneeded vessels for optimal perfusion occurring during the maturation of new capillaries; this process is thought to be an adjustment to the oxygen surplus, while the surrounding ECM exerts mechanical strain that provides traction and orientation for angiogenic microvessels (Krishnan L. *et al.,* 2008).

7) Raising of the local oxygen level due to the blood flow to the newly vascularized area once tube formation is complete, resulting in a decrease in VEGF levels and the end of angiogenic process (Ferrara N. *et al.,* 2003).

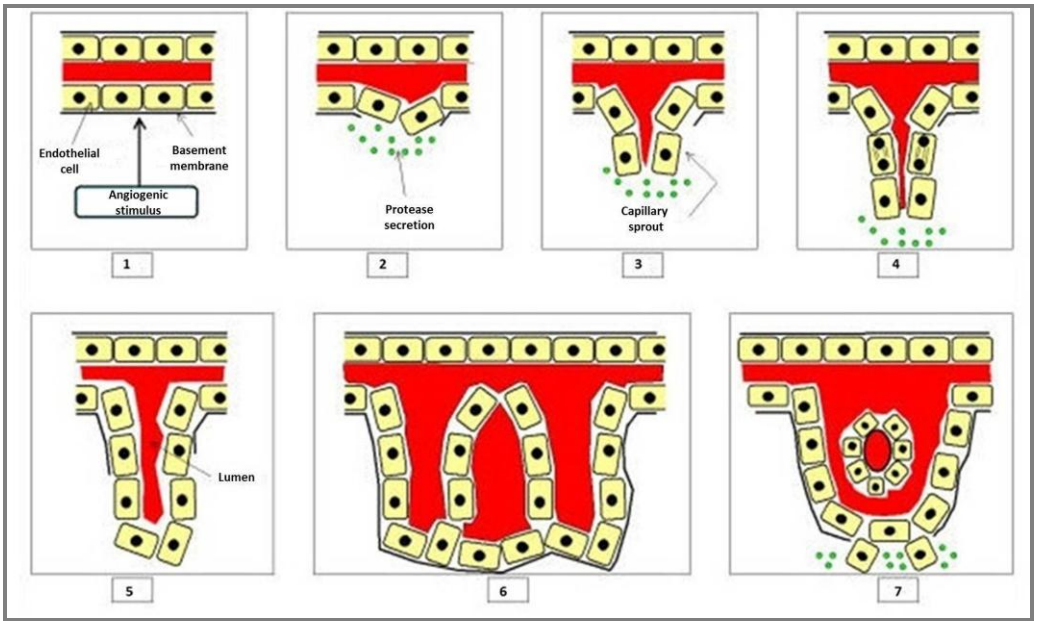

Fig. 1 Angiogenesis is a complex dynamic process. At least seven critical steps have so far been identified to occur during this tightly regulated process (Grizzi F. *et al.*, 2005).

It is well recognized that among the multiple angiogenic factors, vascular endothelial growth factors (VEGFs) are essential for the initiation and overall, for the regulation of vascular growth and patterning (Ferrara N.*et al.*, 2003). VEGFs encompass a family of structurally related proteins that include placental-derived growth factor (PDGF), VEGF-A, VEGF-B, VEGF-C, VEGF-D, and VEGF-E. Human VEGF-A monomers exist as five different isoforms, of which $VEGF_{165}$ is the most abundant and active form and is generally referred to as VEGF. VEGF plays major roles in regulating the functions of ECs. It is a potent angiogenic agent that regulates all the key steps of the angiogenic process, including EC proliferation and migration (Zachary A. *et al.*, 2005). Following activation by hypoxia, reactive oxygen species (ROS), and angiotensin II, VEGF is produced by several types of cells like ECs, vascular smooth muscle cells and also cancer cells, and it modulates EC functions via auto and paracrine pathways (Chua C.C.*et al.*, 1998). Notably, the responses of ECs to VEGF are regulated by the nature, frequency, and distribution of other receptors and interacting molecules. VEGF exerts its effects after binding to homologous membrane tyrosine kinase receptors, VEGFR-1 (Flt-1), VEGFR-2 (Flk1/KDR), and VEGFR-3 (Flt4), that are expressed mainly by blood vessel ECs and lymphatic ECs (Olsson A.K. *et al*., 2006). Although they have different biological activities, VEGFRs all play essential roles in VEGF induced angiogenesis because knockout mice for VEGFR-1, VEGFR-2, and VEGFR-3 are all embryonic lethal as a result of vascular defects (Goishi K. *et al.*, 2004). Intriguingly, the affinity of VEGFR-1 for VEGF is much higher than that of VEGFR-2, but the signaling induced by the latter is the major way by which VEGF regulates EC migration (Waltenberger J. *et al.*, 1994). Like other tyrosine kinase receptors, VEGFR-2 undergoes ligand induced dimerization and oligomerization, which activates its intrinsic tyrosine kinase activity resulting into phosphorylation on specific tyrosine residues in the cytoplasmic domain **(Fig.2)**.

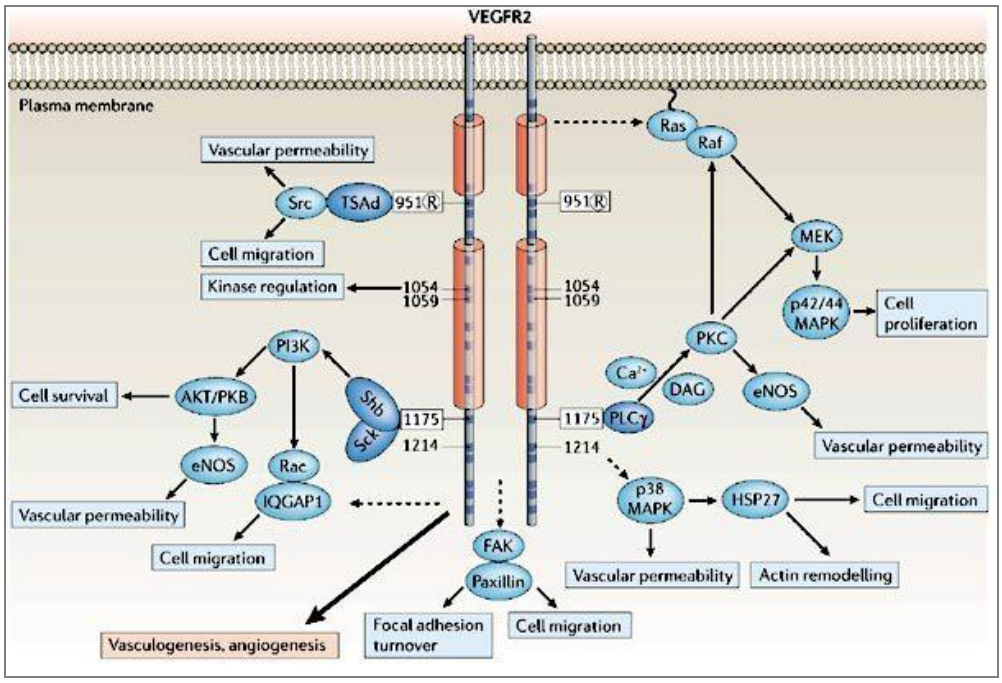

Fig. 2 VEGFR2 phosphorylation sites and signal transduction. Schematic representation of the intracellular domains of dimerized and activated VEGFR2; the different tyrosine-phosphorylation sites that are indicated by the amino acid residue's numbers. The position of the tyrosine residues within the receptor are indicated by dark blue squares. The signaling molecules (dark blue ovals) binding to specific phosphorylation sites (boxed numbers) initiate signaling cascades (light blue ovals), which leads to the establishment of specific biological responses (pale blue boxes). Dashed arrows indicate that the signal initiation is not certain. The biological responses are highlighted by pink boxes. DAG, diacylglycerol; EC, endothelial cell; eNOS, endothelial nitric oxide synthase; FAK, focaladhesion kinase; HPC, haematopoietic progenitor cell; HSP27, heat-shock protein-27; MAPK, mitogen-activated proteinkinase; MEK, MAPK and ERK kinase; PI3K, phosphatidylinositol 3' kinase; PKC, protein kinase C; PLCγ, phospholipase C-γ; Shb, SH2 and β-cells; TSAd, T-cell-specific adaptor (Olsson A.K. *et al*., 2006).

Once phosphorylated the tyrosine residues function as docking sites recruiting molecules carrying SH2 or PTB domains, conveying migratory signals to downstream pathways (Olsson A.K. *et al*., 2006). Y1175 and Y1214 are the two major phosphorylation sites on VEGFR-2 (Takahashi T. *et al.*, 2001; Lamalice L. *et al.*, 2004). Other putatively important phosphorylated sites include Y951 in the kinase insert domain and Y1054 and Y1059 in the tyrosine kinase catalytic domain (Olsson A.K. *et al*., 2006).

1.1 TUMOR ANGIOGENESIS

Angiogenesis is a highly ordered process which not only occurs in physiological conditions but also in a broad range of human diseases. Aberrant angiogenesis is associated with an excess of growth-promoting signals and a lack of sufficient cues to spatially and temporally coordinate vessel growth, remodelling, maturation and stabilization. During pathological conditions such as the growth of a tumor, the angiogenic cascade is persistent and unresolved, fuelled in part by tumor-secreted factors and tumor hypoxia (Chung A.S. *et al.*, 2010).

Tumors begin as an avascular mass of host-derived cells that proliferate, lacking the ability to control their growth (Papetti M. *et al.,* 2002). An avascular tumor is reliant on passive diffusion for the supply of the required oxygen and nutrients and the removal of its waste products. This imposes a limiting size of approximately 2mm to which it can grow (Folkman J., 1971); once it has reached this size, the tumor is described as dormant. Hypoxic tumor cells are known to produce growth factors, including VEGF (Shweiki D. *et al*., 1992); they also produce some endogenous inhibitors of angiogenesis, such as transforming growth factor-beta (TGF-β) (Bikfalvi A., 1995). Moreover, macrophages, which congregate in the region of the abnormal growth, respond to the presence of the tumor and its secretions by producing both pro and anti-angiogenic substances (Bingle L. *et al.*, 2002). These molecules diffuse through the tissue and are detected by the ECs of proximal capillaries. Initially, the inhibitors outweigh the growth factors and the ECs remain quiescent. However, if the tumor is able to produce enough growth factors and/or suppress the expression of inhibitors, it may succeed in flipping the 'angiogenic switch' and promote the growth of new vessels (Hanahan D. *et al*., 1996). ECs from capillaries adjacent to the tumor become activated: they loosen the tight contacts with neighbouring cells (Papetti M.*et al.*, 2002) and secrete proteolytic enzymes or proteases. The first target of the ECs-secreted proteases is the BM to allow their movement through the induced gaps into the ECM. Neighbouring ECs move in to fill the gap and subsequently follow the leading cells into the ECM (Pepper M. S., 2001). Following extravasation, the ECs continue to secrete proteolytic enzymes, which also degrade the ECM. This is necessary to create a pathway along which the cells can move and also allows the release of growth factors, such as VEGF, that are normally sequestered by the matrix, thus augmenting the angiogenic signals (Hirschi K. K. *et al*., 1996). ECs continue to move away from the parent vessel and towards the tumor, thus forming small sprouts which elongate through the recruitment of additional ECs from the parent vessel. These sprouts may initially take the form of solid strands of

cells, but the ECs subsequently form a central lumen, thereby creating the necessary structure for a new blood vessel (Pepper M.S., 2001) **(Fig. 3)**.

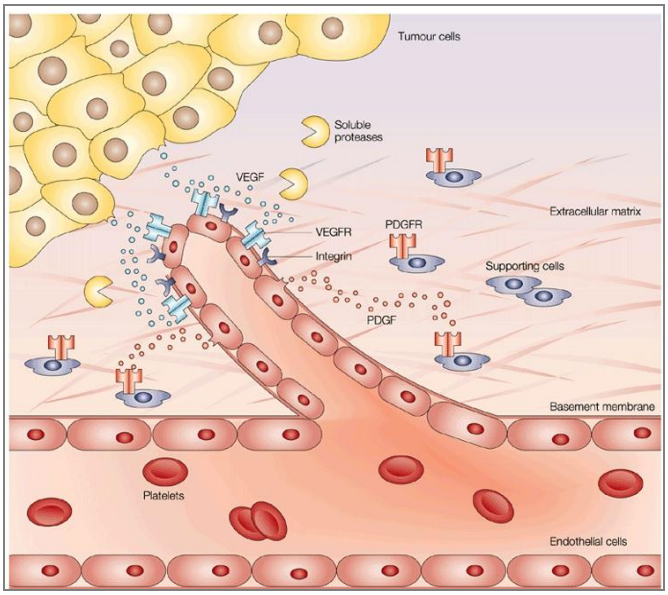

Fig. 3 The key steps underlying during tumor angiogenesis. Schematic representation of the different processes occurring during the formation or tumor-stimulated blood vessels. Tumour cells release pro-angiogenic factors, such VEGF, which diffuse into nearby tissues and bind to receptors on the ECs of pre-existing blood vessels, leading to their activation. Such interactions between ECs tumour cells lead to the secretion and activation of various proteolytic enzymes, such as matrix metalloproteinases (MMPs), which degrade the BM and the ECM. Degradation allows activated ECs, which are stimulated to proliferate by growth factors and to migrate towards the tumour. Integrin molecules, such as $\alpha_v\beta_3$-integrin, help to pull the new sprouting blood vessel forward. The ECs deposit a new BM and secrete growth factors, such as platelet-derived growth factor (PDGF), which attract supporting cells to stabilize the new vessel. PDGFR, PDGF receptor; VEGFR, VEGF receptor (Cristofanilli M. *et al*., 2002).

Although tumors possess the means to recruit and develop a new and ongoing blood vessel supply, this is not to suggest that such blood vessels are normal in either structure or function. Indeed, in solid tumors the vasculature is characterized by a number of prominent abnormalities **(Fig. 4)**. These abnormalities have been hypothesized to have a significant impact on tumor growth, progression and response to various anticancer therapies. Among the structural and morphologic abnormalities are the presence of excessively dilated blood vessels, vessels with areas containing absent or abnormal BM, vessels having extreme corkscrew-like tortuosities, a relative lack of supporting perivascular cellular elements such as pericytes, or abnormalities in the

pericyte population and excessive vascular leakiness (Carmeliet P. *et al.*, 1996). These aberrations can be quite variable within a solid tumor mass and such heterogeneity can also extend to the relative density of blood vessels, which can be quite high in certain areas and low in others (Cooney M. M. *et al*., 2006).

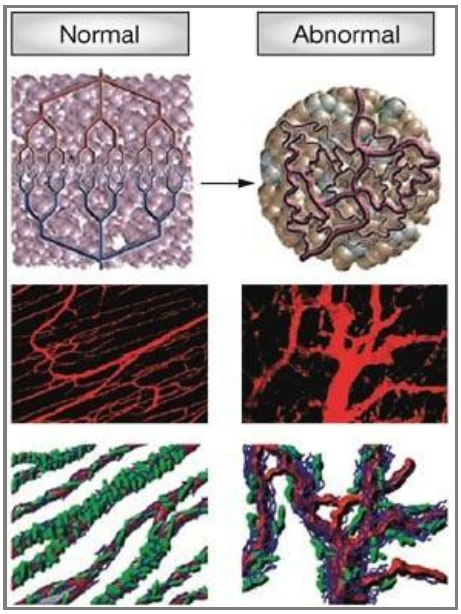

Fig. 4 Features of tumor blood vessels. Unlike healthy blood vessels, tumor vessels consist of disorganized, leaky and primitive vascular networks, which display abnormal functions (Cooney M. M. *et al*., 2006).

As a result of all of these features, blood flow and perfusion within tumors can be highly heterogeneous and often sluggish, with some areas therefore being deprived of oxygen and nutrients, leading to adjacent areas of elevated hypoxia. This may account for slow growth of tumors in some regions and more rapid growth in others. In addition the marked leakiness/hyperpermeability of the tumor vasculature can lead to enhanced extravasation of high molecular weight plasma proteins and fluid into the extracellular microenvironment within tumors. It has been hypothesized that this can limit or retard the diffusion of certain drugs, especially monoclonalAbs or vectors used for gene therapy, as well as immune effector cells from the blood through the interstitium of the tumors. Thus tumor blood vessels, while necessary for progressive tumor growth and metastasis, may also limit the efficacy of anticancer drugs and treatments, including chemotherapy and radiation therapy (De Vita V. *et al*., 2007).

1.1.1 VEGF/VEGFR2 SIGNALING IN TUMOR ANGIOGENESIS

Like the normal angiogenic process, tumor angiogenesis is reliant on VEGF and other angiogenic proteins. Increased levels of VEGF and its receptor VEGFR-2 have been observed in many cancers, including metastatic human colon carcinomas, where increased levels were shown to directly increase tumor vascularization (Takahashi Y. *et al.*, 1995). Breast cancer patients with higher levels of VEGF expression have increased intratumoral vascularization and a worse prognosis (Toi M. *et al.*, 1996). Experiments with monoclonal Abs against VEGF, or genetic inactivation of VEGF (or VEGFR-2), lead to dramatic decreases in angiogenesis and neovascularization in several different forms of cancer (Ferrara N. *et al*., 1996). In addition to the endovascular stimulation attributed to VEGF, it can also increase vascular permeability (Kevil C.G *et al*., 1998), explaining the leaky blood vessels observed in tumors. Indeed, due to its pleiotropic effects in tumor angiogenesis, inactivation of VEGF/VEGFR2 signaling has been extensively attempted as a therapeutic approach. At present, inhibitors of the VEGF pathway are the most clinically advanced, and bevacizumab, a humanized variant of a murine anti-VEGF-A monoclonal antibody that was used in early proof-of-concept studies, is an FDA-approved antiangiogenic treatment for cancer therapy (Ferrara N. *et al*, 2005). Several strategies to inhibit VEGF/VEGFR2 signaling are being generated **(Fig. 5)**. These include monoclonal antibodies targeting VEGF-A **(a)** or the VEGF receptor **(b)** and chimeric soluble receptors such as the 'VEGF-trap' (domain 3 of VEGFR-2 fused to a Fc fragment of an antibody) **(c)**. Additional extracellular inhibitors are aptamers that bind the heparin-binding domain of $VEGF_{165}$ (pegaptanib) **(d)**. A variety of small-molecule VEGFRTK inhibitors that inhibit ligand-dependent receptor autophosphorylation of VEGFR-2 are being tested **(e)**. Additional strategies to inhibit VEGF signaling include antisense and siRNA targeting VEGF-A or its receptors.

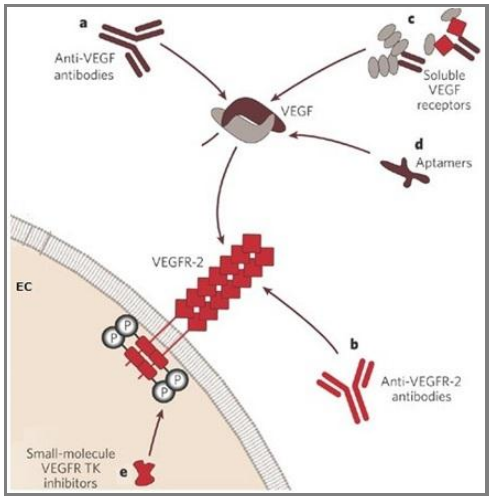

Fig. 5 Schematic representation of the different methods employed for the VEGF /VEGFR2 pathway inhibition. (Ferrara N. *et al.,* 2005).

2. THE EXTRACELLULAR MATRIX

The cells of the microenviroment are embedded in a supporting network of ECM constituents that include collagens, elastin, proteoglycans and various glycoproteins. The importance of the ECM relies on the fact that it does not constitute a mere structural scaffold but it also elicits profound influences on cell behavior, affecting cell growth, differentiation, motility and viability (Bissell M.J. *et al.*, 2005). These effects are further magnified by the intrinsic property of the ECM molecules to function as reservoirs of growth factors, cytokines, matrix metalloproteinases and processing enzymes (Sternlicht M.D.*et al.*, 2001). The relative availability of these elements increases once the ECM rearranges during wound healing or tumor progression.

Several studies taking into account the role of components of the microenvironment indeed established that the ECM plays an important role in tumor vascularization (Wernert N.*,* 1997). Cancer cells per se accumulate over time numerous mutations thus acquiring the ability to be self-sufficient in growth signaling, insensitive to antigrowth signals, unresponsive to apoptotic events and capable of limitless replication (Hanahan D., 2000). Although all of these neoplastic properties are necessary for tumor development, they are not sufficient to give rise to clinically relevant cancers unless the tumor is able to recruit its own blood supply. During the different stages of tumor angiogenesis, temporal and spatial regulation of ECM remodeling events allows for local changes in net matrix deposition or degradation, which in turn contributes to the control of EC growth, migration and differentiation. In this context discovering the roles played by novel ECM proteins in vascularization is a crucial step in the process of creating new treatments for pathological angiogenesis.

2.1 ROLE OF ECM MOLECULES IN ANGIOGENESIS

The ECM is composed of a network of glycosaminoglycans (GAGs) and of fibrous proteins.

GAGs are carbohydrate polymers that form proteoglycans and are involved in both keeping the ECM and surrounding cells hydrated and trapping and storing growth factors. Therefore, GAG molecules may employ a variety of regulatory effects on the accessibility of angiogenic factors (Rouet V. *et al.,* 2005) including their degradation through the activation of proteolytic enzymes and the consequent release of growth factors such as VEGF. Heparan sulfate glycosaminoglycans (HSGAGs) are a diverse family of GAGs that include the syndecans, glypicans, perlecan and agrins. Members of this group of proteins play a key role in the modulation of angiogenesis. EC-bound HSGAGs have the ability to either inhibit or promote neovascularization by mediating signaling through VEGF receptors (Iozzo R.V. *et al.,* 2001) or bFGF (Walker A. *et al.,* 1994).

Major ECM fibrous proteins that promote angiogenesis include collagen, laminin and fibronectin. Collagen IV and laminin are the predominant proteins of the basal lamina that provide structural support for ECs and separate them from the adjacent perivascular cells. The majority of ECM proteins mediate angiogenesis through arginine-glycine-aspartic acid (RGD) motifs which bind to integrins that mediate outside-in and inside-out signaling. Induction of angiogenesis and remodelling of the ECM is characterized by increased permeability and cytoskeletal and cell-to-cell contact changes, which results in newly formed focal contacts mediated primarily by integrins. Fibronectin is produced by both activated endothelial and smooth muscle cells; levels of fibronectin are augmented during angiogenesis by the delivery of fibronectin from the circulation due to the increased vascular permeability. Fibronectin is one of the ECM molecules containing the RGD motif that binds to integrin $\alpha_5\beta_1$, an integrin receptor markedly up-regulated during angiogenesis. The collagen integrin receptors $\alpha_1\beta_1$ and $\alpha_2\beta_1$ also play a positive role during angiogenesis. Furthermore, α_1 chain-derived laminin peptides were demonstrated to mediate angiogenesis *in vitro* (Malinda K.M. *et al.,* 1999).

Interestingly the matrix remodeling occurring during angiogenesis, besides offering a path for ECs to move through and inducing the release of growth factors, produces an additional effect which further increases the complex regulations of this phenomenon. In fact, matrix degradation prompts the release of ECM cryptic sites that may have different properties on angiogenesis respect to the entire molecules. Indeed, the cleavage of collagen XVIII and the α_1, α_2 and α_3 chains

of collagen IV release the angiogenic inhibitors endostatin, arrestin, canstatin and tumstatin, respectively (Kalluri R., 2003).

Another group of ECM proteins which have been recently demonstrated to play an important role in angiogenesis are a disintegrin and metalloproteinases (ADAMs) and a disintegrin and metalloproteinase with thrombospondin motifs (ADAMTs). Besides the presence of thrombospondin (TSP) motifs on these proteases, while the ADAMs are associated with the membrane, the ADAMTs are secreted proteins (Dunn J.R. *et al.*, 2006). These molecules belong to a family related to MMPs and many of them have been found to regulate angiogenesis directly or through expression of MMPs. ADAM-17 has been reported to play a key role in angiogenesis: the inhibition of ADAM-17 not only alters the EC's morphology but it also decreased their proliferation leaving apoptosis unchanged. ADAMTS1 and ADAMTS8 instead contain the thrombospondin anti-angiogenic domain (TSR1). Both these proteins inhibit EC proliferation and suppress growth factor induced vascularization (Vázquez F. *et al.,* 1999).

2.1.1 THE ECM MOLECULES IN TUMOR ANGIOGENESIS

Many ECM proteins surrounding the vasculature have pro-angiogenic properties capable of promoting EC survival, proliferation, migration, and tube formation (Sottile J., 2004). Indeed ECM display intrinsic properties that affect angiogenesis; the most studied molecules in this context are listed below:

- Fibronectin is a fairly ubiquitous and abundant ECM protein that becomes assembled into fibrils at the cell surface. Fibronectin is necessary for vasculogenesis, as the fibronectin-null mice die before birth due to defects of the mesoderm, neural tube, and vascular bed (Linask KK. *et al*., 1988). An alternatively-spliced form of fibronectin that contains an extra B domain has been found in fetal and neoplastic tissues but not in normal adult tissues. In situ hybridization analyses performed on malignant astrocytoma samples have revealed that this isoform is synthesized by vascular cells (Castellani P. *et al.,* 2002) and its expression appears to be a precise diagnostic marker of the highest grade of glioma or glioblastoma. These findings are consistent with those obtained using other types of tumors in which this isoform has been shown to be a marker of angiogenesis (Santimaria M. *et al.*, 2003).

- Osteopontin is expressed by several stromal cells and also by ECs; it contains an RGD sequence that promotes cell attachment and migration through the interaction with multiple integrins. Osteopontin overexpression has been correlated with increased angiogenesis and *in vivo* tumor growth (Hirama M. *et al.,* 2003). The pro-angiogenic function of osteopontin, at least in part, can be attributed to its ability to promote VEGF-directed dermal microvascular EC migration (Senger DR. *et al.,* 1996) and to increase MMP-2 levels in an RGD-dependent manner (Teti A. *et al.,* 1998). Additionally, osteopontin-bound integrin $\alpha_v\beta_3$ inhibits the NF-κB dependent EC apoptosis (Cooper CR. *et al.,* 2002).

- Tenascin-C is a glycoprotein composed of six subunits covalently associated at their amino-terminus by disulfide bonds. Different human tenascin-C isoforms are generated by alternative splicing of one transcript which is aberrantly regulated in neoplastic tissues (Jones P.L. *et al.,* 2000). It is expressed around angiogenic vessels in many tumors and there is evidence that it promotes and regulates angiogenesis *in vitro* and *in vivo*. For instance the treatment of glioma patients with Abs directed against Tenascin-C induced a significant inhibition of tumor angiogenesis.

- Heparan sulphate proteoglycans (HSPGs) are necessary for stable binding of the proangiogenic growth factor bFGF to its receptor (Ornitz D.M. *et al.,* 1992). HSPGs consist of a core protein with attached heparan sulphate (HS) glycosamminoglycan side chains. Alterations in HS glycosamminoglycan in breast carcinoma have been shown to result in an increase in bFGF binding and receptor complex assembly.

- Perlecanis a HSPG deposited along blood vessels BM and it is thought to mediate structural interactions between collagen type IV and laminin networks through its interaction with entactin/nidogen (Iozzo R.V., 2005; Mongiat M. *et al.,* 2003). Intact perlecan is thought to be a proangiogenic HSPG as its expression is altered during embryonic vasculogenesis and in neoplasia (Zhou Z. *et al.,* 2004); perlecan-null mice show severe and sometimes fatal vascular and chondrogenic defects (Costell M. *et al*., 1999); antisense targeting of perlecan blocks tumor growth and angiogenesis *in vivo* (Sharma B. *et al.,* 1998); increased perlecan expression stimulates angiogenesis (Jiang X. *et al.,* 2003). Tumor cell-secreted perlecan

promotes EC sprouting and proliferation, thereby promoting angiogenesis (Jiang X. *et al.,* 2004). This property may also depend on the characteristic of perlecan to organize and structurally support the newly deposited ECM of angiogenic vessels. Interestingly a degradation product of perlecan, called endorepellin, exerts an opposite effect (Mongiat M. *et al.,* 2003).

- Transmembrane chondroitin sulphate proteoglycan NG2 is another protein involved in tumor angiogenesis. This molecule has been shown to promote EC spreading and migration as well as proliferation of microvascular ECs in response to PDGF stimulation (Ozerdem U. *et al.,* 2003). An additional proangiogenic mechanism by which NG2 promotes angiogenesis includes its ability to bind and sequester angiostatin, thus blocking its antiangiogenic function (Chekenya M. *et al.,* 2002).

On the contrary, several ECM molecules have been reported to counteract the sprouting of new blood vessels:

- Thrombospondin-1 (TSP-1) and thrombospondin-2 (TSP-2) have been shown to be potent inhibitors of angiogenesis (Teng-nan L.T.N.*et al*., 2003). Accordingly, their expression in tumor tissues is often inversely correlated with angiogenesis (Adams J.C. *et al*., 2004; Armstrong L.C. *et al.,* 2003). The mechanisms by which they can inhibit angiogenesis include the induction of EC apoptosis by the binding of TSP-1, and potentially TSP-2, to CD36 on microvessel ECs, thereby inducing Fas ligand (FasL) expression (Nor J.E. *et al.*, 2000; Jimenez B. *et al.,* 2000); the clearance of MMP-2 through the association of TSP-2 with MMP-2, the internalization of this complex and its lysosomal degradation (Armstrong L.C. *et al.*, 2002; Rodriguez-Manzaneque JC. *et al.,* 2001); the inhibition of EC proliferation (Armstrong LC. *et al.*, 2002).

- Angiostatin, the cleavage product of plasminogen, is another well-known anti-angiogenic molecule, the only not-ECM protein among the molecules described above. Angiostatin inhibits EC proliferation and motility and down-regulates the levels of cyclin-dependent kinase 5 (cdk5), a cdk absent in quiescent ECs whose expression is induced following bFGF

treatment (Sharma M.R. *et al*., 2004). Angiostatin also acts by upregulating the mRNA levels of FasL and reducing the level of c-Flip which activates the extrinsic apoptotic pathway.

As mentioned above cryptic fragments originated from ECM degradation represent an important contribution to the anti-angiogenic molecules; below the most known active fragments are listed:

- Endostatin is a specific and potent anti-angiogenic factor generated from the proteolytic cleavage of collagen XVIII by matrix metalloproteinases, elastases or cathepsins (Kim H.S. *et al*., 2009). Endostatin is strong angiogenic inhibitor impairing EC proliferation and migration. It halts EC division blocking the cells in the G1 phase of the cell cycle and the treatment of EC with this molecule induces a cell-specific apoptotic death (Dhanabal M. *et al.*, 1999). These properties have provided clues for the development of an anti-tumor strategy with proven therapeutic effectiveness in numerous models of neoplasia (Folkam J. *et al*., 2006).

- Vastatin derived from the NC1 domain of the α_1 chain of collagen VIII. Endostatin and vastatin display similar potency in inhibiting EC proliferation, although the two molecules share only about 12% sequence homology (Xu R. *et a*l., 2001).

- Restin is a fragment of the α_1 chain of collagen XV. Restin inhibits EC migration and angiogenesis, though it differs from endostatin in its ability to inhibit angiogenesis induced by VEGF or FGF-2, in its affinity for binding partners in the ECM, and localization (Sasaki T.*et al*., 2002).

- Tumstatin is a 28-kDa fragment derived from the C-terminal NC1 domain of the α_3 chain of type IV collagen. Tumstatin is anti-proliferative and pro-apoptotic for ECs, but also exerts an immunomodulating effect and anti-proliferative activity on tumor cells. These activities are mostly mediated by $\alpha_v\beta_3$ and $\alpha_5\beta_1$ integrins (Sudhakar A. *et al*,2008). This fragment binds $\alpha_v\beta_3$ integrin, resulting in the inhibition of FAK activation; it inhibits CAP-dependent protein translation via phosphatidylinositol-3 kinase (PI3K)/Akt/mTOR and 4E-BP1, causing in EC apoptosis (Sudhakar A. *et al*, 2003).

- Arrestin is a 26-kDa fragment from the NC1 domain of the α_1 chain of type IV collagen. It inhibits EC proliferation and migration through mechanisms involving cell surface proteoglycans and $\alpha_1\beta_1$integrin on ECs (Mundel T.M. *et al*., 2008).

- Endorepellin derives from the C-terminal module of perlecan, a ubiquitous basement membrane heparan sulfate proteoglycan (Mongiat M. *et al*., 2003). It has high homology with the G-domain of the long arm of laminin-1. Endorepellin binds to several extracellular matrix proteins, growth factors, and receptors (Bix G. *et al.*, 2005). It affects EC functions relevant to angiogenesis by interacting with the $\alpha_2\beta_1$ integrin as well as VEGFR1 and VEGFR2, leading to transcriptional repression of VEGF production (Goyal A. *et al*., 2011).

- Pigment epithelial-derived factor (PEDF) was initially identified as an anti-angiogenic protein whose expression associates with a decreased microvessel density and suppression of tumor growth in a number of tumors, including glioma as well as prostate carcinoma and melanoma (Abe R. *et al.,* 2004). Accordingly, an increased microvessel density is found in tissues from PEDF deficient mice (Doll J.A. *et al.*, 2003), while it blocks the growth factor-promoted neovascularization in rat cornea angiogenesis assays. The mechanism whereby PEDF acts to inhibit angiogenesis is probably associated, at least in part, with its ability to bind collagen and to potentially interfere with the interaction of collagen with the cell (Meyer C. *et al.*, 2002). Additional mechanisms likely include the induction of the expression of Fas on the EC surface and the down-regulation of VEGF mRNA levels (Takenaka K. *et al*., 2005).

3. THE EMILIN/MULTIMERIN PROTEIN FAMILY

EMILINs are a family of ECM glycoproteins whose distinguishing feature is the presence of a cysteine-rich EMI domain at the N-terminus; in addition most of the members of this family also display a gC1q-like domain at the C-terminus (Doliana R. *et al*., 2000; Mongiat M. *et al.,* 2000). These glycoproteins can be clustered into three main groups on the basis of the arrangement of the major protein domains (Braghetta P. *et al.,* 2004).

The first is characterized by the presence of the EMI domain at the N-terminus followed by a coiled-coil region and by a gC1q domain at the C-terminus, and it includes EMILIN1 (Doliana R. *et al.,* 2000), EMILIN2 (Doliana R. *et al.,* 2001), MULTIMERIN1 (Hayward C.P. *et al.,* 1991) and MULTIMERIN2 (Christian S. *et al.,*2001) **(Fig. 6)**.

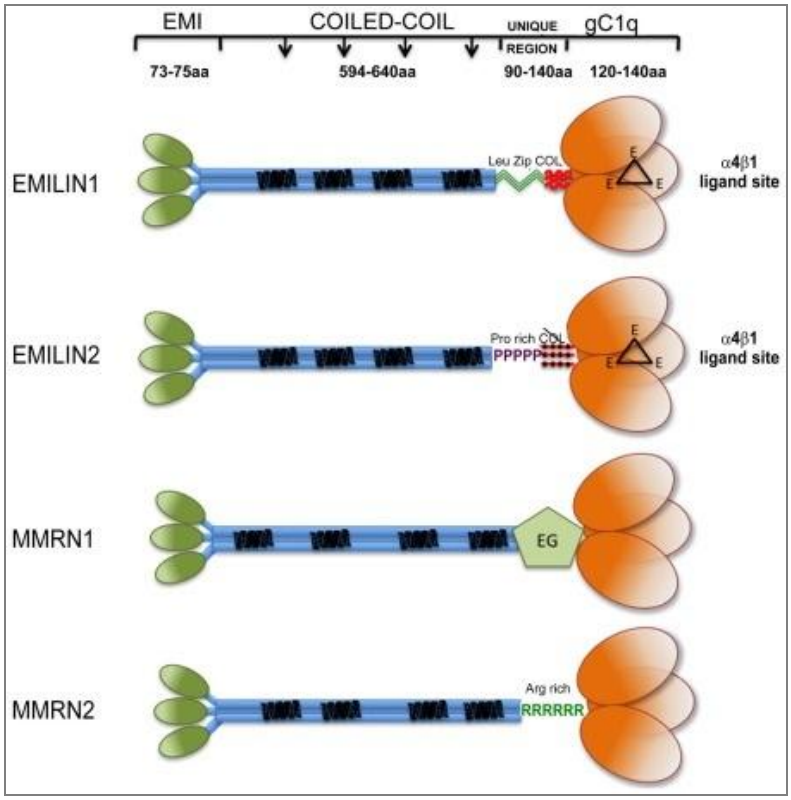

Fig. 6 Schematic representation of the first group of EMILIN/MULTIMERIN family members. (EMI) EMI domain; Coiled-coil region; (C1q) gC1q-like domain; (PR) prolin-rich domain; (RR) arginine-rich domain; (EG) region with partial similarity with EGF domain (Colombatti A. *et al.*, 2011).

The second group comprises only one gene named EMILIN3 displaying a structure similar to the first group except for the lack of the gC1q domain (Leimeister C. *et al.,* 2002); EMILIN3 presents a different pattern expression from other EMILIN/Multimerin proteins and is able to function as an extracellular regulator of the activity of TGF-β ligands (Schiavinato A*. et al*., 2012).

The third cluster includes two genes, Emu1 and Emu2, which share only the presence of EMI domain at N-terminus with the previous group but, since most of the sequence is collagenous, display a completely different structure compared to the other members (Leimeister C. *et al.,* 2002).

3.1 EMILIN1

EMILIN1 is the archetype molecule of the family and it was originally identified during the attempts to isolate elastic tissue-specific glycoproteins. These efforts led to the isolation of a 115 kDa glycoprotein from the heterogeneous fraction of newborn chick aorta extracts. The glycoprotein was next demonstrated to specifically localize at the interface between the amorphous elastin surface and microfibrilshence the acronym (Elastin Microfibril Interface Located proteIN) (Bressan G. *et al.,* 1993). EMILIN1 is highly expressed at the level of large blood vessel wall and in the connective tissue of a wide array of organs (Colombatti A. *et al.,* 1985). During mouse development, EMILIN1 mRNA is expressed along the blood vessels, perineural mesenchyme and somites at 8.5 days (Braghetta P. *et al.,* 2002). Intense labeling is identified in the mesenchymal component of many organs including lung and liver and in different mesenchymal condensations such as limb bud and branchial arches. At late gestation times staining is widely distributed in the interstitial connective tissue and in smooth muscle cell-rich tissues. After birth, the EMILIN1 mRNA expression levels decline with the age increase. EMILIN1 was demonstrated to be involved in multiple functions. As an ECM component EMILIN1 has adhesive and migratory properties for different cell types. It is a ligand for the $\alpha_4\beta_1$ integrin and the interaction occurs through the gC1q1 domain (Spessotto P. *et al.,*2003). EMILIN1-deficient animals display an hypertensive phenotype likely due to a decreased diameter of the arteries which is significantly narrower in EMILIN1-null mice compared to the wild type mice. The molecular mechanism underlying this outcome relies on the binding of EMILIN1 to the immature form of the pro-TGF-β via the EMI domain, thus preventing TGF-β maturation by furin-convertases

(Raman M. *et al*., 2006). EMILIN1 is also highly expressed along the lymphatic vessels and it was demonstrated to be an important constituent regulating the structure and function of lymphatic vessels, as well as lymphangiogenesis (Danussi C. *et al*., 2008). In fact EMILIN1 deficiency results in hyperplasia and enlargement of the superficial and visceral lymphatic vessels which often display an irregular pattern. EMILIN1 deficiency also lead to a significant reduction of anchoring filaments, and this correlates with the functional defects observed, such as mild lymphedema, an enhanced lymph leakage and a highly significant decrease of lymph drainage. EMILIN1-deficient mice also develop larger lymphangiomas if compared to wild type mice (Danussi C. *et al.,* 2008). EMILIN1 deficiency causes skin and lymphatic vessel hyperplasia and structural anomalies in lymphatic vasculature. An EMILIN1-negative microenvironment promotes tumor cell proliferation as well as dissemination to lymph nodes (Danussi C. *et.al*., 2012).

3.2 EMILIN2

EMILIN2 was identified following a yeast two-hybrid screen, using the gC1q1 domain of EMILIN1 as bait (Doliana R. *et al.,* 2001). The protein is secreted extracellularly and was demonstrated to be deposited in the ECM with a meshwork pattern. In the mouse embryos EMILIN2 mRNA expression is more restricted compared with that of EMILIN1; early expression includes somites, neural tube and mesenchyme of branchial arches, limb buds, intervertebral disks and perineural tissue. Weak staining is also found in mesenchymal cells of most organs, including lung, liver, intestine and bladder at the beginning of organogenesis. The strongest EMILIN2 expression was detected in the heart, starting at E8.5 and reaching the highest levels at E11.5. The labeling was restricted to the myocardium, while the endocardium was negative. Unlike other members of the family, staining for EMILIN2 was found in the central nervous system. In the adult tissues, EMILIN2 mRNA amplification was most evident in spleen and uterus and weak in kidney and gut (Braghetta P. *et al*., 2004). Moreover, EMILIN2 was found to be one of the major basilar membrane components in the cochlea (Amma L.L. *et al*., 2003). At the fanctional level, EMILIN2 was found to significantly impair tumor growth inducing tumor cell apoptotic death. EMILIN2 was demonstrated to adopt a totally different mechanism from other ECM proteins that promote cell death; in fact it bears the unique property to directly interact with and activate death receptors, in particular DR4. The activation of the extrinsic apoptotic pathway leads to a dramatic decrease of tumor cell viability

and to anti-tumorigenic properties as demonstrated by *in vitro* and *in vivo* studies (Mongiat M. *et al.,* 2007). EMILIN2 stimulated blood vessel development and displayed a pro-angiogenic effect (Mongiat M. et al., 2010) in particular, blocking with specific antibody or silencing, EMILIN2 expression reduced EC proliferation (Bronisz A. *et al.*, 2012). EMILIN2 represents a negative regulator of tumor development: the gene is frequently methylated in breast, lung and colorectal tumors and this suppression correlates with poorer clinical outcome and increased lymph node metastasis in breast cancer patients (Hill V.K. *et al*., 2010).

3.3 MULTIMERIN1

MULTIMERIN1 (MMRN1) is a soluble S–S linked homopolymer stored in platelets, megakaryocytes, and ECs and deposited in ECM (Hayward C.P., 1997; Adam F. *et al*., 2005). It supports the adhesion of platelets, neutrophils, and ECs via integrin $\alpha_v\beta_3$ and $\alpha_{IIb}\beta_3$ (Adam F. *et al.*, 2005). It binds to collagen and it is able to enhance von Willebrand factor-dependent platelet adhesion to collagen thus supporting thrombus formation. MMRN1 has a high affinity for factor V (Jeimi S.B. *et al*., 2008) and this facilitates the co-storage in platelet α-granules. When MMRN1 is released from platelets during platelet activation, it regulates thrombin formation limiting thrombus formation. This protein is playing an important homeostatic control in platelets aggregation and its consequences. Unfortunately, all these multiple functions have not been assigned to any of the domains of MMRN1 apart from cell adhesion that depends on an RGD sequence at the N-terminus (Adam F. *et al*., 2005).

3.4 MULTIMERIN2

MULTIMERIN2 (MMRN2) also known as EndoGlyx-1, was identified during a screening for new antigenic markers of the vascular endothelium, using a monoclonal antibody (mAb) H572 raised against the human umbilical vein EC (Sanz-Moncasi MP. *et al.,* 1994) **(Fig. 7).**

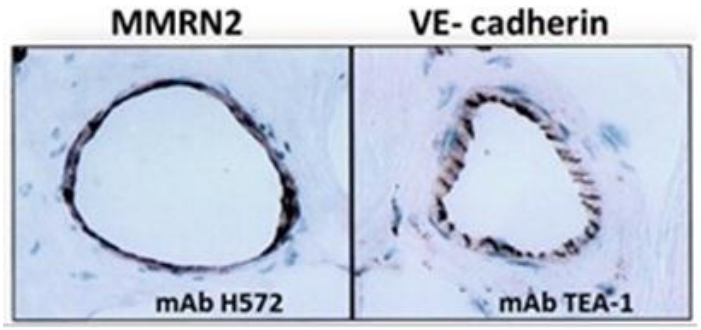

Fig.7 Immunohistochemical staining of MMRN2 on human blood vessels. Sections of normal breast tissue stained with the H572 mAb detecting MMRN2 or with TEA-1 mAb detecting VE-Cadherin (Christian S. *et al.,* 2001).

Unlike other members of the family, MMRN2 is characterized by a short cluster of charged amino acids (10 out of 27 residues) located between the coiled-coil region and the C1q-like domain. The basic amino acids are arranged in a sequence similar to that of the consensus motifs responsible for the ionic interactions with glucosaminoglycans, such as heparin and heparan sulfate (Hileman RE. *et al.*, 1998) and are also found in heparin binding proteins such as the von Willebrand factor (Sobel M. *et al.,* 1992). In an extensive immunohistochemical survey of normal human fetal and adult tissues as well as human cancer tissues, MMRN2 was found to be exclusively expressed at the blood vessel endothelium level. Notably, these include capillaries, veins, arterioles, and muscular arteries, but interestingly no immunoreactivity was observed in the sinusoidal endothelial cells of the spleen and liver. In neoplastic tissues MMRN2 was consistently found to be deposited along tumor capillaries and, in certain tumors, in the “hot spots” of neoangiogenesis (Sanz-Moncasi MP. *et al.,* 1994). The staining pattern revealed a uniform cell surface and cytoplasmic distribution of the antigen and, in some cases, an accentuated immunoreactivity at the abluminal side of the EC layer. Prior to this investigation, the function of this molecule has remained elusive. Given its specific deposition along the blood vessels we have hypothesized that it could play an important role in the regulation of EC homeostasis and in the angiogenetic processes and the results from these investigation are reported in this thesis.

MATERIALS AND METHODS

1. Cell Lines

The HT1080 cell line was obtained from ATCC and cultured in Dulbecco's modified Eagle medium (DMEM) containing 10% fetal bovine serum (FBS) (GIBCO BRL). HUVEC (Human Umbilical Vein Endothelial Cells) were isolated from the human umbilical cord vein. Cells were cultured in M199 medium (GIBCO) supplemented with 20% FBS, 1% Penicillin-Streptomycin, 50 mg/ml heparin (SIGMA) and bovine brain extract (0,5%). Cells were grown in flasks pre-coated with 1% porcine skin gelatin. 293-EBNA (Epstein-Barr Nuclear Antigen) cells were a gift from Rupert Timpl and cultured in DMEM, 10% FBS. All cells were maintained al 37°C in a humidified 5% CO_2 atmosphere.

2. Isolation of HUVEC cells

HUVEC were obtained from human umbilical cord veins according to Jaffe method (Jaffe EA. *et al.*, 1973). A sterile technique was utilized during all the required manipulations. Briefly, both ends of the cord were cut off and the vein was perfused with a Phosphate Buffer Saline (PBS) solution containing 50 mg/ml gentamycin and 250 ng/ml fungizone to wash out the blood. Then one end of the cord was tightly clamped and a 0,25% Collagenase A (Roche) solution pre-warmed at 37°C was injected in the vein to facilitate EC detachment. After 20 minutes of incubation at room temperature, the collagenase solution was flushed out from the cord and the vein was washed with M199 medium. The collected cells were then centrifuged for 10 min at 500g, resuspended in M199 complete medium and seeded onto gelatin-coated flasks.

3. Antibodies and other reagents

The anti-MMRN2 polyclonal antibody was obtained upon immunization of a rabbit with 150 mg of a recombinant MMRN2 fragment corresponding to the N-terminal gC1q domain preceded by the proline-rich domain. The antibody was affinity purified from the rabbit serum by means of the CNBr-activated Sepharose 4B resin (Amersham, GE-Healthcare, Milan, Italy). The anti-FLAG and anti-SMA antibodies, the FLAG peptide, and the anti-FLAG M2 affinity gel were from Sigma-Aldrich (Milan, Italy). The secondary horse radish peroxidase (hrp)-conjugated antibodies were from Amersham (GE-Healthcare, Milan, Italy). The secondary antibodies conjugated with Alexa Fluor 680 and 488 and TO-PRO-3 were from Invitrogen. The Ni-NTA agarose was from QIAGEN (Milan,

Italy). BD Adeno-X™ Rapid Titer Kit was from BD Biosciences (Milan, Italy). The AngioKit was from TCS CellWorks (Buckingham, UK). The anti-mouse anti-CD31 antibody and Matrigel were from BD Biosciences. Anti-VEGFR2 and anti phospho-VEGFR2 (Tyr1175) and (Tyr1214), anti-FAK and anti-phospho-FAK (Tyr576/577), anti-p38 and anti-phospho-p38, anti-β-actin antibodies were from Cell Signaling Technology Inc. (Danvers, MA, USA).The anti-VEGF-A antibody was from Sigma-Aldrich (Milan, Italy). Anti-VEGF-B and anti-PlGF were from Santa Cruz Biotechology Inc. (California, USA). The hypoxyprobe-1 was from HPI, Inc. (Burlington, MA, USA). The *in situ* Cell Death Detection Fluorescein Kit was purchased from Roche Diagnostics S.p.a. (Milan, Italy). The Gv39M antibody recognizing the VEGFR2-bound VEGF-A (Brekken et al., 1998) was a kind gift from Dr. R. Brekken (UT Southwestern Medical Center, Dallas, TX, USA).

4. Cell transfection, expression and purification of recombinant proteins

Human MMRN2 cDNA was retro-transcribed from total RNA extracted from HUVEC cells and cloned into pCEP-Pu vector containing the sequence of the BM40 signal peptide. The MMRN2 coding sequence has been divided into two parts; the first one, corresponding to N-terminal region, was cloned using the restriction enzymes *Pme I* and *Not I*, the second, corresponding to the C-terminal region of the molecule, using *Not I* and *Xho I*. The following oligonucleotides were used:

Forward: 5'-GGGTTTAAACGGACTACAAGGACGACGATGACAAGGCTGCTTCCAGTACTAGCCTC-3',containing the *Pme I* site and a FLAG sequence.

Reverse: 5'-GTGCAGCTGGCGCACCTCGT-3', containing the *Not I* site.

Forward: 5'-GACGAGGTGGGCGCGCTGAA-3', containing the *Not I* site.

Reverse: 5'-CGGGATCCATGGTGATGGTGATGATGGGTCTTAAACATCAGGAAGC-3', containing the *XhoI* site and an His-tag sequence.

For the generation of the MMRN2 deletion mutants, the MMRN2 coding sequence was divided in different fragments: Δ1 (aa residues 24 to 134), Δ2 (aa residues 135 to 949) and Δ3 (aa residues 369 to 949). The fragments were cloned into pCEP-Pu vector using the following oligonucleotides and restriction enzymes:

MMRN2 fragments	Oligo sequence	Restriction enzyme	Tag sequence
Δ1 Forward	5'-CTAGCTAGCCCATCATCACCATCACCATGCTTCCAGTACTAGCCTC-3'	Nhe	His
Δ1 Reverse	5'-ATAGTTTAGCGGCCGCTCAAAAGCTCCTCCAGATGGG-3'	Not1	
Δ2 Forward	5'-CTACGTAGCCCATCATCACACCATCACCATTCCTTGGAGCAGCTGCTG-3'	Nhe	His
Δ2 Reverse	5'-ATAGTTTAGCGGCCGCTCAGAGGTTGAGCTCCAGGAG-3'	Not1	
Δ3 Forward	5'-GCGACAGCTGTCCATCATCACCATCACCATGGGACCAATGGCAGTCTGGTG-3'	pshAI	His
Δ3 Reverse	5'-CGGGATCCGTCGTGGCTGGGCTCCAG-3'	BamHI	
Δ1-2 Forward	5'-CTAGCTAGCCCATCATCACCATCACCATGCTTCCAGTACTAGCCTC-3'	Nhe	His
Δ1-2 Reverse	5'-ATAGTTTAGCGGCCGCTCAGAGGTTGAGCTCCAGGAG-3'	Not1	

293-EBNA cells were transfected by electroporation with the different pCEP-Pu constructs and selected in the presence of 0,5 mg/ml of puromycin and 250 mg/ml of G418. Positive clones were isolated and the expression analyzed by Western blotting. To this purpose when the clones reached sub-confluency, the medium was replaced with serum-free DMEM. After 24-48 hours conditioned media were collected and equilibrated with a buffer containing 50 mM NaH_2PO_4, 150 mM NaCl, 10 mM imidazole. The proteins were purified by means of the Ni-NTA resin and eluted with the elution buffer (50 mM NaH_2PO_4, 300 mM NaCl, 250 mM imidazole). The different fractions were analyzed by SDS-PAGE followed by Coomassie blue staining or Western Blot. Protein fractions were then dialyzed in PBS and concentrated using polyethylene glycol (PEG).

In addition the MMRN2 cDNA was sub-cloned into pcDNA3.1/Myc-His vector by *Hind III* and *Xho I* restriction and HT1080 cells were stably transfected by calcium phosphate transfection.

5. Recombinant adenovirus

For MMRN2 over-expression, tetracycline-inducible recombinant adenoviruses were constructed according to the manufacturer's instructions using the Adeno-X Tet-On Expression System 2 (Clontech Laboratories, Milan Italy). HUVEC were co-transduced with a regulatory virus Adeno-X Tet-On and the MMRN2 recombinant virus at a specific multiplicity of infection ratio (400 : 160). Doxycycline was employed at a final concentration of 0.5 mg/ml.

For the down-regulation of endogenous MMRN2, the Knockout RNAi System was used (Clontech). The targeted sequences were:

siRNA 1: 50-GAGGAACCTCTCAGAGCTGCACATGACCA-30;

siRNA 2: 50-GGATGAGATCAAGGAACTGTACTCCGAAT-30;

siRNA 3: 50-CCTCATCAAGTACGTGAAGGACTGCAATT-30;

siRNA 4: 50-GCAGACAGTGAAGTTCAACACCACATACA-30.

6. MTT and TUNEL assays

Cell proliferation was evaluated using MTT assay. Cells were transduced (or not) with the adenoviruses, as previously described, or treated with the indicated molecules and 72 hours later cell viability was analyzed. The MTT (3-(4,5-Dimethylthiazol-2-yl)-2,5-diphenyltetrazolium bromide, a tetrazole) reagent was added to the cells at a final concentration of 0,3 mg/ml and incubated for 4 hours at 37°C in complete medium. MTT is processed into to purple formazan crystals by the mitochondria of living cells. The medium was then discarded and the crystals solubilized with dimethyl sulfoxide (DMSO). The reduced form of the colorimetric substrate was then quantified at the spectrophotometer at 560 nm.

For the TUNEL assay ECs adhered on coverslips were transduced or not with the adenovirus carrying the MMRN2 sequence and after 72 hours the apoptotic rate was determined using the ApopTag Fluorescein *In Situ* Oligo Ligation Apoptosis Detection Kit (CHEMICON International, Temecula, CA), according to the manufacturer's instructions. The percentage of apoptotic cells was evaluated through the counting of positive cells versus the total number of cells.

7. Cell migration, haptotaxis, scratch test

EC migration in response to ECM substrates was assessed by fluorescence assisted transmigration invasion and motility assay (FATIMA) (Spessotto P. *et al*., book chapter 2009). The procedure is based on the use of Transwell-like inserts carrying fluorescence shielding porous polyethylene terephthalate (PET) membranes (polycarbonate-like material with 8 µm pores) provided by the HTS FluoroblokTM inserts (Becton- Dickinson, Falcon, Milan, Italy). For the migration tests, the HTS Fluoroblok membranes were coated on the upper side with 10 µg/ml of MMRN2 or type I collagen used as control, in the presence of 0,1M bicarbonate buffer at 4°C overnight. The next day the membranes were saturated with 1% BSA in PBS for 2 hours at room temperature. Cells were labeled with DiI (Molecular Probes) for 20 minutes at 37°C before being seeded on the Fluoroblok upper chamber and then incubated at 37°C for the indicated times. Migratory behavior of the cells towards the FBS chemotactic stimulus in the bottom plate was then monitored at different time-intervals by independent fluorescence detection from the top (corresponding to non-transmigrated cells) and bottom (corresponding to transmigrated cells) side of the membrane using the computer-interfaced GENios Plus instrument (TECAN Italia S.r.L.).

Haptotaxis was assessed by plating the molecules on the underside of the membranes.

To study the migratory response of HUVEC cells in presence of the MMRN2 fragments regular transwells were employed. The transwell membranes carrying 8 µm pores were coated on the upper side with 10 µg/ml of MMRN2 or the Δ1, Δ1-2 and Δ3 fragments in the presence of 0,1M bicarbonate buffer at 4°C overnight. Also in this case type I collagen was used as a control. The next day the membranes were saturated with 1% BSA in PBS for 1 hour at room temperature. Cells were placed on the top layer of the permeable membrane in serum free M199 medium containing 0,1% BSA and 10 µg/ml of MMRN2 or either the Δ1, Δ1-2 and Δ3 purified fragments, or type I collagen. In the bottom chamber VEGF-A (10 µg/ml) was added to the medium as migratory stimulus. Following an overnight incubation, the migrated cells were stained with Crystal violet for 30 minutes and counted.

For the scratch test ECs were seeded in a 24-multiwell dish and allowed to grow until they reached confluency. Cells were then starved overnight and the day after a scratch wound across each well was made using a sterile pipet tip. Cells were washed to remove any loosely held cells and then incubated with medium containing 0,5 % serum in the presence of 10 µg/ml of purified MMRN2 or PBS as a control. The open gap was then inspected over time with the microscope. Time course

analysis was carried out by means of the LEICA AF6000 Imaging System (LEICA, Wetzlar, Germany) until some of the well displayed the closure of the wounded area.

8. Matrigel tube formation assay

The Tube Formation Assay is based on the ability of ECs to form three dimensional capillary-like tubular structures when cultured on a gel of basement membrane extract. Matrigel (BD, Bioscience) was thawed at 4°C overnight; 300 µl were quickly added to each well of a 48-multiwell dish using cold pipettes and was allowed to solidify for 30 min at 37°C. Once solid, $4x10^4$ HUVEC cells were resuspended in medium containing 0,5% serum and 10 µg/ml of purified MMRN2 or type I collagen used as a control and then seeded in each well. Tube formation was monitored for 24 hours. Time course analysis was carried out by means of a microscope associated with a camera (LEICA STP 6000).

To evaluate tube formation in a more complex environment, the TCS CellWorks AngioKit was used. This kit provides a co-culture of human ECs among other stromal cells embedded in a culture matrix. In this environment ECs initially form small islands and then begin to proliferate and migrate to form threadlike tubule structures. The co-coltures were treated for 11 days with purified recombinant MMRN2 at different concentrations, or PBS as control. At the end of the treatment cells were fixed and stained with the anti-CD31 antibody provided with the kit. Vessels density was calculated by means of an Image Tool software.

9. 3D *in vitro* angiogenesis assay

For the 3D *in vitro* experiments we have set up a previously described angiogenesis assay (Nakatsu M. N. *et.al* , 2007). Briefly, 4 x 10^2 HUVEC cells per cytodex microcarrier were employed. HUVEC cells were incubated with the beads for 4 hours at 37°C, shaking every 20 minutes. After the incubation time, the coated beads were transferred into a flask containing complete medium and were incubated overnight at 37°C. The next day the coated beads were embedded into a fibrin gel with or without MMRN2 (5 µg/ml). Normal Human Dermal Fibroblasts (NHDF) were layered on top of the gel after resuspension in medium containing or not MMRN2. The NHDF provide the required soluble factors that promote EC sprouting from the surface of the beads. After 7 days, vessels were formed and could be observed under phase-contrast and time-lapse microscopy.

Spheroids were fixed with 4% (w/v) paraformaldehyde for 15 minutes at room temperature and stained with the anti-CD31 antibody (vessels) and with SYTOX (nuclei).

10. CAM assay

CAM assays were performed as previously described (Mongiat M. *et al*., 2003). Twenty eggs were used for each point. A square window was opened in the egg's shell and 150 ng of VEGF-A or bFGF with or without 150 ng of MMRN2 were allowed to be absorbed by the sponges (Gelfoam, Upjohn Company, Kalamazoo, MI, USA). PBS or full-length MMRN2 used as a control. After 4 days the CAMs were fixed with Bowen and pictures were taken at the Stereo Microscope (Leica Microsystems GmbH). The vessels directed toward the sponge were evaluated by counting.

11. RTK array

Analysis of Tyrosine Kinase Receptors (RTKs) activation following treatment of ECs with MMRN2 was evaluated using the Human Phospho-Receptor Tyrosine Kinase kit (R&D Systems). This tool consists of 42 different antibodies recognizing phosphorylated human RTKs spotted in duplicate on nitrocellulose membranes. For this analysis HUVEC cells were incubated with conditioned media from HUVEC cells transduced with the MMRN2 or the control adenoviral vectors (collected 72 h post transduction). The incubation was conducted for 30'. Following incubation, the cells were lysed and the lysates diluted to a final volume of 1,5 ml with the provided buffer. Cell lysates were deposited over the array and incubated overnight at 4°C. A pan hrp-conjugated anti-phospho-tyrosine antibody was then used to detect phosphorylated tyrosines by chemiluminescence. The spots were revealed by exposure to X-ray films and spots' intensity was evaluated with the Image Tool software (University of Texas Health Science Center, San Antonio, TX, USA).

12. Preparation of cell lysates and Western Blotting analysis

To analyze the degradation of MMRN2 following an angiogenic stimulus, HUVEC cells were incubated with VEGF-A (100 ng/ml) for different times in the presence or not of GM6001 (4 µg/ml) and then lysed in cold HNTG buffer (0,1% TrytonX100, 20mM HEPES pH 7.5, 10% glycerol, 150 mM

NaCl) containing a protease inhibitors cocktail (Roche) and 1 mM sodium orthovanadate. After incubation on ice for 20 min, the lysates were centrifuged at max speed for 20 min at 4°C and the supernatants recovered.

For the phosphorylation studies, HUVEC cells were treated with VEGF-A (15ng/ml) with or without MMRN2 (5 μg/ml) for different intervals of time. The cells were then lysed in a cold specific buffer (1mM $CaCl_2$, 1mM $MgCl_2$, 15mM Tris-HCl pH 7.2, 150mM NaCl, 1% TrytonX100, 0,1% SDS, 0,1% Na Deoxycholate) containing 25 mM NaF, 1 mM DTT, 1 mM Na_3VO_4 and the protease inhibitors cocktail (Roche).The samples were then treated as described above.

For the Western blot analyses proteins were resolved in 4-20% Criterion Precast Gels (Bio-Rad Laboratories) and transferred onto Hybond-ECL nitrocellulose membranes (Amersham, GE-Healthcare). Membranes were blocked with 5% dry milk in TBS-T (100mM Tris-HCl pH 7.5, 0,9% NaCl, 0,1% Tween 20) and probed with the appropriate antibodies. The blots were finally developed using ECL (Western blotting detection, Amersham Biosciences) and exposed to X-ray films. Alternatively the Odyssey infrared imaging system was used (Li-COR Biosciences, Lincoln, NE, USA).

13. Radioligand displacement studies, ELISA

For the displacement of HUVEC-bound ^{125}I-VEGF-A (Perkin Elmer, Milan, Italy), 2 x 10^5 HUVEC cells were used per point. Cells were incubated with 70 pM ^{125}I-VEGF-A and increasing concentrations of cold-VEGF-A or recombinant full-length MMRN2, incubated on ice for 1 h, collected, and counts obtained with the Wizard 2 GAMMA Counter (Perkin Elmer). In alternative, the recombinant VEGFR2 Fc chimera (R&D Systems, Inc., Milan, Italy) was used and coated on ELISA plates (10 ng/well). Bound ^{125}I-VEGF-A was rescued using 2M NaOH at 50°C and type I collagen was used as a control.

For the ELISA tests, 0.5 μg of MMRN2 or of the VEGFR2 chimera were used to coat the plates, BSA was used as a control. The wells were blocked with 2% BSA and incubated with soluble VEGF-A (100 ng/well) for 1 h at 37°C. In other ELISA test the wells were also incubated with soluble VEGF-B or PlGF. Binding was verified using the specific anti-cytokine antibodies; the ABTS substrate was added and absorbance at 405 nm detected with a spectrophotometer (TECAN, Milan, Italy).

14. *In vivo* experiments

For the *in vivo* experiments ten female athymic nude mice (Harlan S.r.l, Milan, Italy) were injected subcutaneously with one million of HT1080 cells stably transfected with pcDNA3.1 vector carrying the MMRN2 coding sequence or with the empty vector. The left flanks of each mouse were injected with control cells, while the right flanks with cells expressing MMRN2. Two MMRN2 clones were used (clone 4 and 9) for a total number of 20 mice. Tumor growth was monitored over time and tumor size measured with a caliper. The tumor volumes were calculated with the following formula: ($\prod$ x length x width^2)/6. After 19 days the animals were sacrificed and the tumors excised. In all the cases a portion of the tumor was lysed with HNTG buffer and the ectopic expression of human MMRN2 was confirmed by Western blot analysis using a specific antibody.

15. Immunohistochemistry analyses of the tumor sections

For the immunohistochemical analyses, tumors were included in the Optimal Cutting Temperature compound (OCT) and frozen. For microvessel density analysis, 7 µm thick sections were obtained and stained with anti-mouse CD31 and/or α-SMA antibodies. For the co-localization analyses, sections from mock and MMRN2-transfected tumors were stained with anti-human MMRN2 and Gv39M antibodies. Images were acquired with a Leica TCS SP2 confocal system (Leica Microsystems Heidelberg, Mannheim, Germany), using the Leica Confocal Software (LCS). Vessels density was calculated by means of the Image Tool software. Alternatively five mice injected in both flanks as above were treated with 60 mg/kg of pimonidazole HCl 45 minutes prior being killed and sections were stained with the PAb2627 (hypoxyprobe-1, CHEMICON, Temacula, CA, USA) according to the manufacturer instructions.

16. Immunofluorescence analysis of ECs, aortic ring and retina immunostainings

HUVEC cells were grown on cover glass slides placed in a 24 multi-well plate, treated 20 minutes with VEGF-A (10 ng/ml) and MMRN2 (5 µg/ml) at 37°C and then fixed with 4% (w/v) paraformaldehyde for 15 minutes at room temperature. The cells were then permeabilized with a PBS solution containing 1% BSA, 0,2% TRITON X-100 for 5 minutes at room temperature, saturated with blocking buffer (PBS-2% BSA) for 1 hour and incubated overnight at 4°C with the α-VEGFR2

antibody. The antibody incubation was followed by actin staining with phalloidin for 1 hour at room temperature. Slides were finally mounted in Mowiol containing 2,5% (w/v) of 1,4-diazabicyclo-(2,2,2)-octane (DABCO). Images were acquired with a confocal system (Leica Microsystems).

The aortic assays were performed as previously described (Baker M *et al*., 2012). Aortic rings were isolated from C57/BL6 mice and cultivated for 8 days on rat type I collagen containing 30 ng/ml of VEGF-A to induce the sprouting of new vessels. The rings were fixed in 4% (w/v) paraformaldehyde, permeabilized with a PBS solution containing 0,25% TRITON X-100 for 15 minutes at room temperature, blocked with PBS-1%BSA buffer 90 minutes at room temperature. The rings were whole mounted and stained with the anti-VEGFR2 and anti-MMRN2 antibodies; the nuclei with TO-PRO-3. Slides were mounted in Mowiol with 2,5% DABCO and images were acquired with a confocal system (Leica Microsystems).

Retinas were isolated as previously described (Pitulescu M. *et. al.*, 2010) either from adult or P3 C57/BL6 pups. The retinas were fixed in 4% (w/v) paraformaldehyde for 2 hours at 4°C and saturated overnight at 4°C with the blocking buffer (PBS-1% BSA-0,3% TRITON X-100). The next day the retinas were incubated overnight at 4°C with the anti-MMRN2 antibody and with isolectin B. After incubation the retinas were washed with PBS 5 times for 20 minutes, incubated with the secondary antibody for 2 hours at room temperature, washed 4 times for 20 minutes and incubated with TO-PRO-3 for 15 minutes at room temperature. Finally the samples were mounted using Mowiol with 2,5% DABCO. Images were acquired with a confocal system (Leica Microsystems).

RESULTS

1. MMRN2 IMPAIRS TUMOR ANGIOGENESIS AND GROWTH

As mentioned above, the ECM glycoprotein MMRN2 is specifically deposited along the blood vessels in tight contact with ECs, being present also in the luminal side. Nevertheless, since its discovery, the function of this molecule has remained elusive. Given is specific localization and its close proximity to ECs we have hypothesized an involvement of this molecule in the regulation of EC function. To assess this hypothesis we have first tested the ability of ECs to adhere to MMRN2. We have found that indeed ECs specifically bind to MMRN2 even though the interaction strength is lower compared to that exerted by type I collagen, and was not integrin dependent. Thus based on its localization and on the specific interaction with ECs we have thought to further investigate the role of this molecule in regulating ECs and in angiogenesis, with particular interest in tumor angiogenesis, and these investigations will be the subject of the first part of the present thesis.

1.1 MMRN2 DOES NOT AFFECT EC VIABILITY OR THEIR APOPTOTIC RATE

To assess the role of MMRN2 in regulating ECs we next verified if the treatment with MMRN2 could affect EC viability. To this end HUVEC cells were seeded on 48 well plates and challenged with purified recombinant MMRN2 or type I collagen (Coll I) using increasing protein concentrations (from 0,6 µg/ml to 10 µg/ml). Following the incubation with the recombinant molecules, EC viability was evaluated by MTT assays. The results indicate that MMRN2 does not significantly affect HUVEC cell viability **(Fig. 1a)**. To corroborate these results we also performed MTT assays on HUVEC cells trasduced with an inducible MMRN2 adenoviral vector and cultured the cells with or without doxycycline. Also in these conditions, despite the protein was overexpressed in the culture medium at high concentration, MMRN2 did not alter the proliferation of ECs **(Fig. 1b)**.

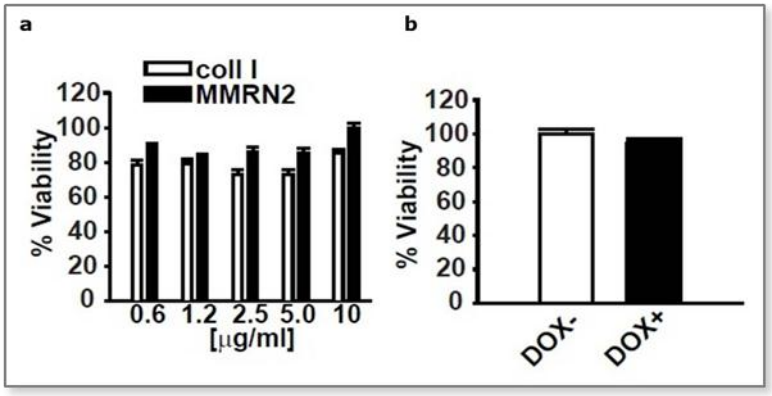

Fig. 1 ECs viability is not affected by MMRN2 treatment. a) MTT assay performed on HUVEC cells treated with increasing concentrations of recombinant MMRN2 or type I collagen (Coll I) as a control. **b)** MTT assay performed on EC transduced with the MMRN2 adenoviral construct in the presence or absence of doxycycline (DOX+ and DOX-, respectively). The values reported represent the mean ± SD of three independent experiments.

Subsequently we also verified whether MMRN2 could affect the viability of ECs. For this purpose HUVEC were treated with 10 μg/ml of recombinant MMRN2 or type I collagen and DNA fragmentation was evaluated by TUNEL assays. As shown in **Fig. 2a**, the apoptotic rate of HUVEC cells treated with MMRN2 was comparable to that observed following type I collagen treatment. This indicates that EC survival is not affected by the presence of MMRN2. A similar outcome was observed following transduction of HUVEC cells with the MMRN2 adenoviral construct and incubation of the cells in the presence or absence of doxycycline **(Fig. 2b)**.

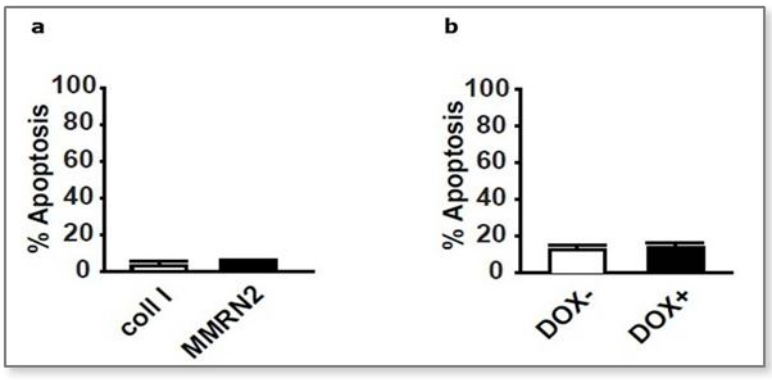

Fig. 2 MMRN2 does not alter the apoptotic rate of ECs. a) TUNEL assay performed on HUVEC cells treated with 10 μg/ml of MMRN2 or type I collagen (coll I). **b)** TUNEL assay performed on HUVEC cells transduced with the MMRN2 adenoviral construct and incubated with or without doxycycline (DOX+ or DOX-, respectively). The values reported represent the mean ± SD of three independent experiments.

1.2 MMRN2 IMPAIRS EC MOTILITY AND TUBULOGENESIS

Another important feature of the angiogenic process is the migration of ECs to form new vessel sprouts. In order to verify whether MMRN2 affected ECs migration, we analyzed the chemotactic response of ECs to soluble factors in the culture medium. HUVEC cells were fluorescently labelled and let migrate towards a VEGF-A stimulus (50 ng/ml) in culture plate inserts (Transwell) previously coated with 10 μg/ml of MMRN2 or type I collagen. Fluorescence measurements at different time intervals revealed that MMRN2, unlike type I collagen, induced a significant reduction of the ECs migration rate **(Fig. 3a)**. As a consequence, the down-regulation of MMRN2 expression by a specific siRNA construct led to an increased motility of HUVEC cells towards the VEGF-A stimulus **(Fig. 3b)**.

In addition, to assess whether MMRN2 could function as a chemoattractant or chemorepulsant for ECs, we set up an haptotactic response assay. For this purpose, MMRN2 or type I collagen were coated on the underside of the Transwells' membranes and fluorescently labelled HUVEC cells were seeded on the upper side of the plate inserts. The EC movement was monitored at different time points by independent fluorescence detection from the top and bottom side of the membranes and the results indicate that MMRN2 does not serve as an aptotactic stimulus for ECs **(Fig. 3c)**.

Furthermore, we also tested the effect of MMRN2 on ECs in a scratch test analysis: HUVEC cells were seeded on 24-multiwell plates, allowed to grow to confluency and scratch wounds were made using a sterile pipette tip. Cells were treated with 10 μg/ml purified MMRN2 or type I collagen and their movement across the area was monitored by time lapse analysis. ECs incubated with type I collagen migrated throughout the scratched area and succeeded in restoring the monolayer, on the contrary in presence of MMRN2 ECs failed to efficiently migrate and close the wounded area **(Fig. 3d)**.

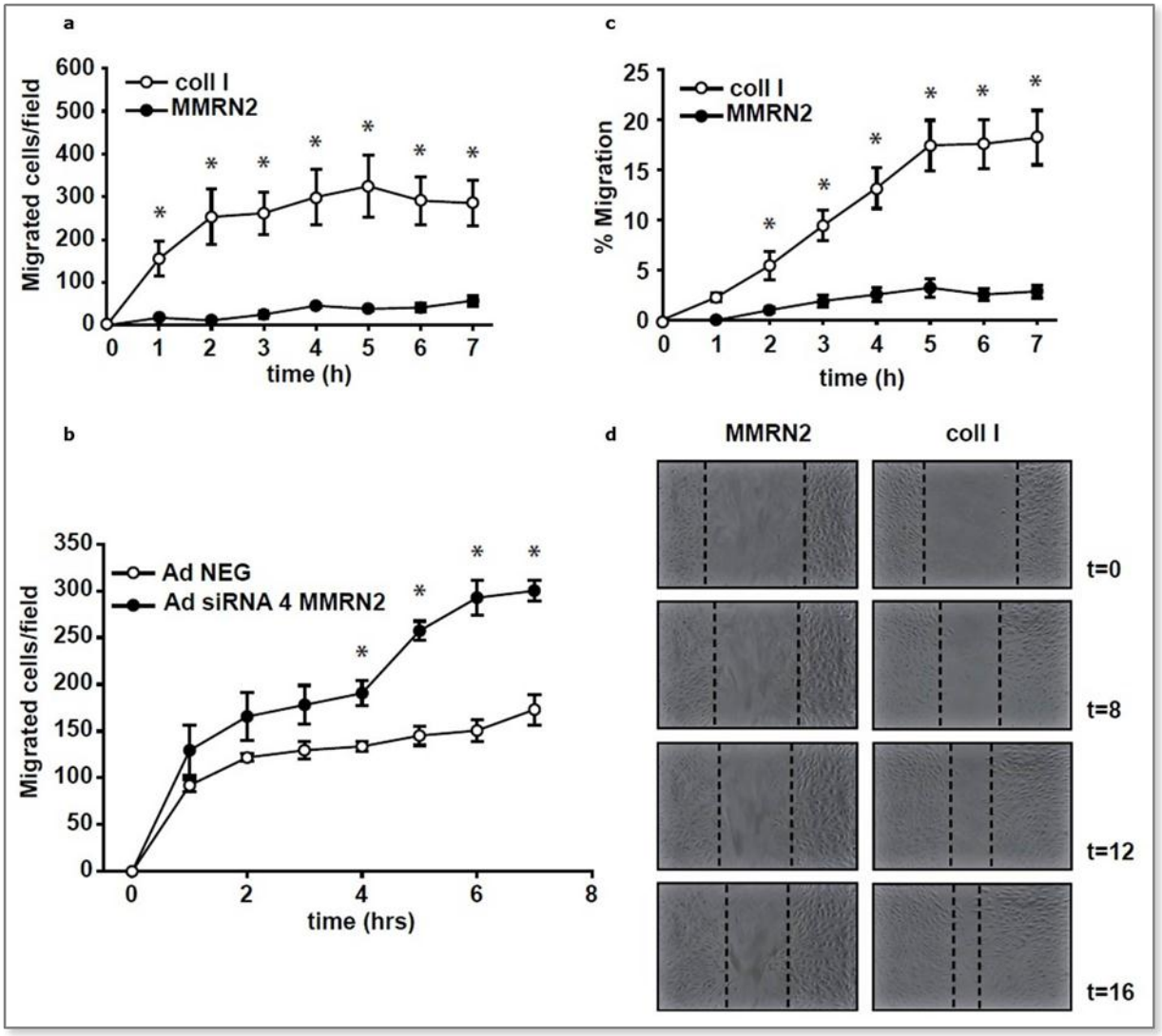

Fig. 3 MMRN2 significantly reduces ECs motility. a) Analysis of HUVEC cell migration toward a VEGF-A stimulus (50 ng/ml) through MMRN2 or type I collagen (coll I) coated on the transwell' membranes (**P*≤0,009). **b)** Migration of HUVEC cells through type I collagen-coated transwells (coll I) toward a VEGF-A stimulus, following transduction with the control (AdNEG) or with the MMRN2 (Ad siRNA 4 MMRN2) siRNA adenoviral constructs (**P*≤0,02). **c)** Haptotaxis assay performed on HUVEC cells let migrate towards a MMRN2 or type I collagen (coll I) stimulus previously coated on the underside of the transwell membranes (**P*≤0,04). **d)** Representative images of the scratch assay performed on HUVEC cells treated with 10 µg/ml purified MMRN2 or type I collagen (coll I). The edge of the moving cells is highlighted by dashed lines.

The differentiation and reorganization of ECs to form tubules is a central step of the angiogenic process. Hence we investigated whether MMRN2 could also play a role in this phenomenon. To this end, a tube formation assay was performed seeding HUVEC cells on pre-gelified matrigel matrix containing either purified MMRN2 or type I collagen and images were captured over time by time-lapse microscopy. MMRN2 impaired the ability of ECs to form tubules on Matrigel and the cells failed to organize functional tubule connections. On the contrary in the presence of type I collagen a complete vessel network was formed **(Fig. 4a)**.

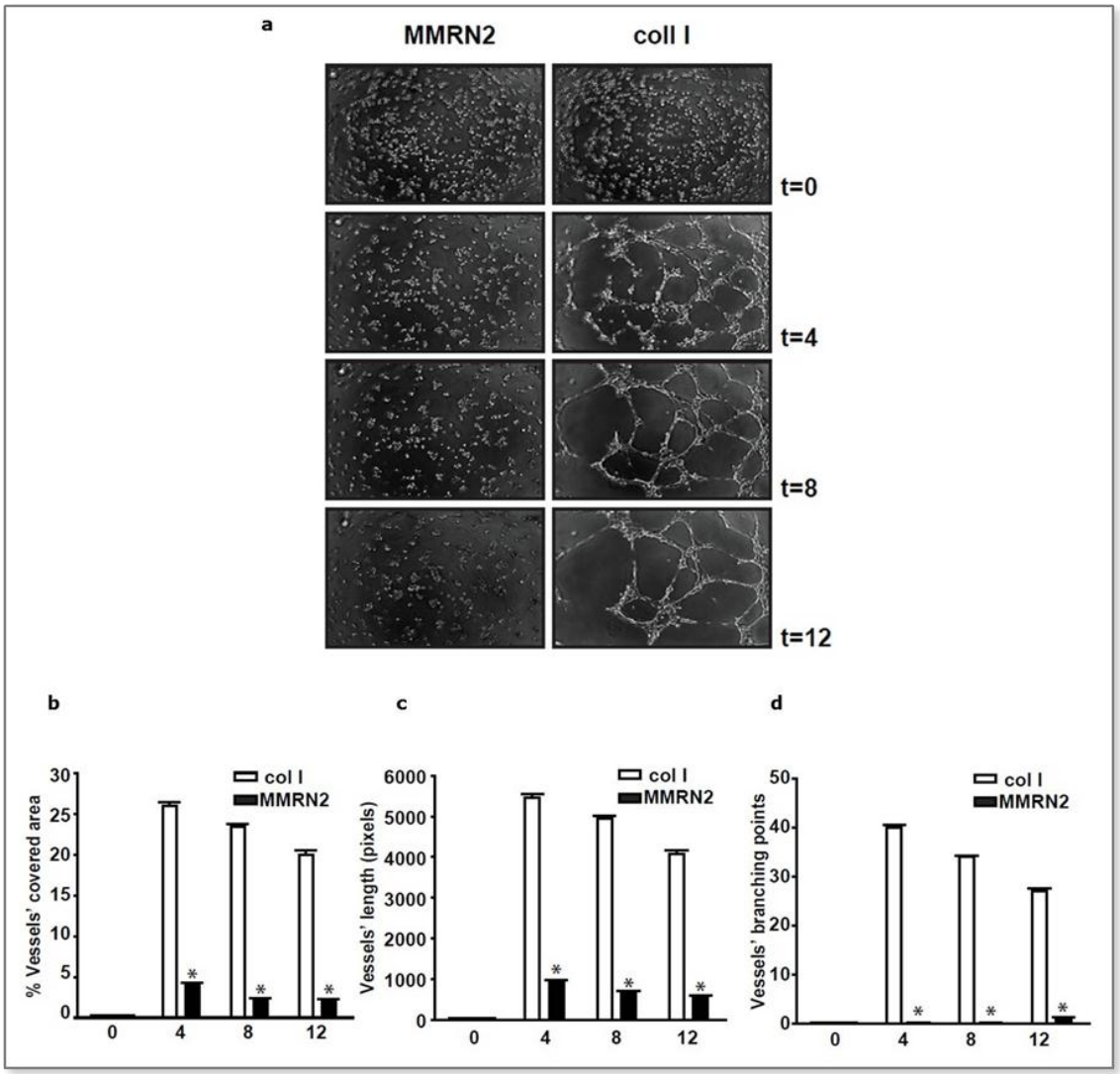

Fig 4. MMRN2 inhibits tubulogenesis. **a)** Representative images of HUVEC cells reorganization to form tubules on Matrigel in presence of 10 µg/ml recombinant MMRN2 or type I collagen (coll I). **b-c-d)** Quantitative analysis of the percentage of the area covered by the vessels, the vessels' length, and branching of the tube formation in the presence of type I collagen (coll I) or MMRN2, respectively; the analysis from three independent experiments was performed by the WinTube software (Wimasis GmbH, Germany), (* $p \leq 0.0001$).

The effect of MMRN2 on tubule formation was also assessed in a more sophisticated setting using the AngioKit, consisting of a co-culture of fibroblast and ECs in a culture matrix. The co-cultures were challenged for eleven days with increasing concentration (from 5 µg/ml to 10 µg/ml) of recombinant MMRN2 or an equal volume of PBS as a control. The reorganization of ECs to form tubules was then evaluated by CD31 staining. The cultures treated with MMRN2 presented a significant reduction of the vessel area compared to the PBS control **(Fig. 5)**. In addition, the negative effect on the tubule structures was dose dependent since the increase of MMRN2 concentration led to a progressive reduction of tubule formation, which was on the contrary improved by VEGF, used as a positive control.

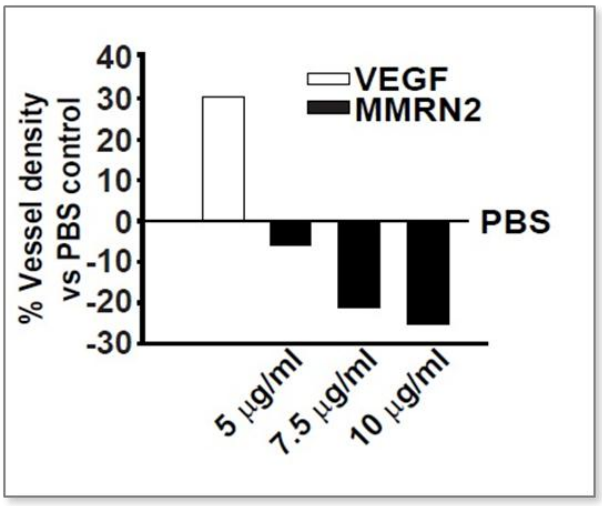

Fig. 5 MMRN2 affects tubule formation in a co-culture experimental setting. Evaluation of the vascular density following treatment of the cell co-coltures provided by the AngioKit with VEGF (10 ng/ml) or with increasing concentrations of MMRN2 or equal volumes of PBS. VEGF was used as a positive control and vessel density was calculated using the Image Tool Software. The data represent the percentage of variation of the vascular density using the values obtained with the PBS vehicle as a reference.

1.3 MMRN2 INHIBITS THE VEGF-A-INDUCED ANGIOGENESIS *IN VIVO*

In order to verify whether MMRN2 could exert anti-angiogenetic effects *in vivo*, we performed the chicken embryo chorioallantoic membrane (CAM) assay, an extensively used model for studying neovascularization. The assay was performed by placing a sponge containing 50 ng of VEGF-A or bFGF with or without 150 ng of MMRN2 over the CAM through a square window open in the egg's shell. After four days of incubation, angiogenesis was evaluated by counting of the newly formed vessels directed towards the sponge in a spoke-weel fashion; the development of novel vessels prompted by the VEGF-A stimulus was significantly impaired in the presence of MMRN2. On the contrary, MMRN2 did not significantly affect the bFGF-induced angiogenesis, suggesting that the effect of MMRN2 depended on an impingement of the VEGF-A signaling **(Fig. 6a-b)**.

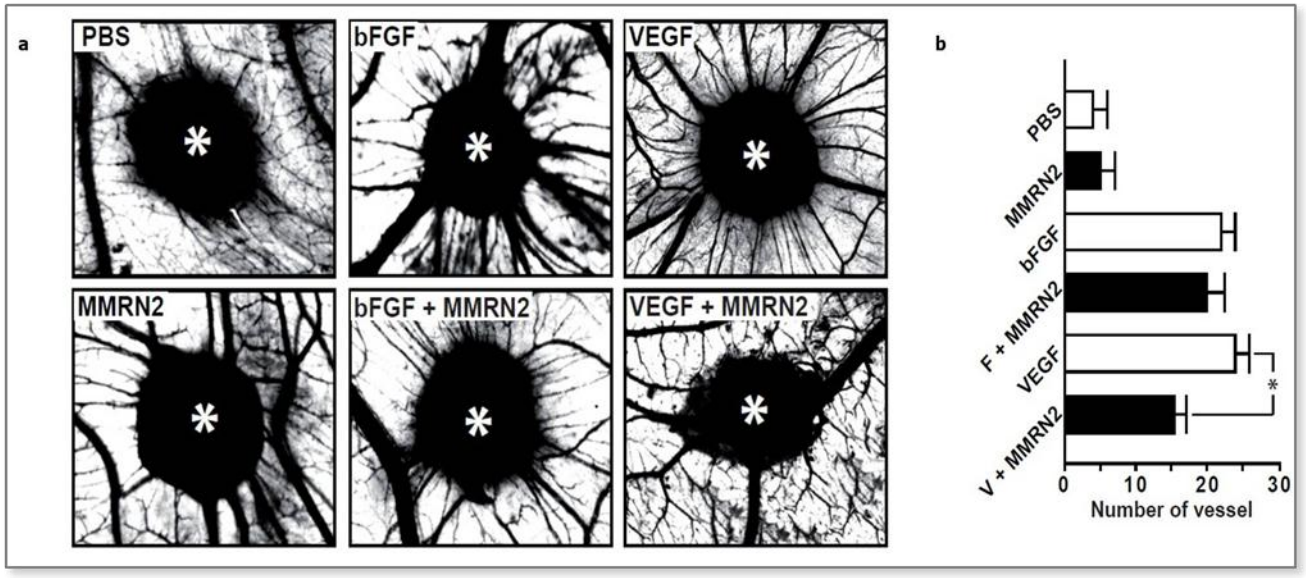

Fig. 6 MMRN2 impairs the development of new vessels in vivo. a) Representative pictures of the CAM assays performed using sponges (white asterisk) containing VEGF-A or bFGF with or without MMRN2. PBS or MMRN2 without stimulus were used as a control. **b)** Quantification of the new vessels directed toward the sponges containing or not VEGF-A or bFGF (V and F, respectively) of the above experiment. Twenty eggs were used for each point and the values represent mean ± s.e. of three independent experiments (*P=0.01).

1.4 MMRN2 DOWN-REGULATES VEGFR2 ACTIVATION BY BINDING VEGF-A

In order to better understand the molecular mechanisms involved in the down-regulation of EC function elicited by MMRN2, we first chose a broad approach and analyzed the activation of an array of receptor tyrosine kinases (RTK) on the EC surface. To this end HUVEC cells were treated with conditioned media containing or not MMRN2 and the effects were assessed by means of a commercially available RTK array. As shown in **Fig. 7a-b,** the treatment with MMRN2 led to a major decrease of VEGFR2 activation, supporting our hypothesis of an involvement of the VEGF-A signaling in the MMRN2-driven anti-angiogenic effects.

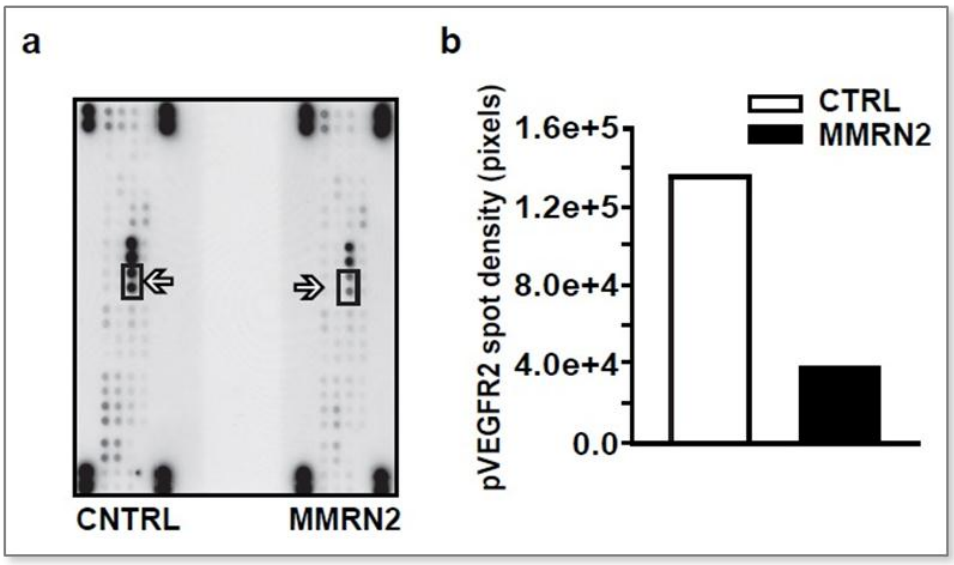

Fig. 7 MMRN2 significantly reduces VEGFR2 activation. a) Image of the RTK array analysis following incubation with lysates from HUVEC cells challenged with conditioned media containing or not MMRN2 (MMRN2 and CNTRL, respectively). The spots corresponding to VEGFR2 are highlighted by an arrow. **b)** Quantitative analysis of the spots corresponding to VEGFR2 phosphorylation as assessed with the Imaging Tool software.

Given that VEGFR2 is one of the most important receptors regulating neoangiogenesis, we thought to better investigate the role of MMRN2 in the regulation of this important signaling pathway. Thus, HUVEC cells were incubated for different time intervals with VEGF-A (15 ng/ml) in presence or not of MMRN2 (5 µg/ml) and VEGFR2 phosphorylation was analyzed by Western blot analysis. A monoclonal antibody directed against the Y-1175 phosphorylation site, which is known to be implicated in EC migration, was used in these studies. As shown in **Fig. 8**, MMRN2 specifically

blocked the VEGF-A-driven VEGFR2 phosphorylation and this effect was accompanied by a significant down-regulation of FAK phosphorylation.

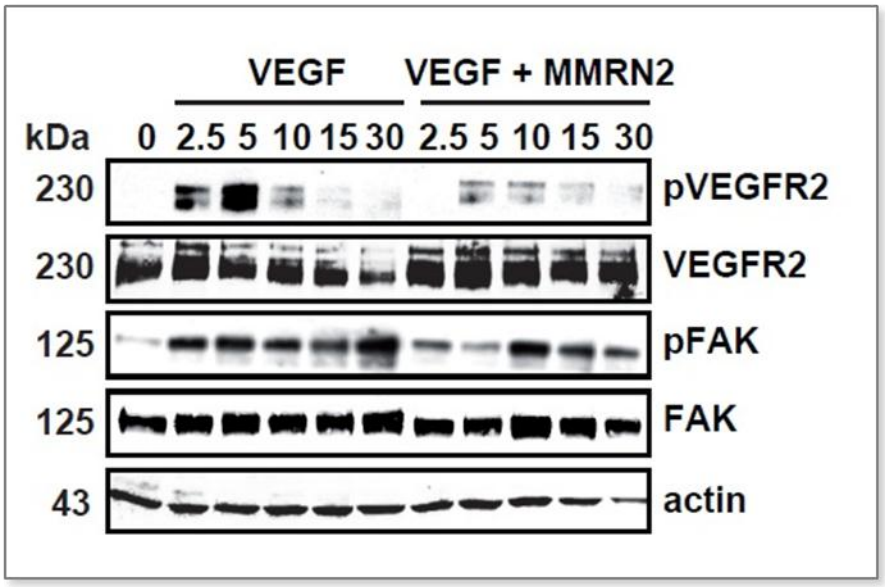

Fig. 8 MMRN2 down-regulates VEGFR2 and FAK phosphorylation. Western blot analysis of VEGFR2 and FAK activation following treatment of HUVEC with VEGF-A with or without MMRN2 for different intervals of time in minutes. Both the total and the phosphorylated forms of VEGFR2 and FAK were analyzed. Actin was used as a normalizer of protein loading.

We next verified whether the down-regulation of VEGFR2 phosphorylation was caused by an interference of MMRN2 with the VEGF-A/VEGFR2 interaction on the EC surface. To this aim, we performed radio-ligand displacement studies following incubation of HUVEC cells with ^{125}I-VEGF-A and challenged with increasing concentrations of cold VEGF-A or MMRN2. MMRN2 induced a considerable displacement of radio-labelled VEGF-A, indicating that this molecule interferes with the VEGF-A–VEGFR binding **(Fig. 9a)**. To verify if this effect did not require other molecules present on the EC surface, we have performed a similar experiment in a cell-free setting, using the recombinant extracellular domain of VEGFR2 immobilized on plastic. In this case the displacement was even stronger, comparable to that obtained with VEGF-A; on the contrary, type I collagen did not displace VEGF-A from its receptor **(Fig. 9b)**.

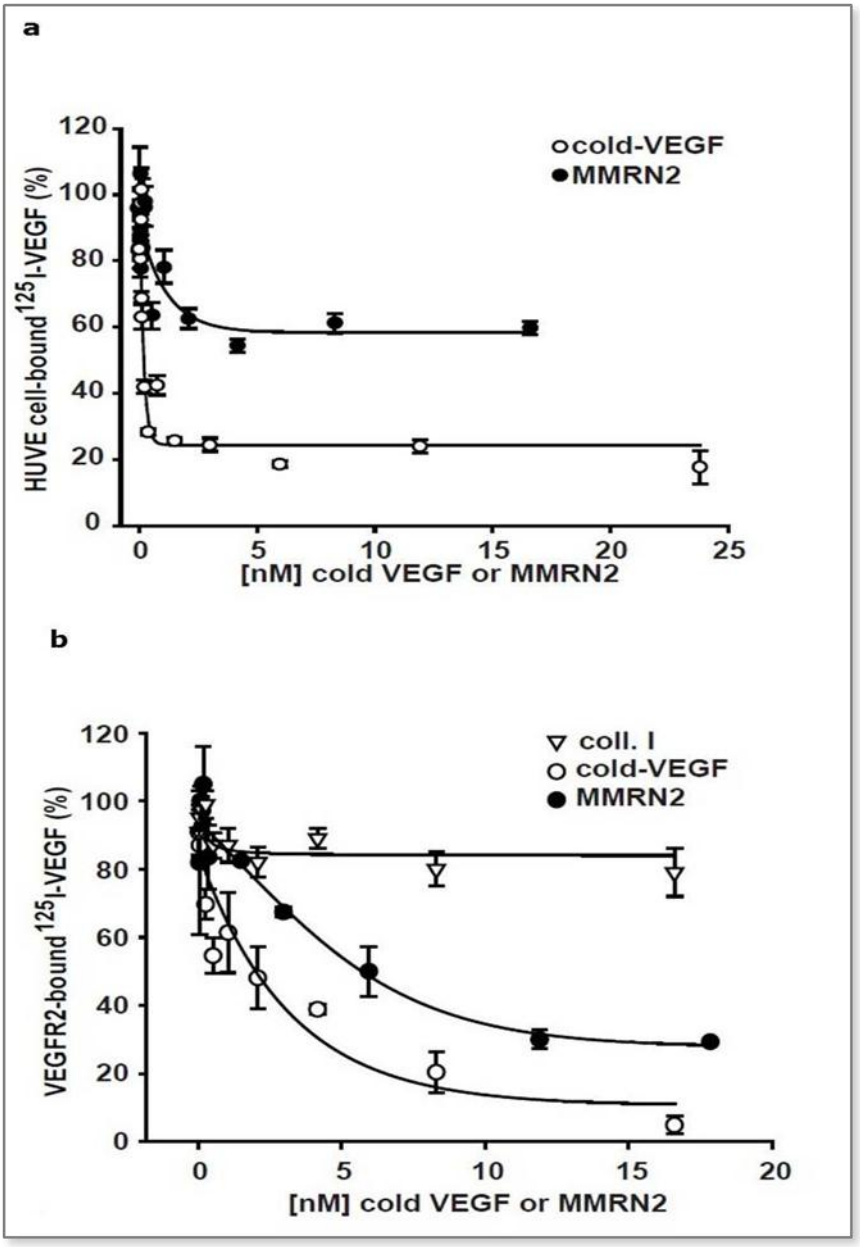

Fig. 9 MMRN2 affects VEGF-A/VEGFR2 interaction on EC surface. a) Graph representing the displacement of ^{125}I-VEGF-A from the EC surface challenging the cells with increasing concentrations of cold VEGF-A or MMRN2. Values are expressed as the percentage referred to the bound ^{125}I-VEGF-A to VEGFR2 in the absence of cold VEGF-A or MMRN2 and are the mean ± s.e. of three independent experiments. **b)** Graph representing the displacement of ^{125}I-VEGFA from recombinant VEGFR2 immobilized on plastic. Type I collagen (coll I) was used as a control. The experiment was performed as above and the values represent the mean ± s.e. of three independent experiments.

In order to confirm the specificity of MMRN2 in negatively affecting the VEGF-A/VEGFR2 interaction, we performed ELISA tests by coating the plates with recombinant VEGFR2, incubating with soluble VEGF-A and challenging with type I collagen or MMRN2 and also in this case we found that MMRN2 significantly displaced VEGA-A from its receptor **(Fig. 10a)**. Next we questioned whether this effect could occur through a direct binding of VEGF-A to MMRN2. To address this question MMRN2 was immobilized on plastic and incubated with soluble VEGF-A; the ELISA test indicated that indeed the two molecules interacted **(Fig. 10b)**.

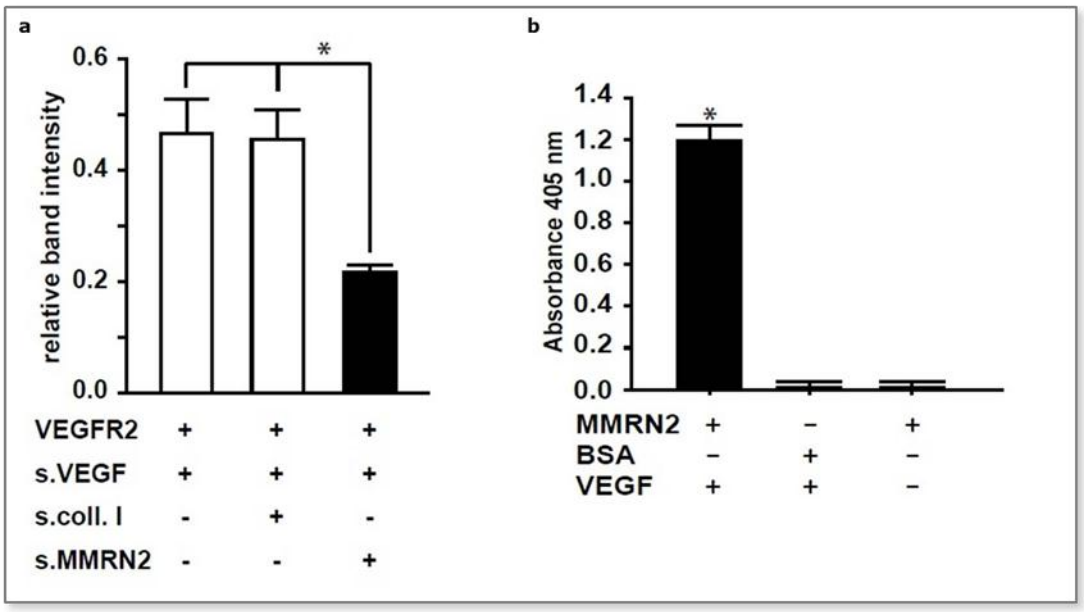

Fig. 10 MMRN2 interferes with the VEGF-A/VEGFR2 interaction by binding VEGF-A. a) Graph representing ELISA test performed following the coating of recombinant VEGFR2 (0,5 µg/well) on 96 well plates and treatment with soluble VEGF-A (50 ng/well) in presence or not of type I collagen (coll I) or MMRN2 (150 ng/well). The experiment was repeated three times in triplicates; (*P≤0.017). **b)** Graph representing the absorbance detected following an ELISA test performed on immobilized MMRN2 (0,5µg/well) or BSA to which soluble VEGF-A was added (100ng/well). Values represent the mean ± s.e. of three independent experiments; (*P=0.0002).

1.5 MMRN2 HALTS THE *IN VIVO* TUMOR GROWTH AND TUMOR ANGIOGENESIS

Given the strong anti-angiogenic effect exerted by MMRN2 *in vitro*, we hypothesized that this molecule could also play a role in tumor angiogenesis and, as a consequence, affect tumor growth. To verify this hypothesis HT1080 cells were stably transfected with the MMRN2 pcDNA construct and the efficient expression of the molecule was verified by Western blot analysis. In order to evaluate if the putative effect on tumor growth was dose dependent (the highly expressing clone 4 (cl 4) and clone 9 (cl 9) characterized by a lower expression of MMRN2) we chose two different clones characterized by different protein expression levels **(Fig. 11a)**. Control mock transfected HT1080 cells were injected in the left flank of ten nude mice, while the MMRN2 over-expressing cells were injected in the right flank. Tumor growth was monitored and the sizes measured with a caliper. After 19 days the animals were sacrificed and tumors excised. In presence of MMRN2 a striking inhibition of tumor growth was observed. Moreover the anti-tumor effect of MMRN2 was stronger when using the high-expressing clone, indicating that the effect was dose-dependent **(Fig. 11b-c)**.

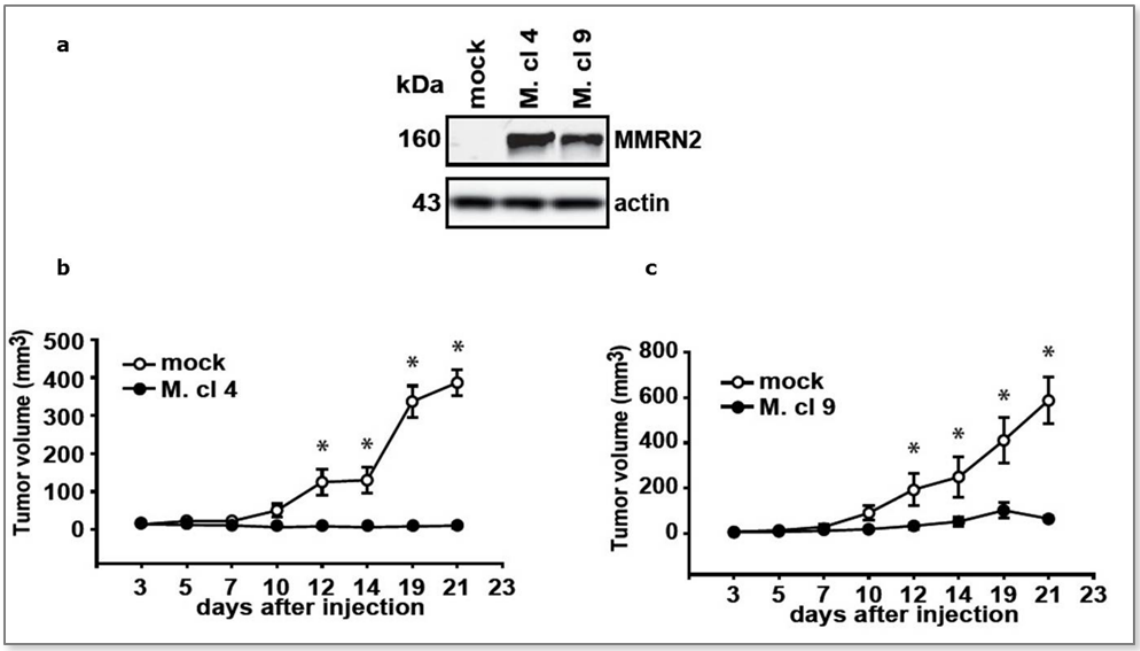

Fig. 11 MMRN2 negatively affects the *in vivo* tumor growth. a) Western blot analysis of the two HT1080 clones stably expressing MMRN2 (M cl4 and M cl9). A mock transfected clone was used as a control. **b-c)** Graphs representing the tumor volumes obtained following the injection of two HT1080 transfected clones over-expressing MMRN2 (M cl4 and M cl9) and the mock transfected cells (mock), used as a control. Ten animals were used for this experiment and the data represent the mean ± s.e. of three independent experiments (*P≤0.003 for M cl4) (*P≤0.04 for M cl9).

In order to verify if the anti-tumorigenic effect of MMRN2 could be exclusively associated with the inhibition of angiogenesis or could also depend on a direct effect on tumor cells, we checked the proliferation and apoptotic rate of HT1080 cells challenged with MMRN2. To this end, HT1080 clones over-expressing MMRN2 were seeded on 48-well plates and after 24 or 48 hours the number of cells was evaluated by MTT assays. The viability of MMRN2 over-expressing clones was comparable to that of the mock transfected cells **(Fig. 12a)**. Next the clones were plated on coverslips and after 48 hours of incubation the apoptotic rate assessed by TUNEL assays. The number of TUNEL-positive nuclei of the clones over-expressing MMRN2 was comparable to that of the mock transfected cells **(Fig. 12b)**.

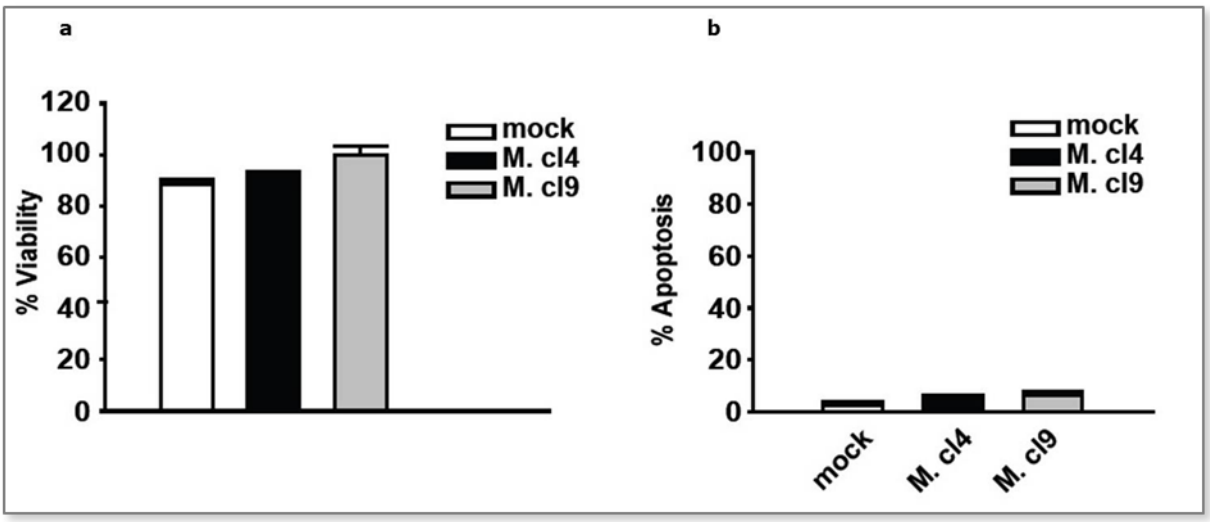

Fig. 12 MMRN2 does not affect HT1080 cell proliferation or their apoptotic rate. a) Graph representing the MTT assays and **b)** TUNEL assays performed using the M. cl4 and M. cl.9 clones over-expressing MMRN2 or the mock transfected cells. The values reported represent the mean ± s.e. of three independent experiments.

Since all these data indicated that the significant decrease of tumor development induced by MMRN2 could not be associated to a direct action of this molecule on cancer cells, we verified whether the lack of tumor growth was due to a reduced intra-tumor angiogenesis. In order to confirm this hypothesis 7 mm cryosections were obtained from the excised tumors. The cryosections were stained with the anti-mouse CD31 monoclonal antibody to specifically detect the blood vessels and the vascular density as well as the vessel length which were evaluated from the images of five independent fields. A striking reduction of the vessel density and of the length

of the vessels was observed in MMRN2 over-expressing tumors compared to the control tumors **(Fig. 13a–b)**.

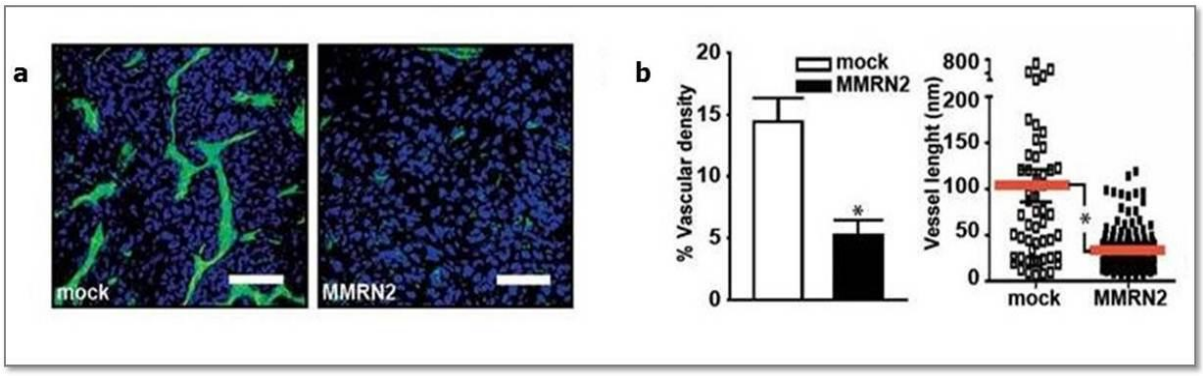

Fig. 13 MMRN2 impairs intratumoral angiogenesis. a) Representative immunofluorescence images of tumor cryosections from tumors generated using mock or MMRN2 transfected HT1080 cells following staining with the anti-CD31 antibody to evaluate the blood vessels. Nuclei were stained with the TO-PRO-3 dye, scale bars: 75 mm. **b)** Graph representing the quantitative analysis of the vascular density (**P*=0.0009) and of the vessel length (**P*=0.02) within the tumor cryosections, as obtained by means of the Image Tool software.

Moreover tumor sections from the same tumors were stained with anti-CD31 and the anti-α-SMA antibodies to detect ECs and pericytes, respectively. The vessels from the MMRN2-positive tumors were less mature displaying a decreased pericyte content **(Fig. 14a-b)**.

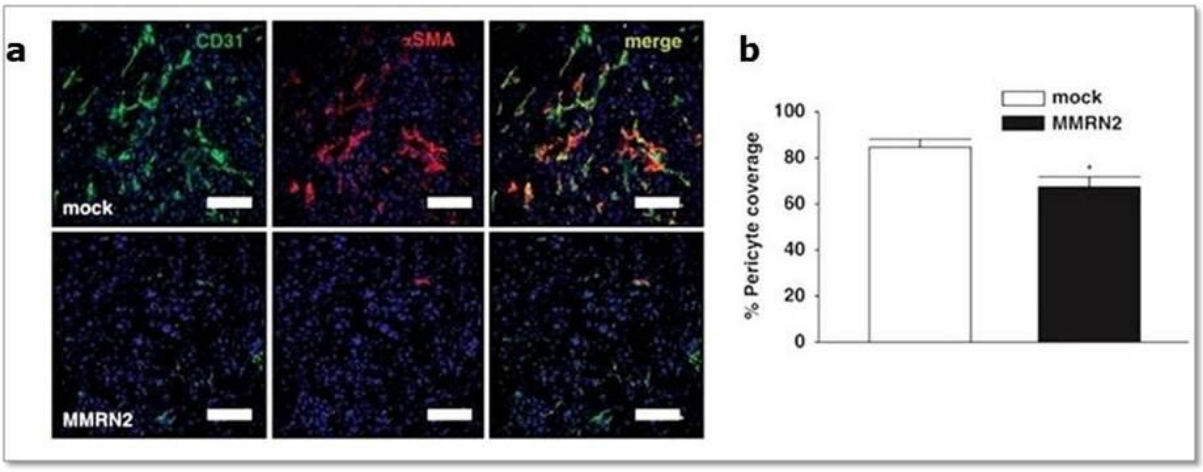

Fig. 14 a) MMRN2-positive tumors are less mature. Representative images of the immunofluorescence analysis using anti-CD31 (ECs) and the anti-α-SMA (pericytes) antibodies on tumor sections from mock and MMRN2-transfected HT1080 cells. Nuclei were stained with the TO-PRO-3 dye, scale bars: 75 mm. **b)** Graph

representing the quantification of the co-localization of the anti-CD31 and the anti-a-SMA staining obtained from the immunofluorescences from mock and MMRN2-overexpressing tumors (*P=0.006).

In order to corroborate the finding that MMRN2 halted *in vivo* tumor angiogenesis, we verified the presence or absence of hypoxic areas on tumor sections from mock and MMRN2-transfected HT1080 cells using the hypoxyprobe-1 detection system. Despite their size, which was significantly inferior compared to the control tumors, the tumors derived from MMRN2-transfected cells displayed extended hypoxic regions **(Fig. 15a-b)**.

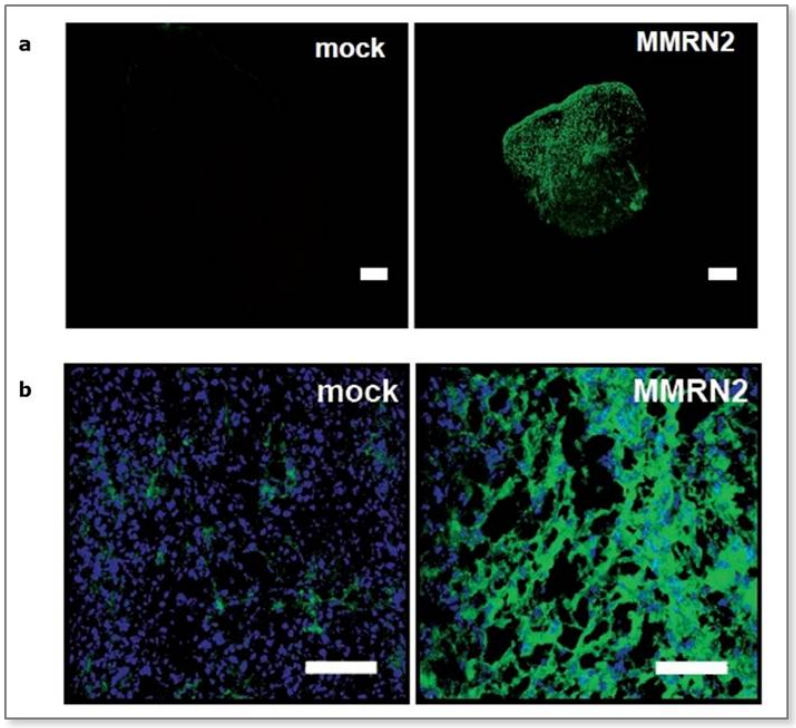

Fig. 15 Tumor expressing MMRN2 present extended hypoxic areas. a) Representative images of the tumor hypoxic areas as detected with the hypoxyprobe-1 on tumor sections from mock and MMRN2-transfected HT1080 cells, scale bars: 500 mm. **b)** High magnification images of the tumor hypoxic areas detected as above. Nuclei are stained with TO-PRO-3 dye, scale bars: 75 µm.

To verify whether in the tumor microenviroment MMRN2 could be associated with VEGF-A/VEGFR2 axis, we analyzed the localization of VEGF-A bound to VEGFR2 on tumor section from mock and MMRN2-transfected HT1080 cells.

To this end we used the anti-CD31 antibody as marker of blood vessels and the Gv39M antibody specifically recognizing the VEGFR2-bound VEGF-A. The Gv39M antibody revealed a diffuse staining in the tumors expressing MMRN2, also in areas distant from the CD31-positive blood vessels **(Fig. 16a-b)**.

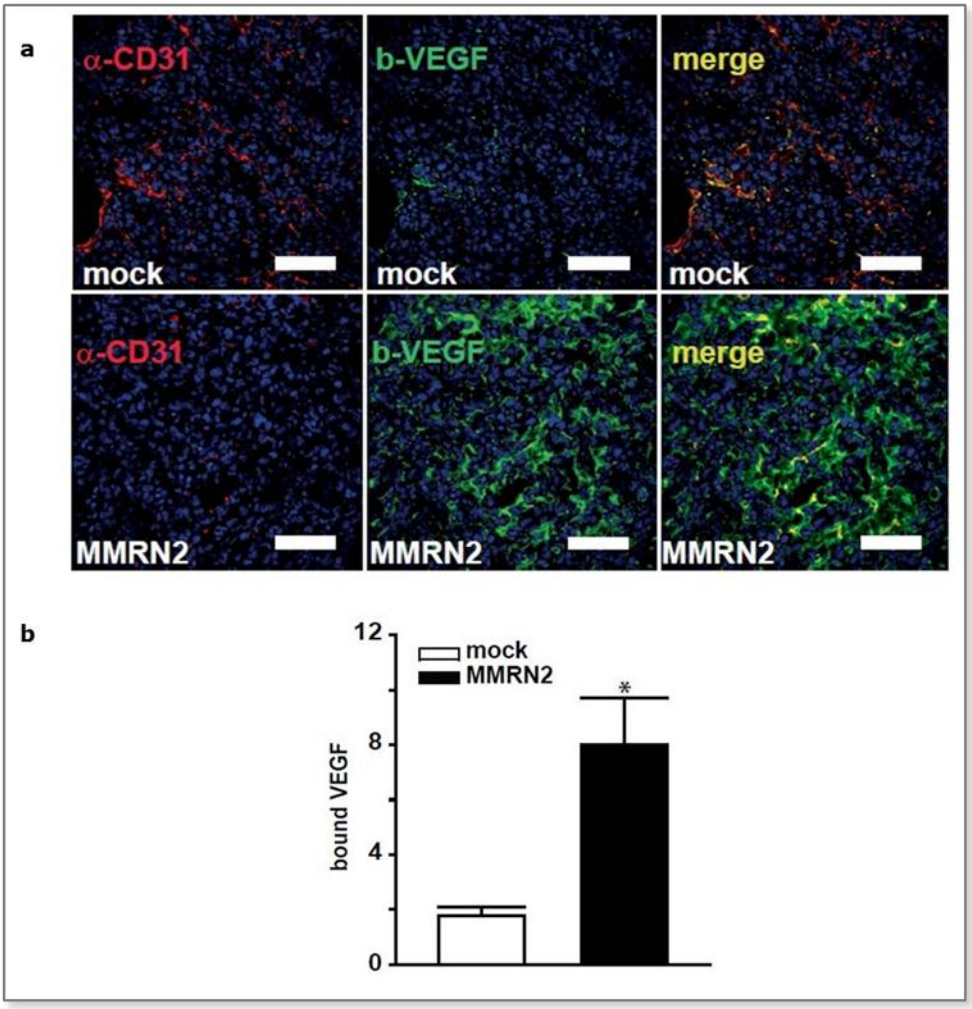

Fig. 16 VEGF-A co-localizes with MMRN2. a) Representative pictures of the immunofluorescence analysis of blood vessels (α-CD31) in mock and MMRN2-positive tumors using the Gv39M antibody to detect bound-VEGF-A (b-VEGF). Nuclei are stained with the TO-PRO-3 dye, scale bars: 75 mm. **b)** Graph representing the quantitative analysis of VEGF-A staining (pixel area) from mock and MMRN2-positive tumors (*P=0.008).

Next, we performed an ELISA test coating recombinant VEGFR2 or MMRN2 (5 µg/ml) and incubating with soluble VEGF; the binding was detected by the primary antibody Gv39M. We demonstrated that the Gv39M antibody also detected the MMRN2-bound VEGF-A **(Fig. 17a)**. In addition we carried out an immunofluorescence analysis on the mock and MMRN2-positive tumor sections using the polyclonal anti-human MMRN2 affinity purified antibody (α-hMMRN2) and the Gv39M antibody. The antibodies revealed that the VEGFR2-bound VEGF-A mainly co-localized with recombinant MMRN2 produced by the transfected HT1080 cells **(Fig. 17b)**, suggesting that MMRN2 may function by sequestering VEGF-A and preventing VEGF-A/VEGFR2 interaction.

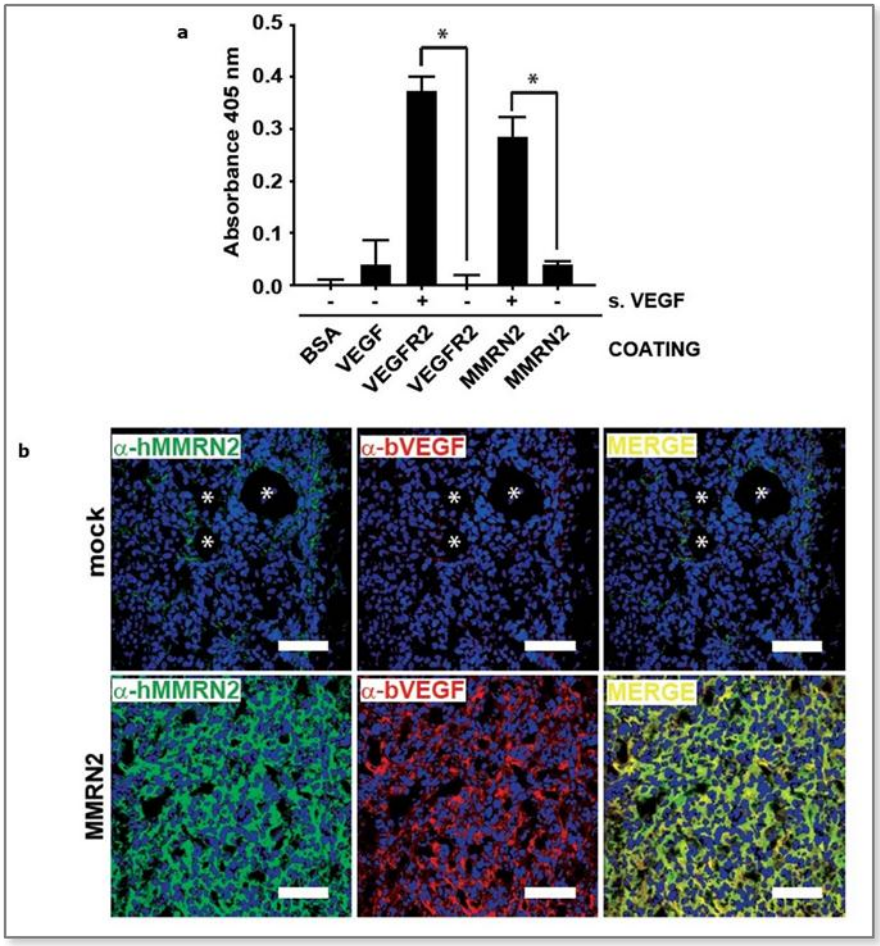

Fig. 17 Sequestration of VEGF-A by MMRN2 in the tumor microenviroment. a) Graph representing the ELISA test performed following the coating of recombinant VEGFR2 and MMRN2 (0,5 µg/well) on 96 well and incubation with soluble VEGF-A (100ng/well). The detection of the VEGFR2-bound VEGF-A was achieved by means of the Gv39M antibody. (*$P \leq 0.0039$). **b)** Representative images of the immunofluorescence staining performed on mock and MMRN2-positive tumor sections using the α-hMMRN2 and the Gv39M antibody. Nuclei are stained with TO-PRO-3 dye. Scale bars: 75 µm.

2. ROLE OF MMRN2 IN BLOOD VESSEL FORMATION AND HOMEOSTASIS

The data reported above and recently published (Lorenzon E. *et al.*, 2012) prompted us to further study the involvement of MMRN2 in the regulation of VEGF signaling and in general in the regulation of blood vessel formation and homeostasis.

In the second part of this thesis I will report new preliminary data generated with the aim of addressing a number of questions that, in part, still remain open:

1. Is MMRN2 involved in the regulation of other specific VEGFR2 phosphorylation sites or other downstream molecules of VEGF-A/VEGFR2 pathway?
2. Can MMRN2 bind to other member of the VEGF family or other growth factor involved in angiogenesis?
3. Which is the region of the molecule responsible for these effects?
4. Must MMRN2 be degraded to allow an efficient sprouting of ECs?

2.1 MMRN2 BLOCKS THE VEGF-A-DRIVEN VEGFR2 PHOSPHORYLATION AT Y1214

First we have questioned whether the presence of MMRN2 affected VEGFR2 activation through the phosphorylation of other tyrosine residues in the intracellular region. In particular, given the major influence of MMRN2 in EC migration, we have analyzed the phosphorylation of Y1214, a key site regulating the activation of different molecules involved in cell migration, actin remodeling and vascular permeability (Lamalice L. *et al*., 2004). To this end, HUVEC cells were incubated with VEGF-A (10 ng/ml) and MMRN2 (5 µg/ml) for 2, 4, 8 and 16 minutes. Cells were lysed and the Y1214 phosphorylation assessed by Western blot using a specific antibody. As shown in **Fig. 18**, we have found that MMRN2 down-regulates also the VEGFR2 receptor phosphorylation at Try1214. Accordingly the down-modulation of VEGFR2 phosphorylation was accompanied by a strong inhibition of the phosphorylation of p38, a molecule downstream of the VEGF-A/VEGFR2 pathway involved in the regulation of cell migration **(Fig. 18)**.

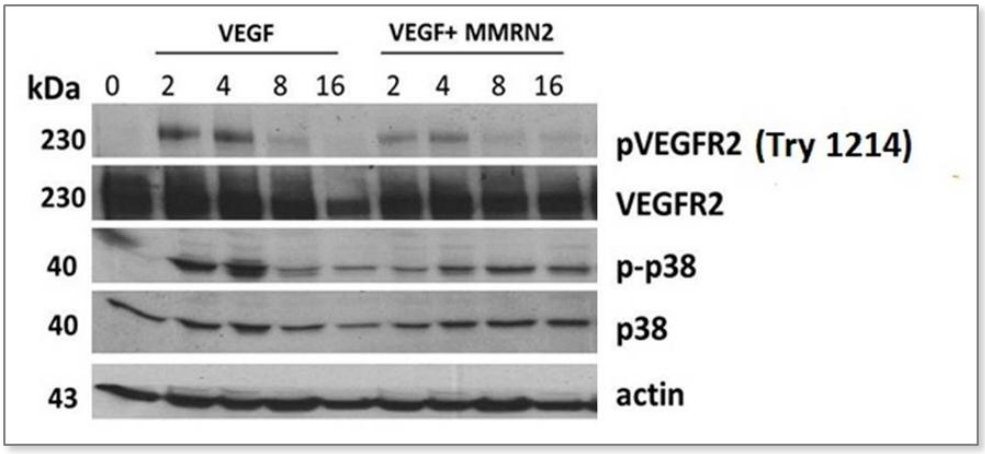

Fig. 18 MMRN2 down-regulates the phosphorylation of VEGFR2 at Y1214 and of p38. Western blot analysis of the phosphorylation of VEGFR2 at Y1214 and of p38 following treatment of HUVEC cells with VEGF-A with or without MMRN2 for different time intervals expressed in minutes. Both the total and the phosphorylated forms of VEGFR2 and p38 were analyzed with specific antibodies. Actin was used as a normalizer of protein loading.

2.2 MMRN2 DOES NOT BIND VEGF-B AND PlGF

We have next evaluated whether the binding of MMRN2 was specific for VEGF-A or if the molecule could also bind to other members of the VEGF family. In particular we have evaluated the binding of VEGF-B and PlGF to MMRN2 by means of ELISA assays. 96 well plates were coated with recombinant MMRN2 (0,5 µg/well) and incubated with soluble VEGF-B and PlGF (150 ng/well) and their binding assessed with specific antibodies. Our preliminary data indicate that the binding is specific for VEGF-A since VEGF-B and PlGF did not lead to any specific signal in the ELISA tests **(Fig.19)**.

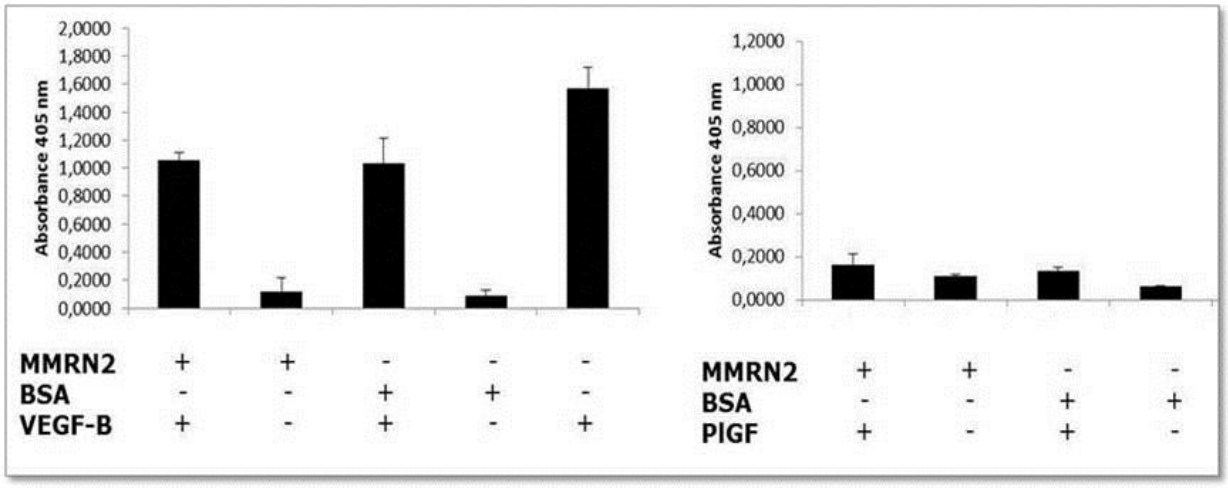

Fig. 19 MMRN2 does not interact with other members of the VEGF family. Graphs representing the absorbance detected following ELISA test following immobilization of MMRN2 (0,5µg/well) or BSA incubation with soluble VEGF-B and PlGF (150ng/well).

2.3 THE N-TERMINAL REGION OF MMRN2 RETAINS THE WHOLE MOLECULE ANTI-MIGRATORY EFFECTS

In order to discover the region of MMRN2 responsible for the anti-angiogenic effects, we have generated a series of deletion mutants. In particular we have generated the fragments: Δ1 (aa residues 24 to 134), Δ2 (aa residues 135 to 949) and Δ3 (aa residues 369 to 949) **(Fig. 20a)**. These fragments were expressed in 293-EBNA cells and we have verified the expression of the molecules by Western blot analysis (data not shown). Since the expression of the fragment Δ2 failed, we have generated a new fragment identified as Δ1-2 encompassing both the Δ1 and the Δ2 regions.

The recombinant fragments were then tested for their ability to inhibit EC migration. For this purpose type I collagen and MMRN2, which served as positive and negative controls respectively, and the different mutants (Δ1, Δ1-2 and Δ3) were coated at equimolar concentrations (37,5 nM) on the upperside of the Transwell membranes. HUVEC cells were then placed on the top of the inserts' membranes and the cells let migrate towards the VEGF-A stimulus (10 ng/ml). As shown in **Fig. 20b**, the Δ1 and Δ1-2 fragments were able to significantly inhibit EC migration similarly to the effect exerted by the whole molecule.

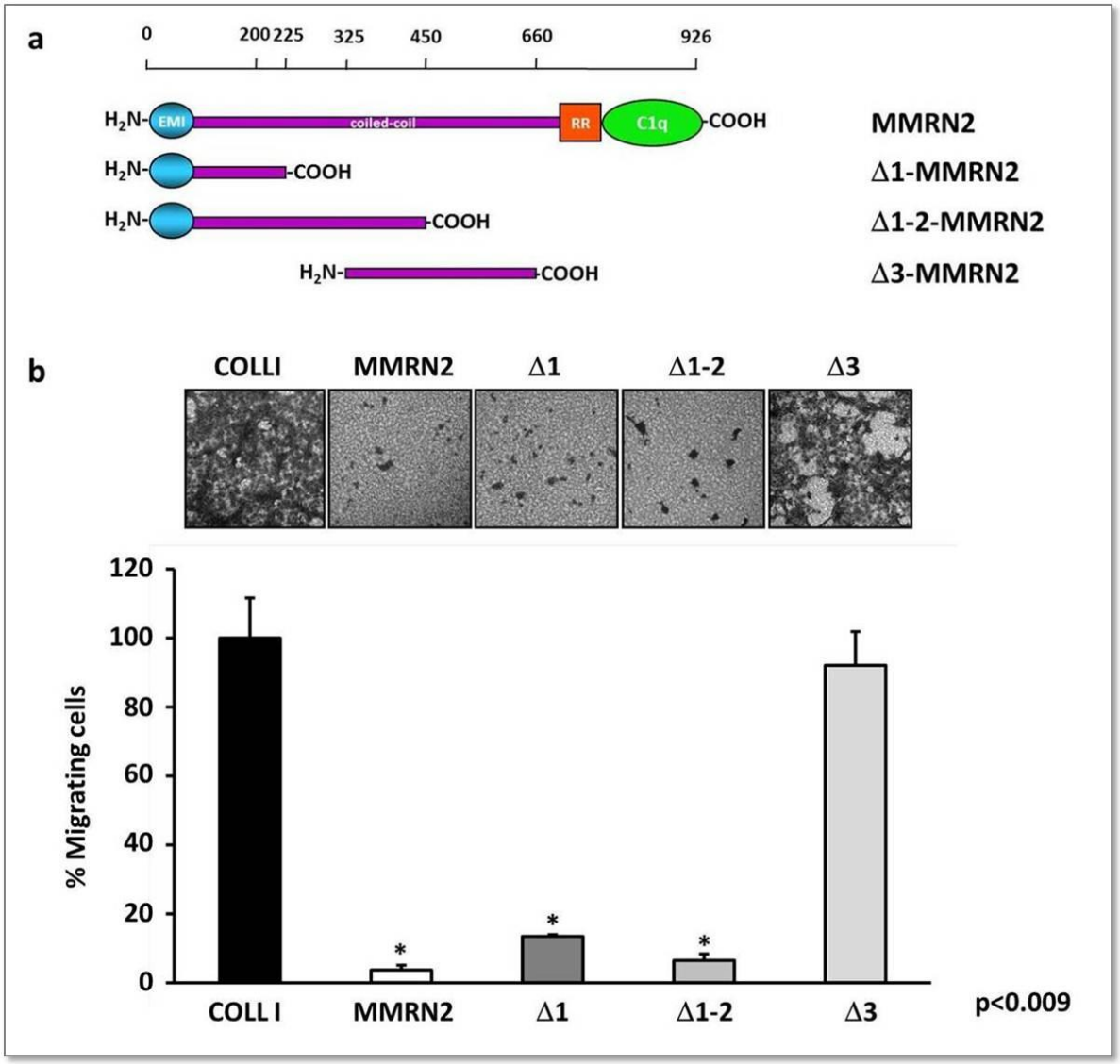

Fig. 20 The region of MMRN2 included between Δ1 and Δ1-2 fragments reduces EC migration. a) Schematic representation of the MMRN2 deletion mutants. **b)** Images representing the migration test toward a VEGF-A stimulus performed using HUVEC cells following transwell's membranes coating with type I (coll I), MMRN2 or the different mutants (Δ1, Δ1-2 and Δ3).

2.4 MMRN2 AFFECTS VEGFR2 DISTRIBUTION ON THE EC SURFACE

Another mechanisms modulating EC function during angiogenesis is the regulation of the availability of the VEGFR2 receptor on the EC surface. We thus questioned whether MMRN2 could also modulate the exposure of VEGFR2 at the EC plasma membrane. For this purpose we have treated HUVEC cells with recombinant MMRN2 (5 µg/ml) following stimulation with VEGF-A (10 ng/ml) for 20 minutes and performed an immunofluorescence analysis for VEGFR2 and actin stress fibers distribution. As shown in **Fig. 21**, the presence of MMRN2 led to a decreased amount of thick stress fibers, structures involved in cell motility. Furthermore MMRN2 also led to an impairment of VEGFR2 expression on the EC surface, the majority of which was present in peri-nuclear structures similarly to the control cells.

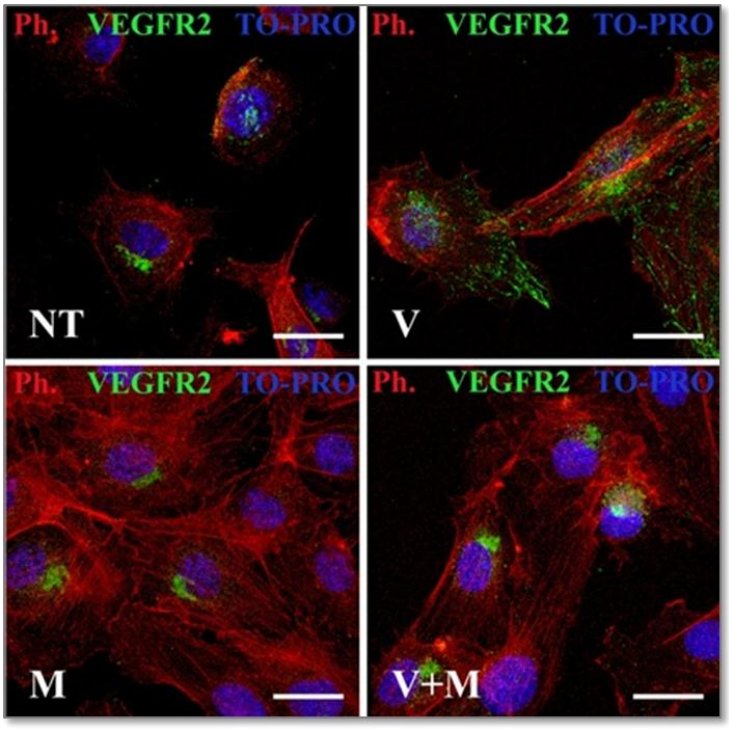

Fig. 21 MMRN2 affects the availability of VEGFR2 on the EC surface. Images representing the immunofluorescence analysis of HUVEC treated with VEGF-A (V) MMRN2 (M) or both (V+M) for 20 min and stained with phalloidin (Ph) and the anti-VEGFR2 antibody. Nuclei were stained with TO-PRO-3. Scale bar: 23.8 µm.

2.5 MMRN2 IMPAIRS THE SPROUTING OF NEW VESSELS IN A 3D CONTEXT

To further investigate on the role of MMRN2 in angiogenesis we have set up a recently described test to verify the development of novel sprouts in a 3D context. This assay will serve for future experiments to simply assess the development on new vessels in a more sophisticated setting in which easily manipulate the expression of different molecules/factors and simultaneously include other cell types involved in vessel formation, such as smooth muscle cells and pericytes. To set up the 3D *in vitro* angiogenesis assay, HUVEC cells were coated onto cytodex microcarriers and embedded into a fribrin gel with or without recombinant MMRN2 (5 µg/ml or NT). The gel was then overlayed with Normal Human Dermal Fibroblasts (NHDF). The plates containing the spheroids were then incubated for 7 days. Following the incubation the structures were fixed and stained with anti-CD31 antibody. As shown in **Fig. 22**, while control spheroids developed numerous and long vessels' sprouts, spheroids treated with MMRN2 failed to form novel vessels, confirming that the over-expression of this molecule significantly impairs angiogenesis also in this experimental setting.

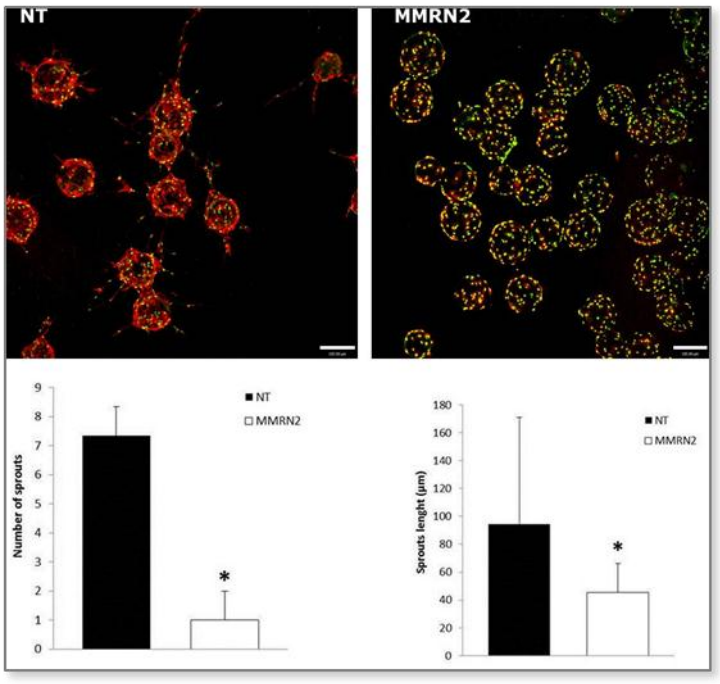

Fig. 22 Recombinant MMRN2 induces a striking reduction of the vessels' sprouts in a 3D setting. a) Representative images obtained following a 3D *in vitro* angiogenesis assay using HUVEC cells coated onto cytodex microcarriers and embedded into a fribrin gel with or without (NT) MMRN2. Spheroids were

stained with α-CD31 (vessels) and SYTOX (nuclei). **b)** Graphs representing the evaluation of the number (*P=0,04) and the length (*P=0,01) of the sprouts as assessed by the Volocity 3D software. Values represent the mean ± s.d. of three independent experiments.

Taken together, the experimental evidences that we have so far generated suggest that MMRN2 may represent a key molecule that stabilizes blood vessels following their formation. Once deposited, MMRN2 may be conceived as an homeostatic molecule that, unless degraded, obstructs the formation of new vessels. To try to address this question, we have recently set up both *in vitro* and *in vivo* studies, in this last case exploiting the C57BL/6 mouse model.

2.6 MMRN2 MAY BE DEGRADED FOLLOWING A VEGF-A STIMULUS

It is known that the angiogenic stimulus induces the activation of several proteases that degrade the ECM and allow the movement of ECs to form new vessels (Iruela-Arispe M.L. *et al*., 2009).

To verify if MMRN2 is a target molecule for degradation in this context we treated HUVEC cells with VEGF-A (100 ng/ml) for different time interval in the presence or not of metalloproteinases inhibitors, and analyzed the putative decrease of the full-length MMRN2 by Western blot analysis. Our preliminary results indicate that, indeed, the treatment with VEGF-A significantly reduces the levels of the full-length MMRN2, as detected by Western blot analysis **(Fig. 23)**. Interestingly, this decrease is abolished by the presence of the metalloproteinase inhibitor GM6001, indicating that the decreased levels of MMRN2 are due to protein degradation rather than impaired synthesis. Further experiments will be necessary to verify this finding and identify the putative cleavage site(s).

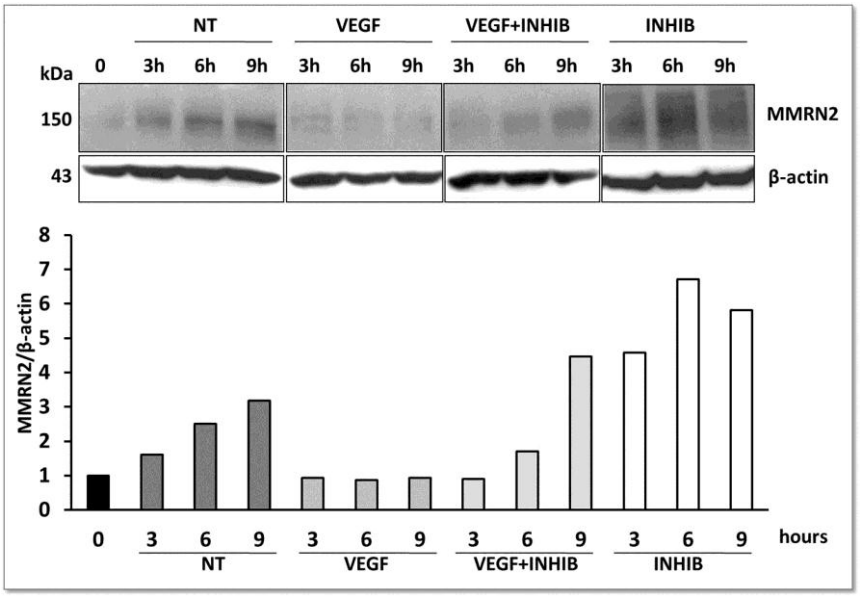

Fig. 23 MMRN2 is degraded following an angiogenic stimulus. Western blot analysis of MMRN2 expression following treatment of HUVEC cells with VEGF-A with or without metalloproteinases inhibitors (INHB) for different time intervals expressed in hours (h). A specific polyclonal antibody was used to detect the MMRN2 band. Actin was used as a normalizer of protein loading.

Based on these preliminary results, it is conceivable to hypothesize that MMRN2 may be deposited at the late stages of blood vessel formation to stabilize the newly formed structures. Only in the presence of a strong angiogenic stimulus the protein could be degraded to allow new blood vessel formation. In order to address this point we have recently started to take advantage of the mouse aortic ring and retina models.

In particular aortic rings from wild type C57BL/6 mice were isolated and cultivated on rat type I collagen containing VEGF-A to induce the sprouting of new vessels. The rings were whole mounted and stained with the anti-VEGFR2 and anti-MMRN2 antibody. As indicated in **Fig. 24**, the tips of the newly formed vessels display a faint staining for MMRN2, suggesting that the tips of the sprouting ECs are devoid of MMRN2 to allow an efficient migration of these cells to form new blood vessels. On the contrary, the formed vessels more adjacent to the ring are already surrounded by MMRN2.

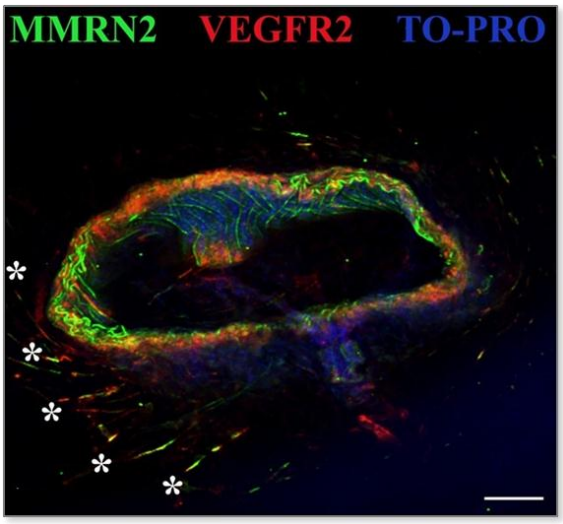

Fig. 24 New vessel sprouts are devoid of MMRN2. Representative image of the immunofluorescence analysis of whole mounted aortic rings from C57BL/6 mice cultivated on rat type I collagen in the presence of VEGF-A. The rings were stained with α-MMRN2 and α-VEGFR2 antibodies and the nuclei with TO-PRO-3. The lack of MMRN2 expression along the tips of the newly vessels is indicated by an asterisk. Scale bar: 150 μm.

These findings are in accordance with the preliminary results so far collected with the staining performed of the retinas collected from C57/BL6 pups or adult animals. In fact, while the vessels of the retinas from adult animals display a strong staining for MMRN2, retinas from P3 pups display only a faint staining mostly localized adjacent to the stock cells. Similarly to what observed in the aortic ring assays the tip cells do not display staining for MMRN2 **(Fig. 25)**.

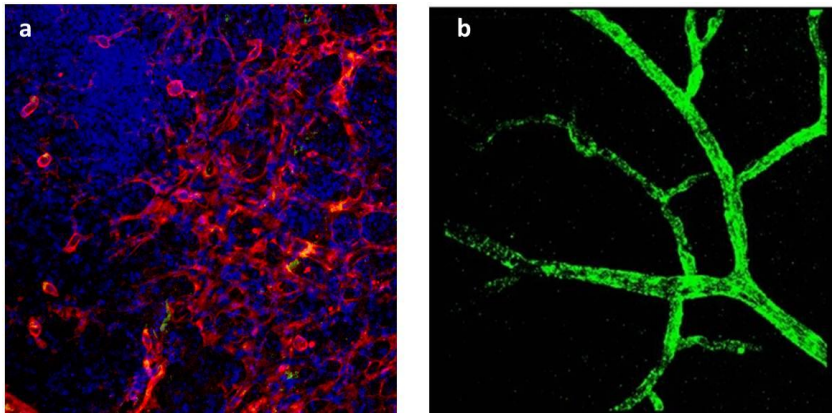

Fig. 25 MMRN2 may be deposited only in the late stages of blood vessels formation. Images of the immunofluorescence analysis performed on the whole mounted retinas from P3 C57BL/6 pups **(a)** and adult mice **(b)** stained with anti-MMRN2 (green) antibody and with isolectin B for vessels (red).

Taken together, the results presented in the last session of this thesis suggest that MMRN2 can be considered an homeostatic molecule that maintains the blood vessel integrity: it is deposited in the last stages of blood vessel development and must be degraded to allow an efficient sprouting of novel vessels.

DISCUSSION

The subject of investigation of my PhD program was to identify the putative role of the ECM protein MMRN2 in the regulation of the angiogenic processes. I mainly focused on two different aspects: first, the effect of MMRN2 in modulating ECs behavior and hence the formation of new vessels, in particular in the context of tumor growth; second, the possible role of this protein in maintaining blood vessels' homeostasis. These two aspects will be discussed separately.

1. Role of MMRN2 in the regulation of ECs behavior and angiogenesis.

The strategic deposition of this molecule along the blood vessels and in tight association with ECs (Christian S.*et al.*, 2001) prompted us to hypothesize that MMRN2 could affect EC behavior and therefore play a key role in the regulation of angiogenesis.

The manipulation of MMRN2 expression in HUVEC cells did not affect their proliferation or their apoptotic rate. By contrast, MMRN2 significantly impaired ECs motility. This effect reflected on a significant impairment of the development of new blood vessels in a number of *in vitro*, *ex vivo* and *in vivo* tests that we have performed, including tubulogenesis on matrigel, aortic ring assays and CAM assays.

These striking effects prompted us to investigate on the molecular mechanisms underlying the anti-angiogenic properties of MMRN2. For this purpose we carried out a broad analysis of the activation of an array of RTKs present on the EC surface and found that the over-expression of MMRN2 induced a prominent down-regulation of VEGFR1 and VEGFR2. Since VEGFR2 accounts for most of the VEGF-A effects on adult ECs (Waltenberger J. *et al*., 1994), we have subsequently concentrated our investigations on the role of MMRN2 in the regulation of VEGFR2 activation. Specifically we have demonstrated that MMRN2 acted by down-regulating the phosphorylation of Tyr1175, which is well known to be also implicated in the regulation of EC migration (Holmqvist K. *et al.*, 2004). In addition, the treatment of HUVEC cells with MMRN2 reduced the phosphorylation of FAK, a molecule known to be down-stream of VEGFR2 signaling which plays a leading role in focal adhesion turnover and cell migration (Abedi H. *et al*., 1997). Taken together, these biochemical data supported the finding that MMRN2 mainly affected the motility of ECs and are in line with our *in vitro* and *in vivo* findings.

The reason why MMRN2 did not alter the proliferation of EC exclusively affecting their migratory potential, remains unclear. This property is unique, in fact most of the ECM molecules that alter VEGFR2 activation also impinge on EC proliferation (Kupprion *et al.*, 1998). Our hypothesis is that this outcome may depend on a simultaneous activation of other molecules affecting cell proliferation in a positive way. This hypothesis is supported by the fact that, unlike that of FAK, the phosphorylation of Erk 1/2 is not altered by the manipulation of MMRN2 expression (data not shown). The complex and multiple regulations that may be exerted by MMRN2, not only on ECs but also on other cell types including smooth muscle cells and pericytes, are likely given the complex multi-domain arrangement of this molecule.

To shed light on the possible mechanisms by which MMRN2 could impair VEGFR2 activation, we verified if MMRN2 could act by sequestering the ligand for this receptor by radioligand displacement assays. MMRN2 indeed displaced ^{125}I-VEGF-A from the EC surface and also from the recombinant extracellular region of VEGFR2 in solid phase assays, suggesting that the MMRN2-driven down-regulation of VEGFR2 signaling could likely depend on an impairment of the VEGF-A/VEGFR2 interaction. The interference of MMRN2 with the VEGF-A/VEGFR2 complex was due to the direct binding of VEGF-A to MMRN2, as demonstrated by ELISA assay. This finding is relevant since, given the tight contact of MMRN2 with ECs, MMRN2 may attain a high pericellular concentration and thus represent an important competitor for the binding of VEGF-A to VEGFR2. In truth, the relatively low density of this receptor on the cell surface (˜10.000–25.000 molecules/cell) (Hotz B.*et al*., 2010) fits with this hypothesis. Thus, the fact that MMRN2 exerted anti-angiogenic effects also in experimental settings where the addition of VEGF-A was not required, could depend on the blockade of endogenous VEGF-A released by the ECs (Roccaro A.M. *et al*., 2006). In fact, for instance, the sprouting of novel vessels in aortic ring assays is highly dependent on endogenously released VEGF-A (Ligresti G. *et al*., 2011). Nonetheless, it cannot be excluded that MMRN2 may affect other molecular pathways or also act on different cell types, when present in the experimental setting.

The promising results obtained *in vitro* and *ex vivo*, prompted us to evaluate whether the dramatic decrease of blood vessel formation induced by MMRN2 could reflect on an impairment of tumor growth *in vivo*. The over-expression of MMRN2 by a sarcoma cell line induced a remarkable decrease of tumor growth when injected in nude mice, in most cases leading to an almost complete regression of the tumor masses. This outcome could have been due to an impingement of the blood supply as our *in vitro* and *ex vivo* data suggested, but also on a direct tumor-

suppressive effect on cancer cells. This second possibility was ruled out by the fact that the ectopic over-expression of MMRN2 did not affect the tumor cell proliferation or viability, reinforcing the likelihood that MMRN2 acted in an indirect way by limiting the development of new vessel to support tumor growth. This hypothesis was corroborated by the analysis of the tumor sections: tumors derived from MMRN2 over-expressing cells displayed a substantial reduction of the blood vessel density suggesting that the lack of an efficient tumor vascularization accounted for the reduced tumor growth. In accordance with these findings, the tumors derived from MMRN2-transfected cells were characterized by extensive hypoxic areas. Furthermore, these tumors displayed a decreased pericyte coverage, thus the reduced maturity of these vessels likely implies a diminished efficiency of these vessels in transporting oxygen and nutrients to support tumor growth. These results in addition to support our results pinpointing MMRN2 as a key regulator of tumor-associated angiogenesis, also suggest that this molecule may also affect the recruitment of pericytes.

The pivotal role of the VEGF-A/MMRN2 interaction in impairing the VEGF-A/VEGFR2 axis *in vivo* and tumor angiogenesis was corroborated by the use of the Gv39M antibody which recognizes only the VEGFR2-bound VEGF-A. Staining of the tumor sections with the Gv39M antibody demonstrated that MMRN2 and VEGF-A co-localized *in vivo*. More importantly in solid phase assays the antibody was able to recognize not only the VEGFR2-bound VEGF-A, but also the MMRN2-bound VEGF-A. This outcome suggests that the binding to MMRN2 is specific and leads to a conformational change of VEGF-A that allows the recognition by the Gv39M antibody, similarly to what occurs following the VEGFR2/VEGF-A interaction. These results indicated that the sequestration of VEGF-A by MMRN2 in tumor microenviroment may prevent the interaction with VEGFR2 leading to a decreased intra-tumoral angiogenesis and consequent impaired tumor growth.

Interestingly, database analysis of MMRN2 expression (www.oncomine.org) indicates that this molecule is differentially expressed in many types of tumors such as brain, breast, kidney and sarcomas, if compared with the normal counterpart. Many of these tumors are highly dependent on angiogenesis. Thus it is conceivable that the dysregulation of MMRN2 expression, through the impingement of the intra-tumoral vascularization, might have an impact on tumor progression.

Taken together these findings are in line with the knowledge that angiogenesis is indispensable for tumor growth (Folkman J.*et al.*, 1971). Based on this hypothesis a novel therapeutic approach

aimed at eradicating tumor vasculature has been proposed to improve patients' survival. Dr. Judah Folkman has been a pioneer in this field of research and for the first time in 1971 he hypothesized the possibility to halt tumor growth developing a new class of drugs: the inhibitors of angiogenesis. Many antiangiogenic therapies have been developed ever since and some of them have entered the clinical practice. However, the use of an antiangiogenic treatment as a single drug has been found to have little or no efficacy (Ribatti D., 2010). For this reason antiangiogenic drugs are exclusively used in combination with conventional chemotherapy. Moreover antiangiogenic drugs have not produced enduring efficacy in terms of either tumor decrease or dormancy or long-term survival; rather, the common result is a delayed tumor progression followed by a period of clinical benefit, which is suggestive of an emergent resistance to the therapy (Paez-Ribes M. *et al.*, 2009). It is therefore necessary to develop new tools to block tumor angiogenesis. In this context the ECM is a direct source of angiogenesis regulatory factors, both stimulators and inhibitors. Major endogenous inhibitors of angiogenesis are matrix molecules or matrix-derived fragments (Bellotti D. *et al.,* 2011). Considering the inhibitory role exerted by MMRN2 in vessel development, we can hypothesize that this molecule, or its putative region responsible for the antiangiogenic effects, may represent a potentially novel and powerful tool for the development of new anti-angiogenic drugs to be employed for cancer treatment.

2. Putative role of MMRN2 in the maintenance of blood vessel integrity

The finding that MMRN2 is an antiangiogenic molecule has given rise to many questions. How does MMRN2 affect EC motility rather than proliferation? Does MMRN2 bind other members of the VEGF family? Which is the region of the molecule responsible for its effects? Must MMRN2 be degraded to allow an efficient sprouting of ECs?

We have so far generated preliminary unpublished results have begun to address some of these questions.

Fist we have verified that MMRN2 reduces also the phosphorylation of Tyr1214 on VEGFR2. This result further reinforces our finding indicating that MMRN2 mostly impairs EC motility, in fact this Tyr1214 is a key site regulating cell migration, actin remodeling and vascular permeability

(Lamalice L. *et al.*, 2004). Accordingly, the down-modulation of Tyr1214 phosphorylation was accompanied by the inactivation of p38, a molecule required for the remodeling of the cytoskeleton occurring to drive actin-based motility (Huttenlocher A. *et. al*., 1995). Thus the inactivation of p38 by may block actin polymerization and reorganization into stress fibers hampering EC motility.

To verify if MMRN2 could bind other members of the VEGF family, we carried out a series of sandwich ELISA test. So far we excluded an interaction with VEGF-B and PlGF, however we will also test other important growth factors as VEGF-C and VEGF-D, which are known to bind VEGFR2 and VEGFR3 (Tammela T.*et al.*, 2005); a possible binding to these factors may further explain the potent anti-angiogenic properties of MMRN2.

In order to dissect the discrete MMRN2 region responsible for the interaction with VEGF-A and for the consequent antiangiogenic effects, we generated a series of deletion mutants of MMRN2 which were tested in migration assays. We found that the region included between Δ1 and Δ1-2 fragments were able to significantly inhibit EC motility similarly to the effect exerted by the whole protein. In order to find an efficient tool to be employed in cancer therapy, we will further dissect this region creating a peptide library of overlapping fragments and evaluate their anti-angiogenic effects.

More recently we have identified a possible mechanism by which MMRN2 may impair VEGFR2 activation: the treatment with MMRN2 induced a reduction of the VEGFR2 from EC plasma membrane. Indeed despite the VEGF-A stimulus VEGFR2 remained mainly perinuclear in the presence of MMRN2 and thus not available for the binding with its ligand. This finding opens the possibility that MMRN2 may regulate VEGFR2 activation not only though the binding to VEGF-A but also affecting the availability of the receptor on the EC surface. This finding is particularly interesting since a putative therapeutic use of this molecule/fragment may allow a simultaneous blockage of both the ligand and the receptor. In addition, following the treatment, ECs showed a decrease of the actin stress fibers, corroborating the findings that MMRN2 regulates ECs migration by inhibiting VEGFR2 pathway.

Taken together these results support the hypothesis that MMRN2 may function as an homeostatic molecule; once deposited MMRN2 may stabilize the blood vessels counteracting the sprouting of new vessels. In this scenario, only a strong angiogenic stimulus and the consequent activation of metalloproteinases by ECs may allow the destruction of this molecule and an efficient sprouting of

novel vessels. This hypothesis is supported by our results generated both *in vitro*, where we observed a significant decrease of MMRN2 following treatment of EC with VEGF-A, as well as in *ex vivo* tests; indeed the tips of the newly form vessels departing from aortic rings embedded in type I collagen matrices are devoid of MMRN2. In accordance with these findings also the developing retinas from P3 pups display a weak MMRN2 deposition as opposed to retinas from adult mice, suggesting that MMRN2 may be deposited only in the final stages of blood vessel development contributing to their stabilization.

In conclusion, with these findings we provided preliminary evidences suggesting that MMRN2 may represent a novel key homeostatic molecule indispensable for the maintenance of blood vessel integrity. In this view MMRN2 may function as a 'biological barrier' keeping ECs in a steady-state condition; in this case only the decrease of the MMRN2 protein levels likely due to the activation of proteases may allow an efficient sprouting out ECs to form new blood vessels.

REFERENCES

Abe R, Shimizu T, Yamagishi S, Shibaki A, Amano S, Inagaki Y, Watanabe H, Sugawara H, Nakamura H, Takeuchi M, Imaizumi T, Shimizu H. Overexpression of pigment epithelium-derived factor decreases angiogenesis and inhibits the growth of human malignant melanoma cells in vivo. *Am J Pathol* 2004 164:1225-1232.

Abedi H., Zachary I. Vascular endothelial growth factor stimulates tyrosine phosphorylation and recruitment to new focal adhesions of focal adhesion kinase and paxillin in endothelial cells. *J. Biol. Chem*. 1997 272, 15442–15451.

Adam F, Zheng S, Joshi N, Kelton DS, Sandhu A, Suehiro Y, Jeimy SB, Santos AV, Massé JM, Kelton JG, Cramer EM, Hayward CP. Analyses of cellular multimerin 1 receptors: in vitro evidence of binding mediated by alphaIIbbeta3 and alphavbeta3. *Thromb Haemost*. 2005 94(5):1004-11.

Adams JC, Lawler J. The thrombospondins *Int J Biochem Cell Biol* 2004 36:961-968.

Amma LL, Goodyear R, Faris JS, Jones I, Ng L, Richardson G, Forrest D. An emilin family extracellular matrix protein identified in the cochlear basilar membrane. *Mol Cell Neurosci* 2003 23(3):460-72

Armstrong LC, Bjorkblom B, Hankenson KD, Siadak AW, Stiles CE, Bornstein P. Thrombospondin 2 inhibits microvascular endothelial cell proliferation by a caspase-independent mechanism *Mol Biol Cell* 2002 13:1893-1905

Armstrong LC, Bornstein P. Thrombospondins 1 and 2 function as inhibitors of angiogenesis *Matrix Biol* 2003 22:63-71

Baker M, Robinson S.D, Lechertier T, Barber P.R, Tavora B, D'Amico G, Jones D.J, Vojnovic B, Hodivala-Dilke K. Use of the mouse aortic ring assay to study angiogenesis *Nature Protoc.* 2012 7: 89–104.

Bazzoni G, Dejana E. Endothelial cell-to-cell junctions: molecular organization and role in vascular homeostasis. *Physiol Rev.*2004 84(3):869-901.

Belotti D, Foglieni C, Resovi A, Giavazzi R, Taraboletti G. Targeting angiogenesis with compounds from the extracellular matrix. *Int J Biochem Cell Biol.* 2011 43(12):1674-85.

Bikfalvi A. Significance of angiogenesis in tumour progression and metastasis. *Eur J Cancer*.1995 31A(7-8):1101-4.

Bingle L, Brown NJ, Lewis CE. The role of tumour-associated macrophages in tumour progression: implications for new anticancer therapies. *J Pathol*. 2002 196(3):254-65.

Bissell MJ, Kenny PA, Radisky DC. Microenvironmental regulators of tissue structure and function also regulate tumor induction and progression: the role of extracellular matrix and its degrading enzymes. *Cold Spring Harb Symp Quant Biol.* 2005 70:343-56.

Bix G, Iozzo RV. Matrix revolutions: "tails" of basement-membrane components with angiostatic functions. *Trends Cell Biol*.2005 15(1):52-60.

Braghetta P, **Ferrari A, De Gemmis P, Zanetti M, Volpin D, Bonaldo P, Bressan GM.** Overlapping, complementary and site-specific expression pattern of genes of the EMILIN/Multimerin family. *Matrix Biol*. 2004 22(7): 549-56

Braghetta P, Ferrari A, De Gemmis P, Zanetti M, Volpin D, Bonaldo P, Bressan GM. Expression of the EMILIN-1 gene during mouse development. *Matrix Biol*. 2002 21(7):603-9

Bressan GM, Daga-Gordini D, Colombatti A, Castellani I, Marigo V, Volpin D. Emilin, a component of elastic fibers preferentially located at the elastinmicrofibrils interface *J Cell Biol* 1993 121(1):201-12

Bronisz A, Godlewski J, Wallace JA, Merchant AS, Nowicki MO, Mathsyaraja H, Srinivasan R, Trimboli AJ, Martin CK, Li F, Yu L, Fernandez SA, Pecot T, Rosol TJ, Cory S, Hallett M, Park M, Piper MG, Marsh CB, Yee LD, Jimenez RE, Nuovo G, Lawler SE, Chiocca EA, Leone G, and

Ostrowski MC. Reprogramming of the tumour microenvironment by stromal PTEN-regulated miR-320. *Nat Cell Biol.* 2012 14: 159-167.

Carmeliet P. Blood vessels and nerves: common signals, pathways and diseases. *Nat Rev Genet.* 2003 4(9):710-20.

Carmeliet P., Mackman N., Moons L. Role of tissue factor in embryonic blood vessel development. *Nature 1996* 6595: 73–75.

Castellani P., Borsi L., Carnemolla B., Biro A., Dorcaratto A., Viale GL., Neri D.,Zardi L. Differentiation between high and low-grade astrocytoma using a human recombinant antibody to the extra domain-B of fibronectin *Am J Pathol* 2002 161:1695-1700

Chekenya M, Hjelstuen M, Enger P, Thorsen F, Jacob AL, Probst B, Haraldseth O,Pilkington G, Butt A, Levine JM, Bjerkvig R. NG2 proteoglycan promotes angiogenesis-dependent tumor growth in CNS by sequestering angiostatin *FASEB J* 2002 16:586-588.

Chua CC, Hamdy RC, Chua BH. Upregulation of vascular endothelial growth factor by H2O2 in rat heart endothelial cells. *Free Radic Biol Med.* 1998; 25:891–897.

Chung AS, Lee J, Ferrara N. Targeting the tumour vasculature: insights from physiological angiogenesis. Nat Rev Cancer. 2010 Jul;10(7):505-14.

Christian S., Ahorn H., Novatchkova M., Garin-Chesa P., Park J.E., Weber G., Eisenhaber F., Rettig W.J., Lenter M.C. Molecular cloning and characterization of EndoGlyx-1, an EMILIN-like multisubunit glycoprotein of vascular endothelium. *J Biol Chem* 2001 276(51):48588-95.

Cristofanilli M, Charnsangavej C, Hortobagyi GN. Angiogenesis modulation in cancer research: novel clinical approaches. *Nat Rev Drug Discov*. 2002 (6):415-26.

Colombatti A, **Bressan GM, Castellani I, Volpin D.** Glycoprotein 115, a glycoprotein isolated from chick blood vessels, is widely distributed in connective tissue. *J Cell Biol* 1985 100(1):18-26.

Colombatti A, Spessotto P, Doliana R, Mongiat M, Bressan GM, Esposito G. The EMILIN/Multimerin family. *Front Immunol.* 2011;2:93.

Cooney MM, van Heeckeren W, Bhakta S, Ortiz J, Remick SC. Drug insight: vascular disrupting agents and angiogenesis--novel approaches for drug delivery. *Nat Clin Pract Oncol.* 2006 3(12):682-92.

Cooper CR., Chay CH., Pienta KJ. The role of alphavbeta3 in prostate cancer progression *Neoplasia* 2002 4:191-194.

Costell M., Gustafsson E, Aszodi A, Morgelin M, Bloch W, Hunziker E, Addicks K, Timpl R, Fassler R. Perlecan maintains the integrity of cartilage and some basement membranes. *J Cell Biol* 1999 147:1109-1122.

Danussi C., Spessotto P., Petrucco A., Wassermann B., Sabatelli P., Montesi M., Doliana R., Bressan G.M., Colombatti A. Emilin1 deficiency causes structural and functional defects of lymphatic vasculature. *Mol. Cell. Biol*. 2008 28:4026–4039.

Danussi C, Petrucco A, Wassermann B, Modica TM, Pivetta E, Del Bel Belluz L, Colombatti A, Spessotto P. An EMILIN1-negative microenvironment promotes tumor cell proliferation and lymph node invasion. *Cancer Prev Res.* 2012 Sep;5(9):1131-43.

De Vita V., **Lawrence T., Rosenberg S.** Cancer principles and practice of oncology 2007 e-book, 7th edition.

Dhanabal **M., Volk R., Ramchandran R., Simons M., Sukhatme V.P.** Cloning, expression, and in vitro activity of human endostatin *Bioch and Bioph Res Comm* 1999 258: 345–352.

Doliana R, Bot S, Bonaldo P, Colombatti A. EMI, a novel cysteine-rich domain of EMILINs and other extracellular proteins, interacts with the gC1q domains and participates in multimerization. *FEBS Lett* 2000 484(2): 164-8.

Doliana R, Bot S, Mungiguerra G, Canton A, Cilli SP, Colombatti A. Isolation and Characterization of EMILIN-2, a New Component of the Growing EMILINs Family and a Member of the EMI Domaincontaining Superfamily. *J Biol Chem*. 2001 276(15): 12003-11.

Doll JA, **Stellmach VM, Bouck NP, Bergh AR, Lee C, Abramson LP, Cornwell ML, Pins MR, Borensztajn J, Crawford SE.** Pigment epithelium-derived factor regulates the vasculature and mass of the prostate and pancreas *Nat Med* 2003 9:774-780.

Dunn JR, Reed JE, du Plessis DG, Shaw EJ, Reeves P, Gee AL, Warnke P, Walker C. Expression of ADAMTS-8, a secreted protease with antiangiogenic properties, is downregulated in brain tumours. *Br J Cancer.* 2006 94(8):1186-93.

Ema M., Rossant J. Cell fate decisions in early blood vessel formation. *Trends Cardiovasc Med.* 2003 13(6):254-9.

Ferrara N. and Kerbel R. S. Angiogenesis as a therapeutic target. *Nature* 2005 438: 967–974.

Ferrara N., Gerber H. P. and LeCouter J. The biology of VEGF and its receptors. *Nature Med.* 2003 9: 669–676.

Ferrara N. Heterozygous embryonic lethality induced by targeted inactivation of the VEGF gene. *Nature* 1996 380, 439–442.

Folkman J. Tumor angiogenesis: therapeutic implications *N Eng J Med* 1971 285:1182-1186.

Folkman J. Angiogenesis. *Annual Review of Medicine 2006* 57:1–18.

Goishi K, Klagsbrun M. Vascular endothelial growth factor and its receptors in embryonic zebrafish blood vessel development. *Curr Top Dev Biol.* 2004 62:127–152.

Goyal A, Pal N, Concannon M, Paul M, Doran M, Poluzzi C, Sekiguchi K, Whitelock JM, Neill T, Iozzo RV. Endorepellin, the angiostatic module of perlecan, interacts with both the α2β1 integrin

and vascular endothelial growth factor receptor 2 (VEGFR2): a dual receptor antagonism. *J Biol Chem*. 2011 286(29):25947-62.

Grizzi F, Russo C, Colombo P, Franceschini B, Frezza EE, Cobos E, Chiriva-Internati M. Quantitative evaluation and modeling of two-dimensional neovascular network complexity: the surface fractal dimension. *BMC Cancer*. 2005 8;5:14.

Hayward CP, Warkentin TE, Horsewood P, Kelton JG. Multimerin: a series of large disulfide-linked multimeric proteins within platelets *Blood* 1991 77(12):2556-60.

Hayward CP. Multimerin: a bench-to-bedside chronology of a unique platelet and endothelial cell protein--from discovery to function to abnormalities in disease. *Clin Invest Med*. 1997 20(3):176-87.

Hanahan D, Folkman J. Patterns and emerging mechanisms of the angiogenic switch during tumorigenesis. *Cell.* 1996 86(3):353-64.

Hanahan D, Weinberg RA. The hallmarks of cancer.*Cell* 2000 100(1):57-70.

Hileman RE, Fromm JR, Weiler JM, Linhardt RJ. Glycosaminoglycan-protein interactions: definition of consensus sites in glycosaminoglycan binding proteins. *Bioessays* 1998 20(2):156-67

Hill VK, Hesson LB, Dansranjavin T, Dallol A, Bieche I, Vacher S, Tommasi S, Dobbins T, Gentle D, Euhus D, Lewis C, Dammann R, Ward RL, Minna J, Maher ER, Pfeifer GP, and Latif F. Identification of 5 novel genes methylated in breast and other epithelial cancers. *Mol Cancer*. 2010 9: 51.

Hirama M., Takahashi F., Takahashi K., Akutagawa S., Shimizu K., Soma S., Shimanuki Y., Nishio K., Fukuchi Y. Osteopontin overproduced by tumor cells acts as a potent angiogenic factor contributing to tumor growth *Cancer Lett* 2003 198:107-117

Hirschi, K.K. and D'Amore, P.A. Pericytes in the microvasculature. *Cardiovasc. Res*. 1996 32, 687–698.

Holmqvist K., Cross M.J., Rolny C., Hagerkvist R., Rahimi N., Matsumoto T. The adaptor protein shb binds to tyrosine 1175 in vascular endothelial growth factor (VEGF) receptor-2 and regulates VEGF-dependent cellular migration. 2004 *J Biol Chem* 279: 22267–22275.

Hotz B., Backer M.V., Backer J.M., Buhr H.J., Hotz H.G. (2010). Specific targeting of tumor endothelial cells by a shiga-like toxin-vascular endothelial growth factor fusion protein as a novel treatment strategy for pancreatic cancer. *Neoplasia* 12: 797–806.

Huttenlocher A, Sandborg RR, Horwitz AF Adhesion in cell migration. *Curr Opin Cell Biol.* 1995 7(5):697-706.

Iozzo RV. Basement membrane proteoglycans: from cellar to ceiling *Nat Rev Mol Cell Biol* 2005 8:646-656

Iozzo RV, San Antonio JD. Heparan sulfate proteoglycans: heavy hitters in the angiogenesis arena. *J Clin Invest.* 2001 108(3):349-55.

Yancopoulos G.D., Davis S., Gale N.W., Rudge J.S., Wiegand S.J., Holash J. Vascular-specific growth factors and blood vessel formation. *Nature* 2000 14: 242-8.

Jaffe EA., Nachman RL., Becker CG., Minick CR. (1973). Culture of human endothelial cells derived from umbilical veins. Identification by morphologic and immunologic criteria. *J Clin Invest* 1973 52(11): 2745-56.

Jeimy SB, Fuller N, Tasneem S, Segers K, Stafford AR, Weitz JI, Camire RM, Nicolaes GA, Hayward CP. Multimerin 1 binds factor V and activated factor V with high affinity and inhibits thrombin generation. *Thromb Haemost*. 2008 100(6):1058-67.

Jiang X, Couchman JR. Perlecan and tumor angiogenesis. *J Histochem Cytochem* 2003 51:1393-1410

Jiang X, Multhaupt H, Chan E, Schaefer L, Schaefer RM, Couchman JR. Essential contribution of tumor-derived perlecan to epidermal tumor growth and angiogenesis. *J Histochem Cytochem* 2004 52:1575-1590.

Jimenez B, Volpert OV, Crawford SE, Febbraio M, Silverstein RL, Bouck N. Signals leading to apoptosis-dependent inhibition of neovascularization by thrombospondin-1 *Nat Med* 2000 6:41-48.

Jones PL., Jones FS. Tenascin-C in development and disease: gene regulation and cell function *Matrix Biol* 2000 19:581-596.

Kalluri R. Basement membranes: structure, assembly and role in tumour angiogenesis. *Nat Rev Cancer.* 2003 3(6):422-33.

Kevil C.G., Keith Payne D., Mire E. and Alexander J.S. Vascular permeability factor/vascular endothelial cell growth factor-mediated permeability occurs through disorganization of endothelial junctional proteins," *Journal of BiologicalChemistry* 1998 24: 15099–15103.

Kim H.S., Lim S.J., Park Y.K. Anti-angiogenic factor endostatin in osteosarcoma *APMIS* 2009 117(10): 716-23.

Krishnan L. Effect of mechanical boundary conditions on orientation of angiogenic microvessels. *Cardiovasc. Res.* 2008 78: 324–332.

Kupprion C., Motamed K., Sage E.H. SPARC (BM-40, osteonectin) inhibits the mitogenic effect of vascular endothelial growth factor on microvascular endothelial cells. 1998 *J Biol Chem* 273: 29635–29640.

Lamalice L, Houle F, Jourdan G, Huot J. Phosphorylation of tyrosine 1214 on VEGFR2 is required for VEGF-induced activation of Cdc42 upstream of SAPK2/p38. *Oncogene*. 2004 15;23(2):434-45.

LeBleu V.S., MacDonald B. and Kalluri R. Structure and Function of Basement Membranes**.** *Experimental Biology and Medicine* 2007 232:1121-1129.

Leimeister C., Steidl C., Schumacher N., Erhard S., Gessler M. Developmental expression and biochemical characterization of Emu family members *Dev Biol* 2002 249: 204–218

Ligresti G., Aplin A.C., Zorzi P., Morishita A., Nicosia R.F. Macrophage-derived tumor necrosis factor-a is an early component of the molecular cascade leading to angiogenesis in response to aortic injury. *Arterioscler Thromb Vasc Biol* 2011 31: 1151–1159.

Linask KK,Lash JW. A role for fibronectin in the migration of avian precardiac cells. I. Dose-dependent effects of fibronectin antibody. *Dev Biol*. 1988 129(2):315-23.

Lobov I.B., Brooks P.C. and Lang R.A. Angiopoietin-2 displays vascular endothelial growth factor-dependent modulation of capillary structure and endothelial cell survival in vivo. Proc. Natl Acad. Sci. 2002 99: 11205–11210.

Malinda KM, Nomizu M, Chung M, Delgado M, Kuratomi Y, Yamada Y, Kleinman HK, Ponce ML. Identification of laminin alpha1 and beta1 chain peptides active for endothelial cell adhesion, tube formation, and aortic sprouting. *FASEB J.* 1999 13(1):53-62.

Meyer C, **Notari L, Becerra SP**. Mapping the type I collagen-binding site on pigment epithelium-derived factor. Implications for its antiangiogenic activity *J Biol Chem* 2002 277:45400- 45407.

Mongiat M., Fu J., Oldershaw R., Greenhalgh R., Gown AM., Iozzo RV. Perlecan protein core interacts with extracellular matrix protein 1 (ECM1), a glycoprotein involved in bone formation and angiogenesis *J Biol Chem* 2003 278(19):17491-9.

Mongiat M., Mungiguerra G., Bot S., Mucignat M.T., Giacomello E., Doliana R., Colombatti A. Self-assembly and supramolecular organization of EMILIN. *J Biol Chem* 2000 275(33): 25471-25480.

Mongiat M, Sweeney SM, San Antonio JD, Fu J, Iozzo RV. Endorepellin, a novel inhibitor of angiogenesis derived from the C terminus of perlecan. *J Biol Chem* 2003 278: 4238–4249.

Mongiat M., Ligresti G., Marastoni S., Lorenzon E., Doliana R., Colombatti A. Regulation of the extrinsic apoptotic pathway by the extracellular matrix glycoprotein EMILIN2 *Mol Cell Biol* 2007 27: 7176-7187.

Mongiat M, Marastoni S, Ligresti G, Lorenzon E, Schiappacassi M, Perris R, Frustaci S, and Colombatti A. The extracellular matrix glycoprotein elastin microfibril interface located protein 2: a dual role in the tumor microenvironment. *Neoplasia*. 2010 12: 294-304.

Mundel TM, Yliniemi AM, Maeshima Y, Sugimoto H, Kieran M, Kalluri R. Type IV collagen alpha6 chain-derived noncollagenous domain 1 (alpha6(IV)NC1) inhibits angiogenesis and tumor growth. *Int J Cancer*. 2008 122(8):1738-44.

Nakatsu M.N., Davis J., Hughes C.C. Optimized Fibrin Gel Bead Assay for the Study of Angiogenesis. 2007 *J. Vis. Exp.*(3).

Nor JE, Mitra RS, Naik Sutorik MM, Mooney DJ, Castle VP, Polverini PJ. Thrombospondin-1 induces endothelial cell apoptosis and inhibits angiogenesis by activating the caspase death pathway *J Vasc Res* 2000 37:209-218.

Olsson AK, Dimberg A, Kreuger J, Claesson-Welsh L. VEGF receptor signaling in control of vascular function. *Nat Rev Mol Cell Biol* 2006 7: 359–371.

Ornitz DM., Yayon A., Flanagan JG., Svahn CM., Levi E., Leder P. Heparin is required for cell-free binding of basic fibroblast growth factor to a soluble receptor and for mitogenesis in whole cells *Mol Cell Biol* 1992 12:240-247.

Ozederm U., Stallcup WB. Early contribution of pericytes to angiogenic sprouting and tube formation. *Angiogenesis* 2003 6:241-249.

Paez-Ribes M., Allen E., Hudock J., Takeda T., Okuyama H., Vinals F., Inoue M., Bergers G., Hanahan D., Casanovas O. Antiangiogenic therapy elicits malignant progression of tumors to increased local invasion and distant metastasis *Cancer Cell* 2009 15: 220-231.

Papetti, M. and Herman, I.M. Mechanisms of normal and tumour-derived angiogenesis. Am. J. Physiol. Cell Physiol. 2002 282, C947–C970.

Pepper MS. Extracellular proteolysis and angiogenesis. *Thromb Haemost*. 2001 86(1):346-55

Pitulescu M.E., Schmidt I., Benedito R., Adams R.H. Inducible gene targeting in the neonatal vasculature and analysis of retinal angiogenesis in mice. *Nat Protoc* 2010 9:1518-34.

Raman M, Cobb MH. TGF-beta regulation by Emilin1: new links in the etiology of hypertension *Cell* 2006 124(5): 893-5.

Raza A, Franklin M.J, Dudek A.Z. Pericytes and vessel maturation during tumor angiogenesis and metastasis. *Am J Hematol.* 2010 85(8):593-8.

Rhodes J. M. and Simons M. The extracellular matrix and blood vessel formation: not just a scaffold. *J. Cell. Mol. Med.* 2007 11: 176–205.

Ribatti D. The inefficacy of antiangiogenic therapies. *J Angiogenes Res*. 2010 10;2:27.

Roccaro AM, Hideshima T, Raje N, Kumar S, Ishitsuka K, Yasui H, Shiraishi N, Ribatti D, Nico B, Vacca A, Dammacco F, Richardson PG, Anderson KC. Bortezomib mediates antiangiogenesis in multiple myeloma via direct and indirect effects on endothelial cells. *Cancer Res.* 2006 1;66(1):184-91.

Rouet V, Hamma-Kourbali Y, Petit E, Panagopoulou P, Katsoris P, Barritault D, Caruelle JP, Courty J. A synthetic glycosaminoglycan mimetic binds vascular endothelial growth factor and modulates angiogenesis. *J Biol Chem*. 2005 280(38):32792-800.

Rodriguez-Manzaneque JC, Lane TF, Ortega MA, Hynes RO, Lawler J, Iruela-Arispe ML. Thrombospondin-1 suppresses spontaneous tumor growth and inhibits activation of matrix metalloproteinase-9 and mobilization of vascular endothelial growth factor *Proc Natl Acad Sci U S A* 2001 98:12485-12490.

Rucker H.K., Wynder H.J., Thomas W.E. Cellular mechanisms of CNS pericytes. *Brain Res. Bull*. 2000 51, 363–369.

Sahni A, Francis CW. Vascular endothelial growth factor binds to fibrinogen and fibrin and stimulates endothelial cell proliferation. *Blood* 2000 96: 3772–3778.

Santimaria M., Moscatelli G., Viale GL., Giovannomi L., Neri G., Viti F., Leprini A., Borsi L., Castellani P., Zardi L., Neri D., Riva P. Immunoscintigraphic detection of the ED-B domain of fibronectin, a marker of angiogenesis, in patients with cancer *Clin Cancer Res* 2003 9:571-579

Sanz-Moncasi MP, Garin-Chesa P, Stockert E, Jaffe EA, Old LJ, Rettig WJ. Identification of a high molecular weight endothelial cell surface glycoprotein, endoGlyx-1, in normal and tumor blood vessels *Lab Invest* 1994 71(3):366-73.

Sasaki T, Hohenester E, Timpl R. Structure and function of collagen-derived endostatin inhibitors of angiogenesis. *IUBMB Life* 2002 53(2):77-84.

Sato H, Takino T, Okada Y, Cao J, Shinagawa A, Yamamoto E, Seiki M. A matrix metalloproteinase expressed on the surface of invasive tumour cells. Nature 1994 370(6484):61-5.

Saunders W. B. Coregulation of vascular tube stabilization by endothelial cell TIMP-2 and pericyte TIMP-3. *J. Cell Biol.* 2006 175: 179–191.

Senger DR., Ledbetter SR., Claffey KP., Papadopoulos-Sergiou A., Peruzzi CA., Detmar M. Stimulation of endothelial cell migration by vascular permeability factor/vascular endothelial growth factor through cooperative mechanisms involving the alphavbeta3 integrin, osteopontin and thrombin *Am J Pathol* 1996 149:293-305

Sharma B, Handler M, Eichstetter I, Whitelock JM, Nugent MA, Iozzo RV. Antisense targeting of perlecan blocks tumor growth and angiogenesis in vivo *J Clin Invest* 1998 102:1599-1608

Sharma MR., Tuszynski GP., Sharma MC. Angiostatin-induced inhibition of endothelial cell proliferation/apoptosis is associated with the downregulation of cell cycle regulatory protein cdk5 *J Cell Biochem* 2004 91:398-409.

Schiavinato A, Becker AK, Zanetti M, Corallo D, Milanetto M, Bizzotto D, Bressan G, Guljelmovic M, Paulsson M, Wagener R, Braghetta P, Bonaldo P. EMILIN-3, peculiar member of elastin microfibril interface-located protein (EMILIN) family, has distinct expression pattern, forms oligomeric assemblies, and serves as transforming growth factor β (TGF-β) antagonist. *J Biol Chem*. 2012 287(14):11498-515.

Shweiki, D., Itin, A., Soffer, D. and Keshet, E. Vascular endothelial growth factor induced by hypoxia may mediate hypoxiainitiated angiogenesis. Nature 359, 843–845.

Sobel M, Soler DF, Kermode JC, Harris RB. Localization and characterization of a heparin binding domain peptide of human von Willebrand factor. *J Biol Chem*. 1992 267(13):8857-62.

Sottile J. Regulation of angiogenesis by extracellular matrix. *Biochim Biophys Acta.* 2004 1654(1):13-22.

Spessotto P, **Cervi M, Mucignat MT, Mungiguerra G, Sartoretto I, Doliana R, Colombatti A.** Beta 1 Integrin-dependent cell adhesion to EMILIN-1 is mediated by the gC1q domain. *J Biol Chem*. 2003 278(8): 6160-7.

Spessotto P., Lacrima K., Nicolosi PA., Pivetta E., Scapolan M., Perris R. Fluorescence-based assays for in vitro analysis of cell adhesion and migration. Book, chapter 16 2009 *Methods in molecular biology, extracellular matrix protocols.*

Sudhakar A, Boosani CS. Inhibition of tumor angiogenesis by tumstatin: insights into signaling mechanisms and implications in cancer regression. *Pharm Res*. 2008 25(12):2731-9.

Sudhakar A, Sugimoto H, Yang C, Lively J, Zeisberg M, Kalluri R. Human tumstatin and human endostatin exhibit distinct antiangiogenic activities mediated by alpha v beta 3 and alpha 5 beta 1 integrins. *Proc Natl Acad Sci U S A*. 2003 100(8):4766-71.

Sternlicht MD,Werb Z How matrix metalloproteinases regulate cell behavior. *Annu Rev Cell Dev Biol.* 2001;17:463-516.

Takahashi Y., Kitadai Y, Bucana C.D., Cleary K.R., Ellis L.M. Expression of vascular endothelial growth factor and its receptor, KDR, correlates with vascularity, metastasis, and proliferation of human colon cancer. *Cancer Research* 1995 18: 3964–3968.

Takahashi T, Yamaguchi S, Chida K, Shibuya M. A single autophosphorylation site on KDR/Flk-1 is essential for VEGF-A-dependent activation of PLC-gamma and DNA synthesis in vascular endothelial cells. *EMBO J*. 2001 20(11):2768-78.

Takenaka K, Yamagishi SI, Jinnouchi Y, Nakamura K, Matsui T, Imaizumi T. Pigment epithelium-derived factor (PEDF)- induced apoptosis and inhibition of vascular endothelial growth factor (VEGF) expression in MG63 human osteosarcoma cells *Life Sci* 2005 77:3231-3241.

Tammela T, Enholm B, Alitalo K, Paavonen K. The biology of vascular endothelial growth factors. *Cardiovasc Res.* 2005 65(3):550-63.

Teng-nan Lin TN, Kim GM, Chen JJ, Cheung WM, He YY, Hsu CY. Differential regulation of thrombospondin-1 and thrombospondin-2 after focal cerebral ischemia/reperfusion. *Stroke.* 2003 34(1):177-86.

Teti A., Farin AR., Villanova I., Tiberio A., Tacconelli A., Sciortino G., Chambre AF., Gulino A., Mackay AR. Activation of MMP-2 by human GCT23 giant cell tumor cells induced by osteopontin, bone sialoprotein and GRGDSP peptides is RGD and cell shape change dependent *Int J Cancer* 1998 77:82-93.

Toi M., Kondo S., Suzuki H. Quantitative analysis of vascular endothelial growth factor in primary breast cancer. *Cancer* 1996 6: 1101–1106.

Vázquez F, Hastings G, Ortega MA, Lane TF, Oikemus S, Lombardo M, Iruela-Arispe ML. METH-1, a human ortholog of ADAMTS-1, and METH-2 are members of a new family of proteins with angio-inhibitory activity. *J Biol Chem*. 1999 274(33):23349-57.

Walker A, Turnbull JE, Gallagher JT. Specific heparan sulfate saccharides mediate the activity of basic fibroblast growth factor. *J Biol Chem*. 1994 269(2):931-5.

Waltenberger J, Claesson-Welsh L, Siegbahn A, Shibuya M, Heldin CH. Different signal transduction properties of KDR and Flt1, two receptors for vascular endothelial growth factor. *J Biol Chem* 1994 269: 26988–26995.

Wernert N. The multiple roles of tumour stroma. Virchows Arch. 1997 430(6):433-43.

Xu R, Yao ZY, Xin L, Zhang Q, Li TP, Gan RB. NC1 domain of human type VIII collagen (alpha 1) inhibits bovine aortic endothelial cell proliferation and causes cell apoptosis. *Biochem Biophys Res Commun.* 2001 289(1):264-8.

Zacchigna L., Vecchione C., Notte A., Cordenonsi M., Dupont S., Maretto S., Cifelli G., Ferrari A., Maffei A., Fabbro C., Braghetta P., Marino G., Selvetella G., Aretini A., Colonnese C., Bettarini U., Russo G., Soligo S., Adorno M., Bonaldo P., Volpin D., Piccolo S., Lembo G., Bressan G.M. Emilin1 links TGF-beta maturation to blood pressure homeostasis *Cell* 2006 124(5): 929-42.

Zachary AA, Montgomery RA, Leffell MS. Factors associated with and predictive of persistence of donor-specific antibody after treatment with plasmapheresis and intravenous immunoglobulin. *Hum Immunol.* 2005 66:364–370.

Zhou Z, Wang J, Cao R, Morita H, Soininen R, Chan KM, Liu B, Cao Y, Tryggvason K. Impaired angiogenesis, delayed wound healing and retarded tumor growth in perlecan heparin sulfate-deficient mice *Cancer Res.* 2004 64:4699-4702.

PUBLICATIONS

Lorenzon E, Colladel R, Andreuzzi E, Marastoni S, Todaro F, Schiappacassi M, Ligresti G, Colombatti A, Mongiat M. MULTIMERIN2 impairs tumor angiogenesis and growth by interfering with VEGF-A/VEGFR2 pathway. *Oncogene*. 2012 Jun 28;31(26):3136-47.

Oncogene (2012) 31, 3136–3147

www.nature.com/onc

ORIGINAL ARTICLE

MULTIMERIN2 impairs tumor angiogenesis and growth by interfering with VEGF-A/VEGFR2 pathway

E Lorenzon[1,4], R Colladel[1], E Andreuzzi[1,2], S Marastoni[1], F Todaro[1], M Schiappacassi[1], G Ligresti[3], A Colombatti[1,2] and M Mongiat[1]

[1]*Experimental Oncology Division 2, CRO-IRCCS, Aviano, Italy;* [2]*MATI Center of Excellence, University of Udine, Udine, Italy and* [3]*Department of Pathology, University of Washington, Seattle, WA, USA*

MULTIMERIN2 (MMRN2), also known as Endoglyx-1, is an extracellular matrix glycoprotein whose function has so far remained elusive. Given its specific localization in tight association with the endothelium we hypothesized that this protein could modulate neo-angiogenesis. By multiple assays we showed that MMRN2 significantly impaired endothelial cell (EC) migration and organization of a functional vessel network. The interaction of ECs with MMRN2 induced a striking impairment of VEGFR1 and VEGFR2 activation. We focused our attention on VEGFR2, a chief regulator of angiogenesis, and clarified that MMRN2 interfered with the VEGF/VEGFR2 axis through a direct binding with VEGF-A. This novel interaction was assessed in several assays and the affinity was estimated (Kd ~ 50 nM). We next questioned whether the anti-angiogenic properties of MMRN2 could impair tumor growth. Although overexpression of MMRN2 by HT1080 cells did not affect their growth and apoptotic rate *in vitro*, it remarkably affected their growth *in vivo*. In fact, MMRN2-positive cells failed to efficiently grow and form well-vascularized tumors; a similar outcome was observed following treatment of established tumors with a MMRN2 adenoviral construct. Tumor-section immunostaining revealed a strong co-localization of VEGF-A with the ectopically expressed MMRN2. These novel findings suggest that VEGF may be sequestered by MMRN2 and be less available for the engagement to the receptors. Taken together these results highlight MMRN2 as a crucial player in the regulation of EC function, neo-angiogenesis and hence tumor growth. We hypothesize that secreted and deposited MMRN2 may function as a homeostatic barrier halting the sprouting of novel vessels, and suggest that these studies may embody the potential for the development of novel tools for cancer treatment.
Oncogene (2012) **31,** 3136–3147; doi:10.1038/onc.2011.487; published online 24 October 2011

Keywords: angiogenesis; extracellular matrix; VEGF

Introduction

The development of new blood vessels is of vital importance for normal growth and development, as well as for pathological conditions such as tumor development. Solid tumors do not grow beyond the size of 1–2 mm unless the homeostatic balance between pro- and anti-angiogenic molecules is altered, and the formation of new blood vessels is induced. The newly formed vessels provide the oxygen and the nutrients necessary for the relentless growth and expansion of the tumor, and favor invasion and metastasis (Folkman, 1971). In the latest years it has become clear that the different cellular and acellular components of the tumor microenvironment are pivotal regulators of tumor development (Hu and Polyak, 2008; Joyce and Pollard, 2009). Indeed, the tumor represents a functional tissue interconnected with the microenvironment. The cellular components are surrounded by and intermingled with a complex network of extracellular matrix (ECM) molecules that sustain and favor communication between the cells and the external milieu. One key role of the ECM that has gained prominent recognition is the regulation of tumor angiogenesis (Cheresh and Stupack, 2008; Nyberg *et al*., 2008). During blood vessel sprouts, endothelial cells (ECs) must not only coordinate cytoskeletal changes to move through the tissues but also secrete proteolytic enzymes to promote matrix degradation that favors invasion and affect angiogenesis (Carmeliet, 2000; Nyberg *et al*., 2008; Campbell *et al*., 2010). Several ECM molecules or degradation products have been reported to negatively (Boehm *et al*., 1997; Lawler, 2002; Mongiat *et al*., 2003) or positively (Hirama *et al*., 2003; Mongiat *et al*., 2010; Ventura *et al*., 2010) affect angiogenesis.

VEGF-A is expressed by most types of tumors (Ferrara, 2002), and is a regulator of vascular development that binds VEGFR1 and VEGFR2 receptor tyrosine kinases (RTKs) expressed on the EC membrane (Mustonen and Alitalo, 1995; Olsson *et al*., 2006). VEGFR1 is important for the recruitment of hematopoietic precursors and migration of monocytes and macrophages, and VEGFR2 is required for EC function and accounts for most of the VEGF-A-mediated downstream signaling occurring during angiogenesis. In particular, tyrosine 1175 (Tyr^{1175}) and tyrosine 951 (Tyr^{951}) phosphorylation have been shown to be primarily implicated in the regulation of EC migration (Olsson *et al*., 2006). VEGF-A

Correspondence: Dr M Mongiat, or Professor A Colombatti, Department of Molecular Oncology and Translational Research, CRO-IRCCS, via Franco Gallini 2, Aviano (PN), Italy.
E-mail: mmongiat@cro.it or acolombatti@cro.it
[4]Current address: Roche Diagnostics GmbH Penzberg, Germany.
Received 29 May 2011; revised 1 September 2011; accepted 15 September 2011; published online 24 October 2011

binds to a number of ECM molecules (Kupprion *et al*., 1998; Gengrinovitch *et al*., 1999; Sahni and Francis, 2000; Wijelath *et al*., 2002; Greenaway *et al*., 2007; Zoeller *et al*., 2009) and ECM-bound VEGF-A either prolongs (Hutchings *et al*., 2003; Chen *et al*., 2010) or impairs VEGFR2 activation (Kupprion *et al*., 1998; Sun *et al*., 2009), thus affecting EC proliferation to a great extent.

MULTIMERIN2 (MMRN2), also known as Endo-Glyx-1, is an ECM member of the EDEN (**E**MI **D**omain **EN**dowed) protein family (Braghetta *et al*., 2004) associated with a high molecular weight glycoprotein complex (Christian *et al*., 2001). The molecule displays a pan-endothelial expression pattern both in normal and tumoral vasculature, including hot spots of neovascularization in some tumors (Sanz-Moncasi *et al*., 1994; Christian *et al*., 2001; Huber *et al*., 2006; Koperek *et al*., 2007). It is specifically deposited along the blood vessels in tight juxtaposition with ECs and is also present in the luminal side of the vessels (Christian *et al*., 2001), however, its function has thus far remained obscure. Here, we show evidence that MMRN2 contributes to the maintenance of blood vessels' homeostasis, and that its overexpression affects EC migration and tumor angiogenesis. MMRN2 interferes with the VEGF-A/VEGFR2 axis by VEGF-A sequestration, thus leading to a striking decrease of tumor growth.

Results

The adhesion of ECs to MMRN2 did not affect their viability or their apoptotic rate

Given that MMRN2 is specifically deposited only in the blood vessels we wondered whether this molecule was secreted exclusively by ECs or also by smooth muscle cells. Western blot analysis performed on human umbelical vein endothelial cells (HUVEC) and pulmonary smooth muscle cells indicated that MMRN2 is produced only by ECs (Supplementary Figure 1a, top). In addition, among several MMRN2-negative tumor cell lines (not shown), no MMRN2 expression was detected in the sarcoma (HT1080) and carcinoma (HeLa) tumor cell lines. In order to analyze its putative effects on ECs behavior we have either used purified recombinant MMRN2 (Figure 1a, left) or induced its overexpression in ECs through adenoviral transduction (Figure 1a, bottom, Supplementary Figure 1a, bottom). As previously demonstrated (Christian *et al*., 2001), the purified recombinant molecule barely entered a 4–12% polyacrylamide gel under non-reducing conditions (Figure 1a, right). Alternatively, endogenous expression was downregulated by specific siRNA sequences, construct 4 giving the highest downregulation, which was optimal at 72 h post transduction (Supplementary Figure 1b and Figure 2d). In accordance with the fact that MMRN2 is located in tight contact with the endothelium (Christian *et al*., 2001), ECs adhered to MMRN2 even though the interaction was weaker compared with the adhesion to type I collagen, and was Ca^{2+} and Mg^{2+} independent (Figures 1b and c). Furthermore, EC adhesion on MMRN2 was not affected by a number of anti-integrin blocking antibodies, including anti-α_1, anti-α_4, anti-α_v and anti-β_1 (data not shown). MMRN2 did not affect the regular EC proliferation or their apoptotic rate (Figures 1d–g). Similarly the down-regulation of endogenous MMRN2 by RNA interference did not change the percentage of cells undergoing apoptosis nor their proliferative potential, a further indication that this molecule does not alter the normal EC growth (Supplementary Figure 1c).

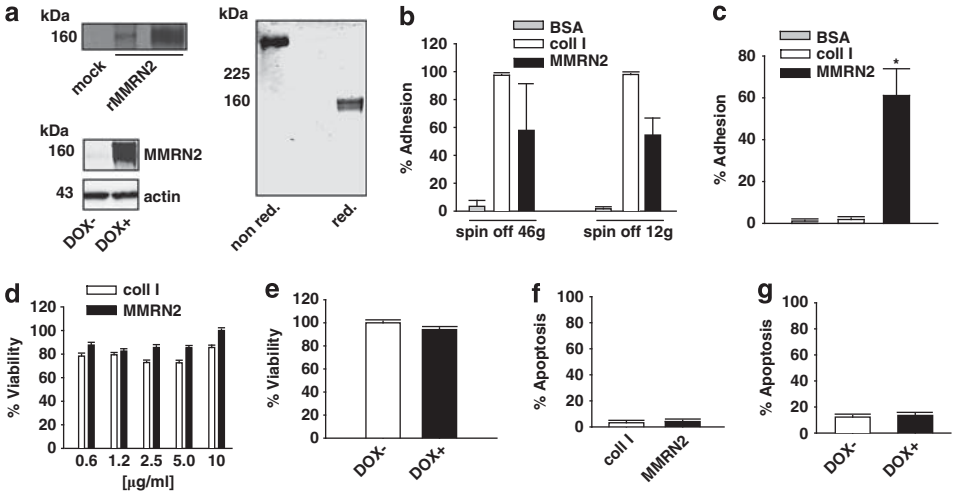

Figure 1 MMRN2 is a substrate for ECs and does not alter their viability or the apoptotic rate. Left panel: SDS–PAGE analysis of two fractions of recombinant His-tagged MMRN2 (rMMRN2) or media from mock-transfected cells (mock). Right panel: Western blot analysis of the conditioned media from HUVEC cells transduced with the MMRN2 adenoviral construct and cultured with or without doxycycline (DOX+ and DOX−, respectively). Actin was used as a normalizer of protein loading (**a**). Adhesion assay (CAFCA, see Materials and methods) performed with HUVEC cells adhered on type I collagen (Coll I), MMRN2 or BSA using two centrifugal forces (spin of 46 or 12 *g*) (**b**). Adhesion assay in the absence of Ca^{2+} and Mg^{2+} (*$P = 0.003$) (**c**). MTT assay performed on HUVEC cells treated with increasing concentrations of Coll I or MMRN2 (**d**). MTT assay performed on HUVEC cells transduced with the MMRN2 adenoviral construct and cultured with or without doxycycline (DOX+ and DOX−, respectively) (**e**). TUNEL assay performed on HUVEC cells treated with 10 μg/ml of Coll I or MMRN2 (**f**). TUNEL assay performed on HUVEC cells transduced with the MMRN2 adenoviral construct and cultured with or without doxycycline (DOX+ and DOX–, respectively) (**g**).

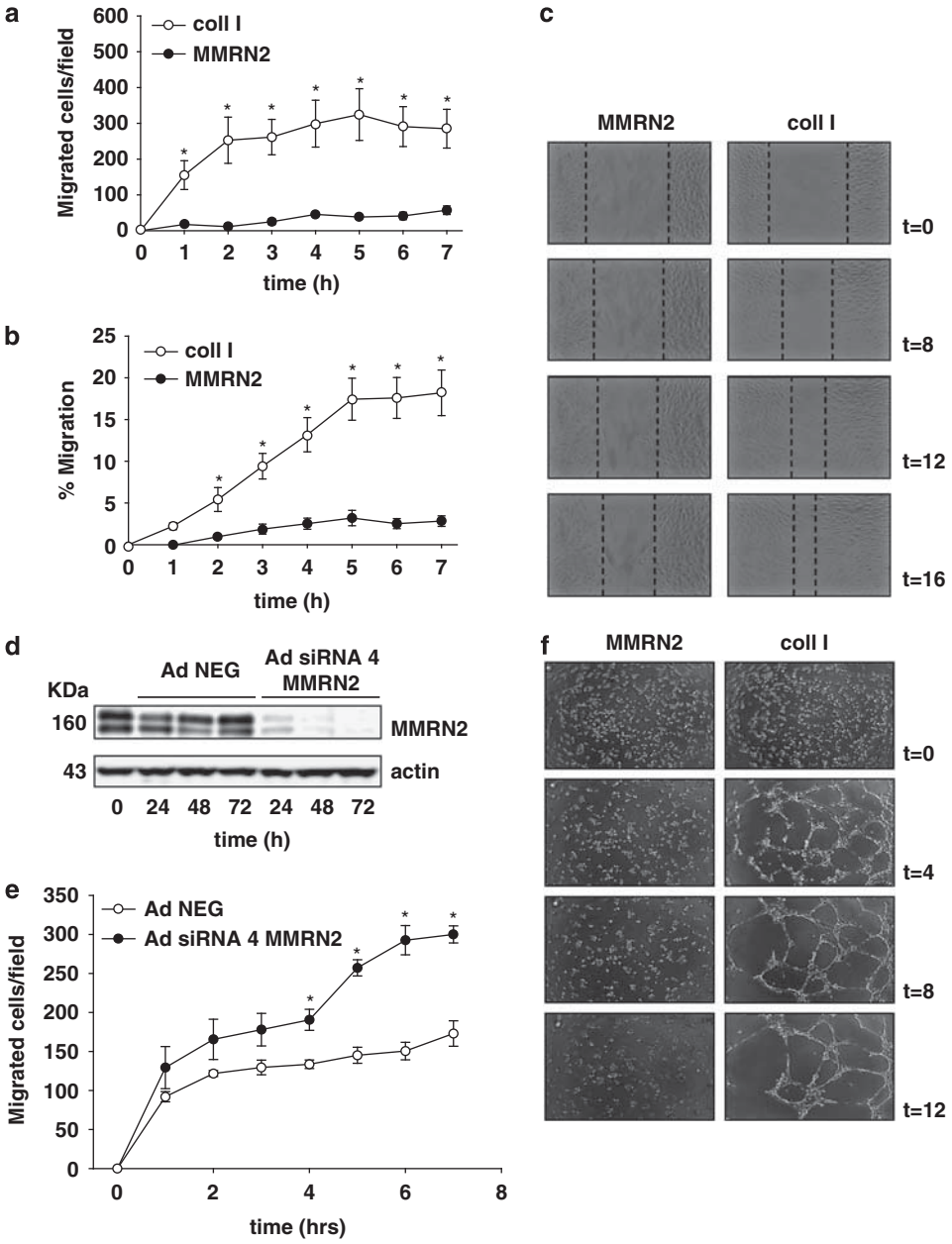

Figure 2 MMRN2 impinges EC motility and tubulogenesis. Analysis of HUVEC cell migration towards a VEGF-A stimulus (50 ng/ml) through type I collagen (Coll I) or MMRN2 coated on the upper side of the transwell membranes (*$P \leqslant 0.009$) (**a**). Haptotaxis of HUVEC cells towards Coll I or MMRN2 coated on the lower side of the transwell membranes (*$P \leqslant 0.04$) (**b**). Representative pictures of the scratch test performed using HUVEC cells challenged with 10 μg/ml of Coll I or MMRN2. The edge of the moving cells is highlighted by dashed lines (**c**). Western blot analysis of MMRN2 expression by HUVEC cells following transduction with the empty or the MMRN2 siRNA adenoviral construct 4 (Ad NEG and Ad siRNA 4 MMRN2, respectively). Actin was used as a normalizer of protein loading (**d**). Migration test of HUVEC cells through Coll I-coated transwells toward a VEGF-A stimulus, following transduction with the control or MMRN2 siRNA adenoviral constructs (Ad NEG and Ad siRNA 4 MMRN2) (*$P \leqslant 0.02$) (**e**). Representative pictures of the Matrigel tubulogenesis test following treatment with 10 μg/ml of Coll I or of MMRN2 (**f**).

MMRN2 significantly reduced EC motility and inhibited tubule sprouting

The ECs' migration towards a VEGF-A stimulus was significantly impaired by MMRN2 (Figure 2a) and, differently from type I collagen, the molecule did not promote haptotactic migration of ECs (Figure 2b). These results were also corroborated by the scratch test analysis, wherein ECs treated with MMRN2 failed to efficiently close the wound (Figure 2c and Supplementary Figure 1d). Accordingly, the downregulation of endogenous MMRN2 led to an increased migration of ECs towards the VEGF-A stimulus (Figures 2d and e). Finally, MMRN2 significantly inhibited tubulogenesis induced by Matrigel (Figure 2f and Supplementary Figures 1e–g).

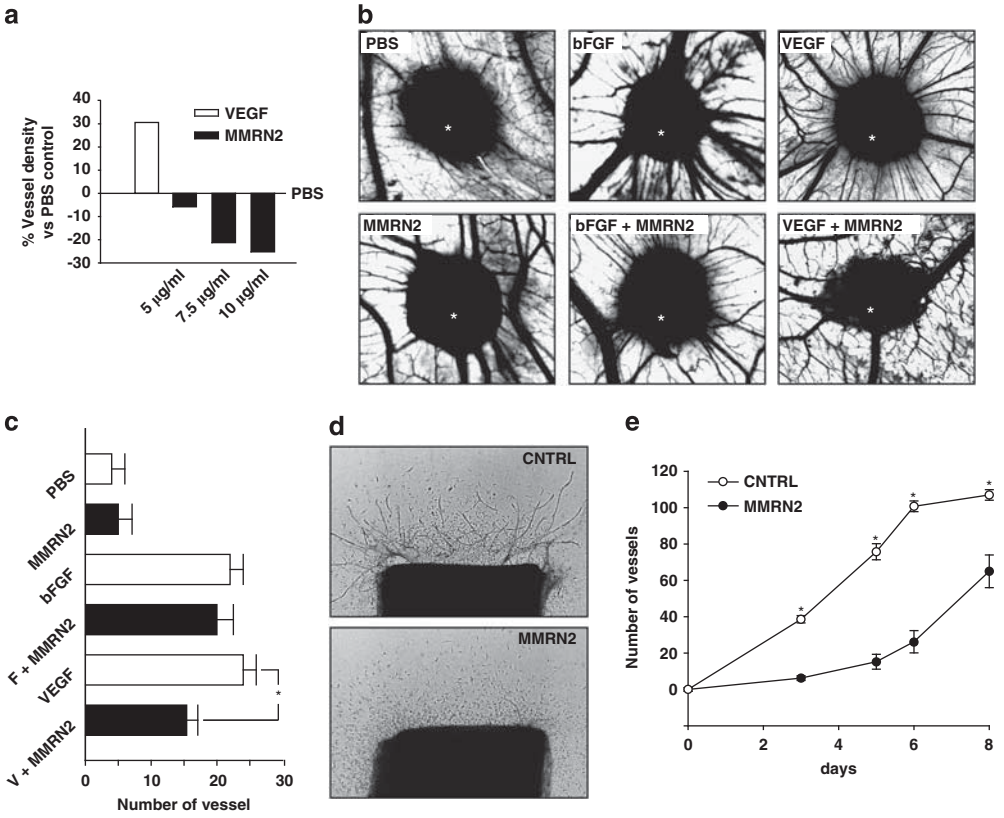

Figure 3 MMRN2 inhibits *in vitro* and *in vivo* angiogenesis. Graph representing the evaluation of the vascular density following treatment of the cells' co-culture from the AngioKit with VEGF-A (10 ng/ml) or with increasing concentrations of MMRN2 (5–10 μg/ml) (**a**). Representative pictures of CAM assays performed using sponges (white asterisk) containing 50 ng of VEGF-A or bFGF with or without 150 ng of MMRN2. Phosphate-buffered saline or MMRN2 without stimulus were used as a control (**b**). Quantification of the newly formed vessels directed toward the sponge by following or not the stimulus with VEGF-A or bFGF (V and F, respectively) of the experiment above. Twenty eggs were used for each point and the values represent mean ± s.e. of three independent experiments ($*P = 0.01$) (**c**). Representative pictures of the aortic ring assay. Aortas were challenged with phosphate-buffered saline (CNTRL) or 10 μg/ml of MMRN2 (**d**). Evaluation of the number of vessels sprouting from the aortas. Four aortas per group were used ($*P \leqslant 0.002$) (**e**).

MMRN2 impaired VEGF-A-induced angiogenesis in vivo *and VEGFR2 activation by sequestering VEGF-A*

We next verified the capability of MMRN2 to affect angiogenesis in a fibroblast/EC co-culture system and found that MMRN2 consistently impaired the formation of microvessels in a dose-dependent manner (Figure 3a). The putative anti-angiogenic activity was subsequently tested *in vivo*. The 'spoke-wheel-like' blood vessel development toward the sponge containing VEGF-A in chorioallantoic membrane (CAM) assays was significantly impaired in the presence of MMRN2 ($P = 0.01$, Figures 3b and c). On the contrary, the decreased blood vessel formation toward a basic fibroblast growth factor (bFGF) stimulus was not significant, suggesting that the effect might specifically involve VEGF-A signaling; moreover, MMRN2 *per se* did not significantly affect angiogenesis in this assay (Figures 3b and c). The anti-angiogenic effect was further confirmed in aortic ring assays; the presence of the molecule dramatically decreased the number of vessels sprouting from the aortas ($P \leqslant 0.002$, Figures 3d and e).

In order to shed light on the molecular mechanisms triggered by MMRN2 that are responsible for the regulation of EC function, we have challenged HUVEC cells with conditioned media containing or not containing MMRN2 and analyzed receptor tyrosine kinase activation with a specific array. The treatment with MMRN2 led to a major decrease of VEGFR2 and VEGFR1 activation (Figures 4a and b and Supplementary Figure 2a), supporting our hypothesis of an involvement of the VEGF-A signaling in the MMRN2-driven anti-angiogenic effects. Given that VEGFR2 is one of the most important receptors regulating neoangiogenesis, HUVEC cells were incubated with VEGF-A alone or with MMRN2 for different time intervals and VEGFR2 phosphorylation was assessed by a specific antibody. MMRN2 specifically blocked VEGF-A-driven VEGFR2 phosphorylation (Figure 4c) and this effect was accompanied by a significant downregulation of FAK phosphorylation (Figure 4c and Supplementary Figure 2b).

We next verified whether the downregulation of VEGFR2 phosphorylation was caused by an interference of MMRN2 with the VEGF-A/VEGFR2 interaction on the EC surface. To this end, displacement experiments following incubation of HUVEC cells with ^{125}I-VEGF-A challenged with increasing concentrations

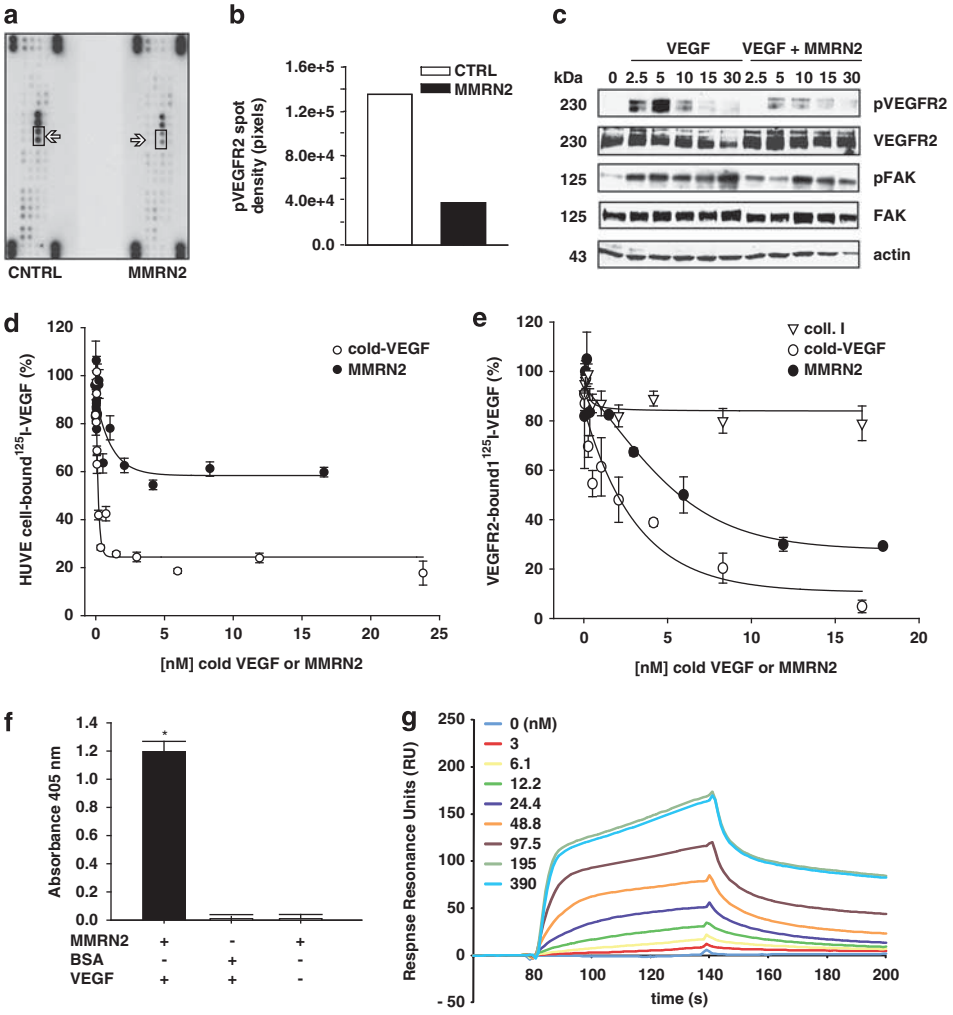

Figure 4 MMRN2 downregulates VEGFR2 activation by binding VEGF-A. RTK array membrane from HUVEC cells challenged with conditioned media containing or not MMRN2 (MMRN2 and CNTRL, respectively). The spots corresponding to VEGFR2 are indicated by an arrow (**a**). Quantitative evaluation of the spots corresponding to VEGFR2 phosphorylation (**b**). Western blot analysis of VEGFR2 and FAK activation following treatment of HUVEC cells with 15 ng/ml of VEGF-A with or without 5 μg/ml of MMRN2 for different lengths of time in minutes. Both the total and the phosphorylated forms of VEGFR2 and FAK were analyzed. Actin was used as a normalizer of protein loading (**c**). Displacement of ^{125}I-VEGF-A from the HUVEC cells' surface with increasing concentrations of cold-VEGF-A or MMRN2. Values are expressed as the percentage referred to the bound ^{125}I-VEGF-A in the absence of cold VEGF-A or MMRN2 and represent the mean ± s.e. of three independent experiments (**d**). Displacement of ^{125}I-VEGF-A from recombinant VEGFR2 immobilized on plastic. Type I collagen (Coll I) was used as a control. The experiment was performed as above and the values represent the mean ± s.e. of three independent experiments (**e**). Absorbance detected following an ELISA test with immobilized MMRN2 or BSA incubated with soluble VEGF-A. Values represent the mean ± s.e. of three independent experiments (*$P = 0.0002$) (**f**). Sensogram expressed in RU obtained from the surface plasmon resonance analysis of different amounts of VEGF-A (the nM concentrations are indicated) interacting with immobilized MMRN2 to a density of 2160 RU. The values of the curves represent the mean of three replicates (**g**).

of cold VEGF-A or MMRN2 were performed. MMRN2 induced a considerable displacement of radiolabelled VEGF-A, indicating that this molecule interfered with the VEGF-A–VEGFR binding (Figure 4d). To verify if this effect did not require other molecules present on the EC surface we have performed a similar experiment using the recombinant extracellular domain of VEGFR2. In this case the displacement was even stronger, comparable to that obtained with VEGF-A; on the contrary, type I collagen did not displace VEGF-A from its receptor (Figure 4e). The specificity of MMRN2 in interfering with the VEGF-A/VEGFR2 interaction was corroborated in ELISA tests following coating of plates with recombinant VEGFR2, incubation with soluble VEGF-A and challenging with type I collagen or MMRN2 (Supplementary Figure 2c). Next, through an ELISA test using soluble VEGF-A and immobilized MMRN2, we confirmed that MMRN2 directly interacted with VEGF-A (Figure 4f). The strength of the MMRN2/VEGF-A interaction was further confirmed by surface plasmon resonance analysis (Kd ~ 50 nM; Figure 4g and Supplementary Figure 2d).

MMRN2 negatively affected tumor angiogenesis and growth

To verify whether MMRN2 could affect tumor angiogenesis and tumor growth *in vivo* we injected stably transfected HT1080 cells in nude mice. Two stable clones were chosen with slightly different expression levels (Supplementary Figure 3a). Strikingly, the ectopic secretion of MMRN2 led to an almost complete blockage of tumor growth (Figures 5a and b and Supplementary Figures 3b and c). The anti-tumor effect of MMRN2 was even more prominent when using the high-expressing clone 4, the mean of the tumor volumes obtained with clone 9 being more than threefold those obtained with clone 4. The MMRN2 effect was so strong that with this approach only two tumors could be excised for further analysis. The ectopic expression of MMRN2 by HT1080 cells, which do not normally express this molecule, did not alter their viability or their apoptotic rate, indicating that MMRN2 did not affect tumor cell behavior (Figures 5c and d). The effect had thus to be indirect and, given our compelling evidences establishing a negative role of MMRN2 in the regulation of angiogenesis, we verified whether the lack of tumor growth was because of reduced intra-tumor angiogenesis. Compared with the controls, the vascular density and overall length of the vessels were significantly lower in the MMRN2-transfected cell tumors (Figures 5e and f). Moreover, the vessels from the MMRN2-positive tumors were less mature and thus likely less efficient in providing oxygen and nutrients to the growing tumors (Figures 5g and h). Accordingly, and unlike the controls, the tumors derived from MMRN2-transfected cells displayed extended hypoxic regions, despite their size, which was much smaller (Figure 6a and Supplementary Figure 3d). To corroborate the limited data obtained with the use of HT1080-transfected cells, where only two tumors were available for the analysis, and to verify whether MMRN2 could be effective also on established tumors, we treated growing tumors with the MMRN2 adenoviral construct. Also with this approach, the reduction of tumor growth was consistent, even though less striking compared with that observed with the use of the MMRN2 stably transfected cells (Figure 6b). In this case we could recover all the tumors for further analysis which suggested that, despite the fact that the vessels' length was similarly reduced, the partial effect could likely depend on a less efficient reduction of the blood vessel density compared with that obtained with the transfected cells (Figures 6c and d). The expression of VEGF-A by the tumors from mock and MMRN2-transfected HT1080 cells was confirmed by RT–PCR and western blot on tumor cell lysates, and by immunofluorescence on frozen sections (Supplementary Figures 3e, f and g). Next, we demonstrated that the Gv39M antibody specifically recognizing the VEGFR2-bound VEGF-A also detected the MMRN2-bound VEGF-A (Supplementary Figure 3h). The Gv39M antibody revealed a diffuse staining in the MMRN2-overexpressing tumors, also in areas distant from the CD31-positive blood vessels (Figures 6e and f). Here the staining mainly co-localized with recombinant MMRN2 produced by the transfected HT1080 cells (Supplementary Figure 3i), again suggesting that MMRN2 may function by sequestering VEGF-A and preventing VEGF-A/VEGFR2 interaction.

Discussion

Despite its discovery dates to the nineties, before this study the function of MMRN2 has been fully obscure. Our investigation was driven by the hypothesis that its specific localization along the blood vessels and the intimate contact with ECs (Christian *et al*., 2001) could affect their behavior and hence play an important role in the regulation of angiogenesis.

Here we provided evidence that MMRN2 was secreted by ECs and did not affect their proliferation or their apoptotic rate, whereas it significantly impaired their motility. The MMRN2-dependent inhibition of EC motility was not likely mediated by integrins because adhesion of EC was independent of Mg^{2+} and Ca^{2+}, and was unaffected by integrin-blocking antibodies. The development of new blood vessels was negatively affected by MMRN2 in all the tests that we have carried out both *in vitro*, including tubule formation and co-culture systems, as well as in *in*/*ex vivo* CAM and aortic ring assays. The negative effect of MMRN2 in regulating angiogenesis may likely depend on the endogenous VEGF-A released by ECs when not added directly in the various tests (Roccaro *et al*., 2006), for instance the sprouting of novel vessels in aortic ring assays is highly dependent on endogenously released VEGF-A (Ligresti *et al*., 2011). Although the inhibition of EC motility was directly linked to MMRN2, it cannot be excluded that the striking effects in halting angiogenesis *in vivo* may also depend on its influence on other cell types that may be responsible for an amplification of the anti-angiogenic effects of this molecule (Anghelina *et al*., 2006; Nicosia, 2009).

The interaction of MMRN2 with ECs led to the downregulation of two RTKs present on the ECs' surface, VEGFR1 and VEGFR2. VEGFR2 accounts for most of the VEGF-A effects on adult ECs (Waltenberger *et al*., 1994) and its phosphorylation in presence of MMRN2 was significantly impaired. The reduced phosphorylation of Tyr^{1175}, which is known to be implicated in the regulation of EC migration (Holmqvist *et al*., 2004), and the impaired phosphorylation of FAK were both in agreement with the biological findings. The inhibition of this pathway by MMRN2 was likely dependent on the interference with the VEGF-A/VEGFR2 axis, as demonstrated by the significant displacement of ^{125}I-VEGF-A from the EC surface and from recombinant VEGFR2. The incomplete displacement of the EC-bound VEGF-A, in addition to its interaction with heparin sulfate proteoglycans, was probably also the consequence of a lower affinity of this interaction ($\sim$50 nM), compared with that of VEGFR1 ($\sim$10–20 pM) (de Vries *et al*., 1992) and of

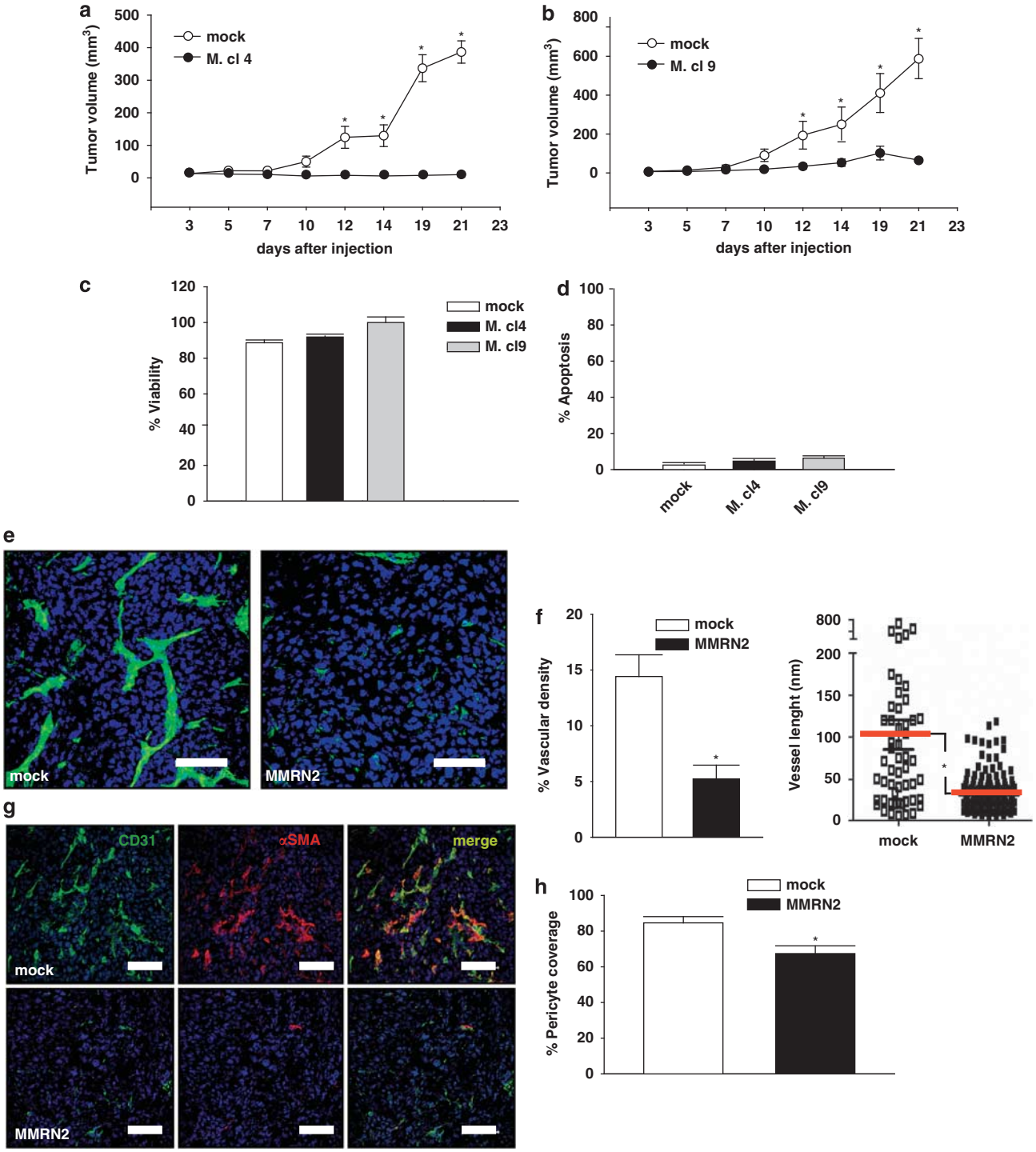

Figure 5 MMRN2 halts *in vivo* tumor growth and tumor angiogenesis. Tumor growth curves obtained following subcutaneous injection of mock or MMRN2 HT1080-transfected cells clone 4 (M. cl 4). Ten animals were used and the data represent the mean ± s.e. of three independent experiments (*$P \leqslant 0.003$) (**a**). Tumor growth curve obtained as above using the MMRN2 clone 9 (M. cl 9) (*$P \leqslant 0.04$) (**b**). MTT assay performed on mock or MMRN2-transfected HT1080 cells. The mock and MMRN2 clones (mock, M. cl 4 and M. cl 9) were analyzed for viability after 48 h in culture (**c**). TUNEL assay performed on the same cells as above (**d**). Representative pictures of the immunofluorescence analysis of the intratumoral vessels performed on the tumor cryosections from mock or MMRN2-transfected cells, following staining with the anti-CD31 antibody. Nuclei were stained with the TO-PRO-3 dye, scale bars: 75 μm (**e**). Evaluation of the vascular density as assessed by means of the Image tool software, (left, *$P = 0.0009$). Values represent the mean ± s.e. of the vessels' pixel areas of at least five fields. Evaluation of the length of the intratumoral vessels from mock or MMRN2 tumor cryosections. The mean of the values is indicated by red bars (right, *$P = 0.02$) (**f**). Representative pictures of the immunofluorescence analysis using anti-CD31 (for ECs) and the anti-α-SMA (for pericytes) antibodies on tumor sections from mock and MMRN2-transfected HT1080 cells. Nuclei are stained with the TO-PRO-3 dye, scale bars: 75 μm (**g**). Quantification of the co-localization of the anti-CD31 and the anti-α-SMA staining obtained from the immunofluorescences from mock and MMRN2-overexpressing tumors (*$P = 0.006$) (**h**).

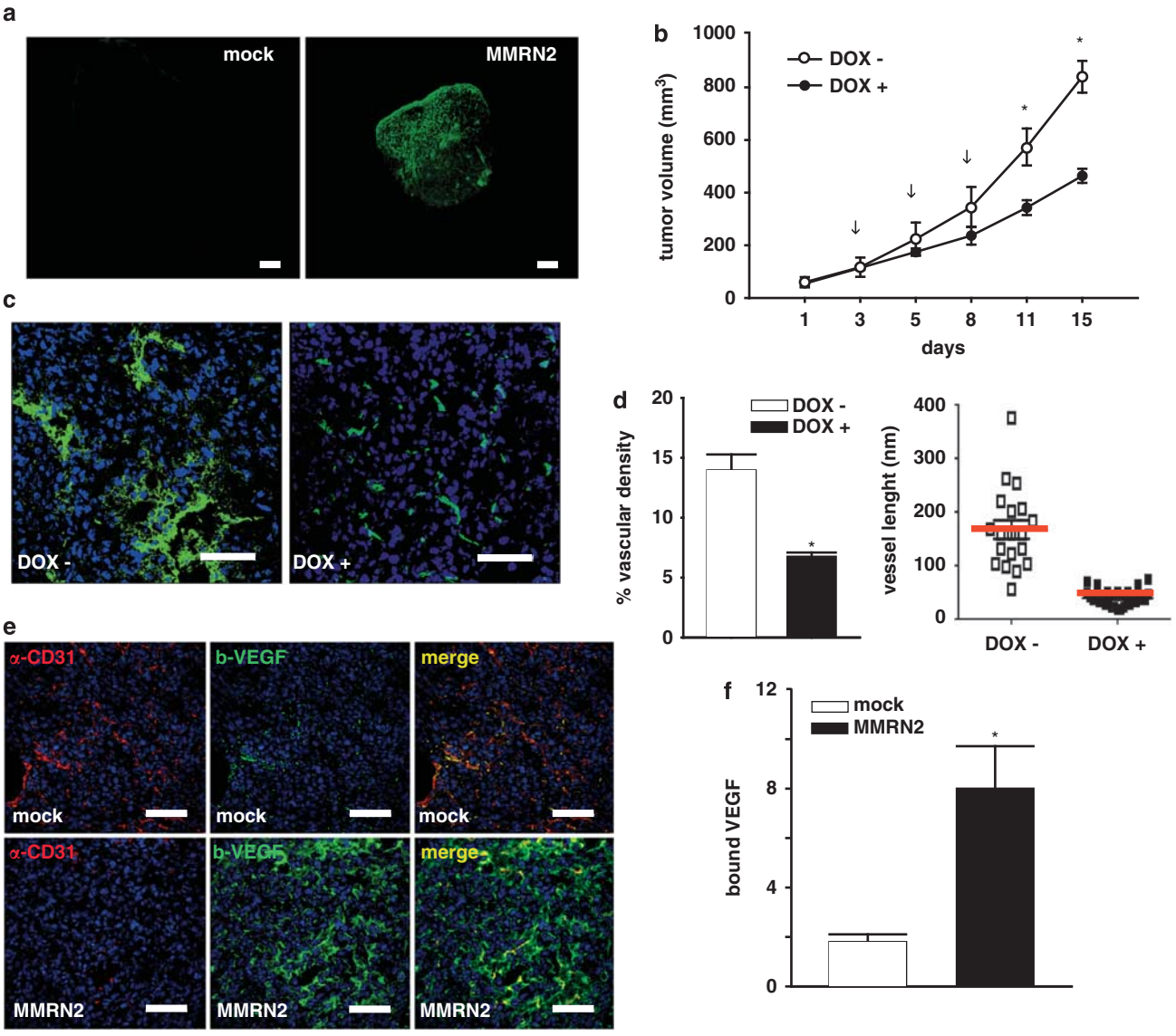

Figure 6 MMRN2 overexpressing tumors lack an efficient mature vasculature. Representative pictures of the tumor hypoxic areas as detected by means of the hypoxyprobe-1 on tumor sections from mock and MMRN2-transfected HT1080 cells, scale bars: 500 μm (**a**). Evaluation of the tumor volumes following intra-tumoral injection of MMRN2 adenoviral particles in established tumors with or without doxycycline (DOX + and DOX–, respectively). Ten mice per group were used and the days of the injections are indicated by an arrow (*$P \leqslant 0.005$) (**b**). Representative pictures of the immunofluorescence analysis of the vessels from the tumor cryosections following treatment of the tumors with adenoviral particles. Nuclei are stained with the TO-PRO-3 dye, scale bars: 75 μm (**c**). Mean ± s.e. of the vascular density expressed in pixel areas (left, *$P < 0.0001$). Evaluation of the length of the vessels from the same tumors as above. The mean of the values is indicated by red bars (left, *$P = 0.002$) (**d**). Representative pictures of the immunofluorescence analysis of blood vessels (α-CD31) in mock and MMRN2-positive tumors using the Gv39M antibody to detect bound-VEGF-A (b-VEGF). Nuclei are stained with the TO-PRO-3 dye, scale bars: 75 μm (**e**). Quantitative analysis of VEGF-A staining (pixel area) from mock and MMRN2-positive tumors (*$P = 0.008$) (**f**).

VEGFR2 (~75–125 pM) (Terman *et al*., 1992) for VEGF-A. The interference of MMRN2 with the VEGF-A/VEFGR interaction was because of a direct binding of VEGF-A to MMRN2, as indicated by both ELISA and surface plasmon resonance analysis. It is reasonable to assume that MMRN2, because of its deposition and localization in tight contact with ECs, may attain a high pericellular concentration and thus represent an important competitor for the binding of VEGF-A to VEGFR2. This hypothesis, also in view of the relatively low density of this receptor on the cell surface (~10 000–25 000 molecules/cell) (Hotz *et al*., 2010), is very likely. The reason why MMRN2 impaired only EC motility remains at the moment elusive, but may depend on a simultaneous activation of other pathways mainly affecting cell proliferation. This hypothesis is supported by the fact that, unlike FAK, Erk 1/2 phosphorylation does not vary in the presence of MMRN2 (data not shown). This effect is unique for MMRN2, as most ECM molecules that bind VEGF-A

also affect cell proliferation (Kupprion *et al*., 1998; Sahni and Francis, 2000).

Our biological results and the elucidation of the molecular mechanisms responsible for the MMRN2 anti-angiogenic activity were consistent with the outcome of the tumor growth studies. The MMRN2-transfected cells were *per se* not affected in their apoptotic nor proliferation rate by the ectopic expression of the molecule, but they almost failed to develop tumors when injected into nude mice. The finding that the MMRN2-positive tumors displayed a significantly lower vascular density suggested that the anti-tumor effects could likely be due to indirect effects hinging on a reduced blood supply, and a consequent depletion of oxygen and nutrients indispensable for tumor growth. The result was similar in tumors treated with MMRN2 adenoviral particles. Here, despite the limitations inherent to the inefficient and incomplete transduction of the tumor cells *in vivo* and the low number of injections performed, a less pronounced reduction of the blood vessel density was obtained as opposed to the higher reduction observed with the use of stably transfected cells. This represented a further indication of an indirect, angiogenic-dependent anti-tumoral role of MMRN2. The effect on vascular density was further exacerbated by the fact that tumor vessels from MMRN2 overexpressing tumors were less mature and thus less efficient, suggesting that MMRN2 may also affect pericyte recruitment. The use of the Gv39M antibody recognizing only the VEGFR2-bound VEGF-A granted further support to our hypothesis of an interference of MMRN2 with the VEGF-A/VEGFR2 axis; VEGF-A co-localized with MMRN2 produced by the transfected HT1080 cells *in vivo*, corroborating the results obtained through the ELISA tests, which indicated that the antibody also recognized the MMRN2-bound VEGF-A. This latter result indicated that the sequestration of VEGF-A by MMRN2 may prevent the interaction with VEGFR2 leading to a decreased intra-tumoral angiogenesis and consequent impaired tumor growth. Interestingly, database analysis for MMRN2 (www.oncomine.org) indicates that this molecule is differentially expressed in many types of tumors such as brain, breast, kidney and sarcomas if compared with the normal counterpart. Many of these tumors are highly angiogenesis dependent and it is conceivable that the dysregulation of MMRN2 expression might have an impact on tumor progression affecting the intra-tumoral vascularization.

In conclusion, with this study we provided evidence that MMRN2 may represent a novel key homeostatic molecule indispensable for the maintenance of blood vessel integrity. These findings were coherent with the hypothesis that MMRN2 may function as a 'biological barrier' keeping ECs in a steady-state condition and that the downregulation of endogenous MMRN2 or even the possible degradation by yet unidentified specific protease(s) could determine efficient sprouting and differentiation of ECs to form novel blood vessels. Our results provide further evidence of the intricate interplay of ECM molecules and cells within the tumor microenvironment, and open the possibility for the development of new anti-angiogenic drugs useful for cancer treatment.

Materials and methods

Cell lines

Human embryonic kidney cells (HEK 293, ATCC CRL-1573, Milan, Italy) were grown in Dulbecco's modified Eagle medium (Cambrex Bio Science, Milan, Italy) containing 10% fetal bovine serum and 1% penicillin–streptomycin. 293-EBNA (Epstein-Barr Nuclear Antigen) cells were a gift from Rupert Timpl. The HT1080 and HeLa cell lines were from ATCC, and cultured in Dulbecco's modified Eagle medium containing 10% fetal bovine serum. Pulmonary artery smooth muscle cells (PASMC) were from Lonza Ltd (Visp, Switzerland) and cultured in the provided medium. HUVEC cells were isolated from human umbilical cord veins as previously described (Jaffe *et al*., 1973). Cells were cultured in Medium 199 (GIBCO, Invitrogen, Milan, Italy) supplemented with 20% fetal bovine serum, 1% penicillin–streptomycin, 50 μg/ml heparin and bovine brain extract (0.5%).

Antibodies and other reagents

The anti-MMRN2 polyclonal antibody was obtained upon immunization of a rabbit with 150 μg of a recombinant MMRN2 fragment corresponding to the *N*-terminal gC1q domain preceded by the proline-rich domain. The *Nae*I and *Xho*I restriction fragment from the full-length pcDNA construct (see below) was sub-cloned into the pQE-30 vector, expressed in bacteria and purified by means of the Ni-NTA resin, and exclusively used for immunization purposes in the present work. The antibody was affinity purified from the rabbit serum by means of the CNBr-activated Sepharose 4B resin (Amersham, GE-Healthcare, Milan, Italy). The anti-FLAG and α-SMA antibodies, the FLAG peptide, and the anti-FLAG M2 affinity gel were from Sigma-Aldrich (Milan, Italy). The secondary horse radish peroxidase-conjugated antibodies were from Amersham. The secondary antibodies conjugated with Alexa Fluor 680 were from Invitrogen. The Ni-NTA agarose was from QIAGEN (Milan, Italy). BD Adeno-X Rapid Titer Kit was from BD Biosciences (Milan, Italy). The AngioKit was from TCS CellWorks (Buckingham, UK). The anti-mouse anti-CD31 antibody and Matrigel were from BD Biosciences. Anti-VEGFR2 and anti phospho-VEGFR2 (Tyr^{1175}), anti-FAK and anti-phospho-FAK ($Tyr^{576/577}$), and anti-VEGF-A were from Cell Signaling Technology Inc. (Danvers, MA, USA). The hypoxyprobe-1 was from HPI, Inc. (Burlington, MA, USA). The *in situ* Cell Death Detection Fluorescein Kit was purchased from Roche Diagnostics S.p.a. (Milan, Italy). The Gv39M antibody recognizing the VEGFR2-bound VEGF-A (Brekken *et al*., 1998) was a kind gift from Dr R Brekken (UT Southwestern Medical Center, Dallas, TX, USA).

Cell transfection, expression and purification of recombinant proteins

Human MMRN2 cDNA was retro-transcribed from total RNA extracted from HUVEC cells and cloned into pCEP-Pu vector. The forward oligonucleotide for the MMRN2 5′ region was: 5′-GGGTTTAAACGGACTACAAGGACGACGATGACAAGGCTGCTTCCAGTACTAGCCTC-3′ and the reverse: 5′-GTGCAGCTGGCGCACCTCGT-3′. For the 3′ region, forward: 5′-GACGAGGTGGGCGCGCTGAA-3′ and reverse: 5′-CGGGATCCATGGTGATGGTGATGATGGGTCTTAAACATCAGGAAGC-3′. The MMRN2 cDNA was then sub-

cloned into pcDNA3.1/Myc-His vector by *Hind*III and *Xho*I restriction. 293-EBNA cells were transfected by electroporation with the pCEP-Pu construct and selected with 0.5 μg/ml of puromycin and 250 μg/ml of G418.

Recombinant adenovirus
For MMRN2 overexpression, tetracycline-inducible recombinant adenoviruses were constructed according to the manufacturer's instructions using the Adeno-X Tet-On Expression System 2 (Clontech Laboratories, Milan Italy). HUVEC cells were co-transduced with a regulatory virus Adeno-X Tet-On and the MMRN2 recombinant virus at a specific multiplicity of infection ratio (800:320). Doxycyline was employed at a final concentration of 0.5 μg/ml.

For the endogenous MMRN2 downregulation, the Knockout RNAi System was used (Clontech). The targeted sequences were: siRNA 1: 5′-GAGGAACCTCTCAGAGCTGCACAT GACCA-3′; siRNA 2: 5′-GGATGAGATCAAGGAACTGT ACTCCGAAT-3′; siRNA 3: 5′-CCTCATCAAGTACGTGA AGGACTGCAATT-3′; siRNA 4: 5′-GCAGACAGTGAAG TTCAACACCACATACA-3′.

Western blotting analysis and immunohistochemistry
Cells were lysed in cold HNTG buffer (1% Triton X-100, 20 mM HEPES pH 7.5, 10% glycerol, 150 mM NaCl) containing a protease inhibitors cocktail (Roche Diagnaostics S.p.a., Milan, Italy) and 1 mM sodium orthovanadate. Proteins were resolved in 4–20% Criterion Precast Gels (Bio-Rad Laboratories, S.r.l., Milan, Italy) and transferred onto Hybond-ECL nitrocellulose membranes (GE-Healthcare). The blots were developed using ECL (GE-Healthcare) and exposed to X-ray films. Alternatively the Odyssey infrared imaging system was used (Li-COR Biosciences, Lincoln, NE, USA). For immunohistochemistry, tumors were included in optimal cutting temperature compound (OCT) and frozen. Sections of 7 μm thickness were made and stained with anti-mouse CD31 and/or α-SMA antibodies. Images were acquired with a Leica TCS SP2 confocal system (Leica Microsystems GmbH, Milan, Italy). Alternatively five mice injected in both flanks as above were treated with 60 mg/kg of pimonidazole HCl 45 min prior being killed and sections were stained with the PAb2627 (hypoxyprobe-1, CHEMICON, Temacula, CA, USA) according to the manufacturer instructions.

Radioligand displacement studies, ELISA and Surface Plasmon Resonance analysis. For the displacement of HUVEC-bound ^{125}I-VEGF-A (Perkin Elmer, Milan, Italy), 2×10^5 HUVEC cells were used per point. Cells were incubated with 70 pM ^{125}I-VEGF-A and increasing concentrations of cold-VEGF-A or recombinant full-length MMRN2, incubated on ice for 1 h, collected, and counts obtained with the Wizard 2 GAMMA Counter (Perkin Elmer). In alternative, the recombinant VEGFR2 Fc chimera (R&D Systems, Inc., Milan, Italy) was used and coated on ELISA plates (10 ng/well). Bound ^{125}I-VEGF-A was rescued using 2 M NaOH at 50 °C and type I collagen was used as a control. For the ELISA tests, 0.5 μg of MMRN2 or bovine serum albumin (BSA) were coated, blocked with 2% BSA and incubated with soluble VEGF-A (100 ng/well) for 1 h at 37 °C. Binding was verified with the anti-VEGF-A antibody; the ABTS substrate was added and absorbance at 405 nm detected with a spectrophotometer (TECAN, Milan, Italy). For BIAcore analysis MMRN2 was immobilized onto CM5-dextran matrix chip from BIAcore Life Sciences (GE Healthcare) using amine coupling to a density of 2160 resonance units (RU); 37 ng/μl of MMRN2 in acetate pH = 4 was used. Different concentrations of $VEGF_{165}$ were injected as analyte and the kinetics of the interaction detected by means of the BIAcore X-100 instrument.

MTT and terminal deoxynucleotidyl transferase-mediated dUTP nick end labeling (TUNEL) assays
Following over- or downregulation of MMRN2 expression or treatment with the recombinant protein, 0.3 mg/ml of MTT (3-(4,5-dimethylthiazol-2-yl)-2,5-diphenyltetrazolium bromide) reagent was added and cells were incubated at 37 °C for 4 h. Absorbance at 560 nm was detected following solubilization of crystals with dimethyl sulfoxide. The apoptotic rate was determined using the ApopTag Fluorescein *in situ* Oligo Ligation Apoptosis Detection Kit (CHEMICON International).

RTK array
RTK activation was evaluated using the Human Phospho-RTK Array Kit (R&D Systems). HUVEC cells were incubated for 30 min with the conditioned media from HUVEC cells transduced with the MMRN2 or control adenoviral vectors (collected 72 h post transduction), the experiment was performed according to the manufacturer's instructions and spots' intensity was evaluated with the Image Tool software (University of Texas Health Science Center, San Antonio, TX, USA).

Cell adhesion, migration, haptotaxis, scratch test and tube formation assays
Centrifugal Assay for Fluorescence-based Cell Adhesion was performed as previously described (Spessotto *et al*., 2000). The miniplates were coated with 10 μg/ml full-length MMRN2 or type I collagen and saturated with 1% denatured BSA. The units were centrifuged upside down for 5 min at 12 or 46 *g* and the fluorescence was measured using the GENios Plus instrument (TECAN). Fluorescence-Assisted Transmigration Invasion and Motility Assay was performed as previously described (Spessotto *et al*., 2000). The transwell membranes were coated with 10 μg/ml of MMRN2 or type I collagen and blocked with 1% BSA. Cells were labeled with DiI (Molecular Probes, Invitrogen) and were let to migrate toward a VEGF-A stimulus (50 ng/ml). Migration was monitored using the computer-interfaced GENios Plus instrument. In alternative, migrated cells were estimated by counting following hematoxylin and eosin staining. Haptotaxis was assessed by plating the molecules on the underside of the membranes. For scratch test analysis, confluent cells were starved overnight and a scratch wound was made using a sterile pipette tip. Cells were washed and incubated with medium containing 0.5% serum in the presence of 10 μg/ml of MMRN2 or type I collagen. Time course analysis was carried out by means of the LEICA AF6000 Imaging System (LEICA, Wetzlar, Germany).

Matrigel tube formation assays were performed as previously described (Mongiat *et al*., 2003). HUVEC cells were resuspended in medium containing 0.5% serum and 10 μg/ml of purified full-length MMRN2 or type I collagen. When using the TCS CellWorks AngioKit, co-cultures were treated for 11 days with MMRN2 or phosphate-buffered saline. Cells were fixed and stained using the anti-CD31 antibody and the DAB substrate was provided. Vessel density was calculated by means of the Image Tool software.

CAM and aortic ring assays
CAM assays were performed as previously described (Mongiat *et al*., 2003). Fifty nanograms of VEGF-A or bFGF with or without 150 ng of MMRN2 was allowed to be absorbed by the sponges (Gelfoam, Upjohn Company, Kalamazoo, MI, USA). Phosphate-buffered saline or full-length MMRN2 only was

used as a control. Twenty eggs each were used. After 4 days the CAMs were fixed and pictures were taken at the Stereo Microscope (Leica Microsystems GmbH). The vessels directed toward the sponge were evaluated by counting.

The aortic ring assays were performed as previously described (Aplin *et al*., 2008). Rat thoracic aortas were dissected and cultured with or without 10 μg/ml of full-length MMRN2. Angiogenesis was measured by counting the number of neovessels over time.

In vivo *tumor growth experiments*

Ten female athymic nude mice (Harlan S.r.l, Milan, Italy) were subcutaneously injected with 1×10^6 HT1080 cells stably transfected with the MMRN2 pcDNA3.1 vector (right flanks) or the empty vector (left flanks). Two MMRN2 clones were used (clone 4 and 9) for a total number of 20 mice. Tumor growth was monitored, and after 19 days the animals were killed and tumors excised. Only two small MMRN2 over-expressing tumors grew and were available for immunohistochemical analysis. Alternatively, 1×10^6 HT1080 cells were subcutaneously injected into 10 female athymic nude mice and let grow to a volume of 40–60 mm^3. Tumors were then injected with 2×10^9 total ifu (AdMMRN2/AdTet-ON, ratio 400:160) three times (dox-adenoviral construct). Three days before the first viral injection 1 mg/ml of doxycycline and 2.5% of sucrose was added to the drinking water of 5 out of 10 animals. Tumor size was measured with a caliper and the volume calculated with the following formula: $(\pi \times \text{length} \times \text{width}^2)/6$.

Conflict of interest

The authors declare no conflict of interest.

Acknowledgements

We thank Dr Philip Thorpe and Dr Rolf Brekken for the generous gift of the Gv39M antibody. We thank the ISS-ACC Program 2, AIRC and MIUR (grant no.RBRN07BMCT) for supporting this work.

References

Anghelina M, Krishnan P, Moldovan L, Moldovan NI. (2006). Monocytes/Macrophages cooperate with progenitor cells during neovascularization and tissue repair: conversion of cell columns into fibrovascular bundles. *Am J Pathol* **168**: 529–541.

Aplin AC, Fogel E, Zorzi P, Nicosia RF. (2008). The aortic ring model of angiogenesis. *Methods Enzymol* **443**: 119–136.

Boehm T, Folkman J, Browder T, O'Reilly MS. (1997). Antiangiogenic therapy of experimental cancer does not induce acquired drug resistance. *Nature* **390**: 404–407.

Braghetta P, Ferrari A, De GP, Zanetti M, Volpin D, Bonaldo P *et al*. (2004). Overlapping, complementary and site-specific expression pattern of genes of the EMILIN/Multimerin family. *Matrix Biol* **22**: 549–556.

Brekken RA, Huang X, King SW, Thorpe PE. (1998). Vascular endothelial growth factor as a marker of tumor endothelium. *Cancer Res* **58**: 1952–1959.

Campbell NE, Kellenberger L, Greenaway J, Moorehead RA, Linnerth-Petrik NM, Petrik J. (2010). Extracellular matrix proteins and tumor angiogenesis. *J Oncol* **2010**: 586905.

Carmeliet P. (2000). Mechanisms of angiogenesis and arteriogenesis. *Nat Med* **6**: 389–395.

Chen TT, Luque A, Lee S, Anderson SM, Segura T, Iruela-Arispe ML. (2010). Anchorage of VEGF to the extracellular matrix conveys differential signaling responses to endothelial cells. *J Cell Biol* **188**: 595–609.

Cheresh DA, Stupack DG. (2008). Regulation of angiogenesis: apoptotic cues from the ECM. *Oncogene* **27**: 6285–6298.

Christian S, Ahorn H, Novatchkova M, Garin-Chesa P, Park JE, Weber G *et al*. (2001). Molecular cloning and characterization of EndoGlyx-1, an EMILIN-like multisubunit glycoprotein of vascular endothelium. *J Biol Chem* **276**: 48588–48595.

de Vries C, Escobedo JA, Ueno H, Houck K, Ferrara N, Williams LT. (1992). The fms-like tyrosine kinase, a receptor for vascular endothelial growth factor. *Science* **255**: 989–991.

Ferrara N. (2002). Role of vascular endothelial growth factor in physiologic and pathologic angiogenesis: therapeutic implications. *Semin Oncol* **29**: 10–14.

Folkman J. (1971). Tumor angiogenesis: therapeutic implications. *N Engl J Med* **285**: 1182–1186.

Gengrinovitch S, Berman B, David G, Witte L, Neufeld G, Ron D. (1999). Glypican-1 is a VEGF165 binding proteoglycan that acts as an extracellular chaperone for VEGF165. *J Biol Chem* **274**: 10816–10822.

Greenaway J, Lawler J, Moorehead R, Bornstein P, Lamarre J, Petrik J. (2007). Thrombospondin-1 inhibits VEGF levels in the ovary directly by binding and internalization via the low density lipoprotein receptor-related protein-1 (LRP-1). *J Cell Physiol* **210**: 807–818.

Hirama M, Takahashi F, Takahashi K, Akutagawa S, Shimizu K, Soma S *et al*. (2003). Osteopontin overproduced by tumor cells acts as a potent angiogenic factor contributing to tumor growth. *Cancer Letters* **198**: 107–117.

Holmqvist K, Cross MJ, Rolny C, Hagerkvist R, Rahimi N, Matsumoto T *et al*. (2004). The adaptor protein shb binds to tyrosine 1175 in vascular endothelial growth factor (VEGF) receptor-2 and regulates VEGF-dependent cellular migration. *J Biol Chem* **279**: 22267–22275.

Hotz B, Backer MV, Backer JM, Buhr HJ, Hotz HG. (2010). Specific targeting of tumor endothelial cells by a shiga-like toxin-vascular endothelial growth factor fusion protein as a novel treatment strategy for pancreatic cancer. *Neoplasia* **12**: 797–806.

Hu M, Polyak K. (2008). Microenvironmental regulation of cancer development. *Curr Opin Genet Dev* **18**: 27–34.

Huber MA, Kraut N, Schweifer N, Dolznig H, Peter RU, Schubert RD *et al*. (2006). Expression of stromal cell markers in distinct compartments of human skin cancers. *J Cutan Pathol* **33**: 145–155.

Hutchings H, Ortega N, Plouet J. (2003). Extracellular matrix-bound vascular endothelial growth factor promotes endothelial cell adhesion, migration, and survival through integrin ligation. *FASEB J* **17**: 1520–1522.

Jaffe EA, Nachman RL, Becker CG, Minick CR. (1973). Culture of human endothelial cells derived from umbilical veins. Identification by morphologic and immunologic criteria. *J Clin Invest* **52**: 2745–2756.

Joyce JA, Pollard JW. (2009). Microenvironmental regulation of metastasis. *Nat Rev Cancer* **9**: 239–252.

Koperek O, Scheuba C, Puri C, Birner P, Haslinger C, Rettig W *et al*. (2007). Molecular characterization of the desmoplastic tumor stroma in medullary thyroid carcinoma. *Int J Oncol* **31**: 59–67.

Kupprion C, Motamed K, Sage EH. (1998). SPARC (BM-40, osteonectin) inhibits the mitogenic effect of vascular endothelial growth factor on microvascular endothelial cells. *J Biol Chem* **273**: 29635–29640.

Lawler J. (2002). Thrombospondin-1 as an endogenous inhibitor of angiogenesis and tumor growth. *J Cell Mol Med* **6**: 1–12.

Ligresti G, Aplin AC, Zorzi P, Morishita A, Nicosia RF. (2011). Macrophage-derived tumor necrosis factor-a is an early component of the molecular cascade leading to angiogenesis in response to aortic injury. *Arterioscler Thromb Vasc Biol* **31**: 1151–1159.

Mongiat M, Marastoni S, Ligresti G, Lorenzon E, Schiappacassi M, Perris R *et al*. (2010). The extracellular matrix glycoprotein elastin microfibril interface located protein 2: a dual role in the tumor microenvironment. *Neoplasia* **12**: 294–304.

Mongiat M, Sweeney SM, San Antonio JD, Fu J, Iozzo RV. (2003). Endorepellin, a novel inhibitor of angiogenesis derived from the C terminus of perlecan. *J Biol Chem* **278**: 4238–4249.

Mustonen T, Alitalo K. (1995). Endothelial receptor tyrosine kinases involved in angiogenesis. *J Cell Biol* **129**: 895–898.

Nicosia R. (2009). The aortic ring model of angiogenesis: a quarter century of search and discovery. *J Cell Mol Med.* **13**: 4113–4136.

Nyberg P, Salo T, Kalluri R. (2008). Tumor microenvironment and angiogenesis. *Front Biosci* **13**: 6537–6553.

Olsson AK, Dimberg A, Kreuger J, Claesson-Welsh L. (2006). VEGF receptor signalling—in control of vascular function. *Nat Rev Mol Cell Biol* **7**: 359–371.

Roccaro AM, Hideshima T, Raje N, Kumar S, Ishitsuka K, Yasui H *et al*. (2006). Bortezomib mediates antiangiogenesis in multiple myeloma via direct and indirect effects on endothelial cells. *Cancer Res* **66**: 184–191.

Sahni A, Francis CW. (2000). Vascular endothelial growth factor binds to fibrinogen and fibrin and stimulates endothelial cell proliferation. *Blood* **96**: 3772–3778.

Sanz-Moncasi MP, Garin-Chesa P, Stockert E, Jaffe EA, Old LJ, Rettig WJ. (1994). Identification of a high molecular weight endothelial cell surface glycoprotein, endoGlyx-1, in normal and tumor blood vessels. *Lab Invest* **71**: 366–373.

Spessotto P, Giacomello E, Perris R. (2000). Fluorescence assays to study cell adhesion and migration in vitro. *Methods Mol Biol* **139**: 321–343.

Sun J, Hopkins BD, Tsujikawa K, Perruzzi C, Adini I, Swerlick R *et al*. (2009). Thrombospondin-1 modulates VEGF-A-mediated Akt signaling and capillary survival in the developing retina. *Am J Physiol Heart Circ Physiol* **296**: H1344–H1351.

Terman BI, Dougher-Vermazen M, Carrion ME, Dimitrov D, Armellino DC, Gospodarowicz D *et al*. (1992). Identification of the KDR tyrosine kinase as a receptor for vascular endothelial cell growth factor. *Biochem Biophys Res Commun* **187**: 1579–1586.

Ventura E, Sassi F, Parodi A, Balza E, Borsi L, Castellani P *et al*. (2010). Alternative splicing of the angiogenesis associated extra-domain B of fibronectin regulates the accessibility of the B-C loop of the type III repeat 8. *PLoS One* **5**: e9145.

Waltenberger J, Claesson-Welsh L, Siegbahn A, Shibuya M, Heldin CH. (1994). Different signal transduction properties of KDR and Flt1, two receptors for vascular endothelial growth factor. *J Biol Chem* **269**: 26988–26995.

Wijelath ES, Murray J, Rahman S, Patel Y, Ishida A, Strand K *et al*. (2002). Novel vascular endothelial growth factor binding domains of fibronectin enhance vascular endothelial growth factor biological activity. *Circ Res* **91**: 25–31.

Zoeller JJ, Whitelock JM, Iozzo RV. (2009). Perlecan regulates developmental angiogenesis by modulating the VEGF-VEGFR2 axis. *Matrix Biol* **28**: 284–291.

Supplementary Information accompanies the paper on the Oncogene website (http://www.nature.com/onc)

ACKNOWLEDGMENTS

This work was performed in the Division of Experimental Oncology 2 at Centro di Riferimento Oncologico (CRO, National Cancer Institute) of Aviano, directed by Prof. Alfonso Colombatti.

I would like to acknowledge the “Tumor microenvironment and Angiogenesis” group, in particular my PhD advisors, Dr. Maurizio Mongiat and Prof. Alfonso Colombatti, for supporting me during these years.